



Project N. 037110

NEAREST

**Integrated observations from NEAR shore sources of Tsunamis:
Towards an early warning system**

Instrument: STREP

Thematic priority: 1.1.6.3 GOCE (Global Change and Ecosystems)

D5: Broad band OBS data analysis

Due date of deliverable: [January 2009](#)

Actual submission date: [January 2009](#)

Start date of the project: [01/10/2006](#) Duration: [36 + 6 months](#)

Organisation name of the lead contractor for this deliverable: [CSIC](#)

Revision: Final

Project Co founded By the European Commission within the Sixth Framework Programme (2002-2006)		
Dissemination Level		
PU	Public	PU
PP	Restricted to other programme participants (Including Commission Services)	
RE	Restricted to a group specified by the Consortium (Including Commission Services)	
CO	Confidential, only for members of the Consortium (Including Commission Services)	

WP2 - Tsunami source characterisation

D5: Wide-Angle Seismic Cruise Report

Task 2.2 Leader:

CSIC

Task 2.2 Responsible:

Valentí Sallarès

Unitat de Tecnologia Marina (UTM) - CSIC
Centre Mediterrani d'Investigacions Marines i Ambientals (CMIMA)
Passeig Marítim de la Barceloneta, 37-49
08003 Barcelona, Spain

Authorship

This report has been compiled by Valentí Sallarès and Marc-André Gutscher based on the different partial contributions made by the scientific and technical cruise members on board the R/V Hesperides during the NEAREST-SEIS survey, hereafter referred as the NEAREST-SEIS cruise party (See section 2: Participants).

Acknowledgements

Many people contributed to the success of the cruise. First, we wish to thank the Captain, Pedro Luis de la Puente García-Ganges, the first officer, José Luis Barón Touriño, the Chief Engineer and the crew of BIO Hesperides for their professional work and their cooperative and helpful attitude which ensured successful operation during the cruise and the acquisition of a vast set of high quality oceanographic data. And the barbecue on the flight deck was great. We deeply thank the UTM-CSIC technical team for their efforts, guidance and assistance throughout the data collection, which ensured the high quality of the marine geophysical data collected, presented in this report. We also thank the members of the UTM-CSIC for the logistics and cruise planning, especially Juanjo Dañobeitia for his support before and during this cruise. The survey was mainly funded through the Spanish ministry Acciones Complementarias Program (NEAREST-SEIS project, Ref. # CGL2006-27098-E/BTE). Additional support was obtained from European Union FP6 by means of the Nearest Project (Coordinator Nevio Zitellini) and is gratefully acknowledged. We also thank Heike Schmitt and the rest of the German ZDF camera team for their hard work in filming the difficulties and successes of oceanographic work in the Northeast-Atlantic in the late autumn.

Table of contents

1. Introduction and objectives	5
2. Participants	7
2.1. <i>Scientific and technical personnel</i>	7
2.2. <i>Participating institution</i>	8
3. The vessel (BIO Hesperides)	11
4. Geological setting of the Gulf of Cadiz	13
4.1. <i>Generalities of the SW Iberian margin</i>	13
4.2. <i>Potential sources of large earthquakes</i>	15
4.3. <i>Long-term geodynamic evolution of the SW Iberian margin</i>	16
5. Cruise plan	18
5.1. <i>The case for a Wide-Angle Seismic experiment</i>	18
5.2. <i>Wide-Angle seismic transects</i>	20
6. Swath bathymetry and acoustic backscatter	23
6.1. <i>Technical description</i>	23
6.2. <i>Bathymetry data</i>	24
6.3. <i>Acoustic backscatter mosaics</i>	26
7. Parametric sub-bottom profiler	28
7.1. <i>Technical description</i>	28
7.2. <i>TOPAS data samples</i>	29
8. Gravimetry	31
8.1. <i>Technical description</i>	31
8.2. <i>Gravity data samples</i>	31
9. Instrumentation for Wide-Angle Seismic data acquisition	35
9.1. <i>French OBS (MicrOBS)</i>	35
9.2. <i>Spanish OBS (LC2000)</i>	37
9.3. <i>Land stations (Hathor LEAS)</i>	39
9.4. <i>Airgun system</i>	41
10. Wide-Angle Seismic data samples	45
10.1. <i>Seismic records of airgun shooting along P1</i>	45
10.2. <i>Seismic records of airgun shooting along P2</i>	60
10.3. <i>Local earthquakes recorded by OBS</i>	72
11. Conclusions	75
12. References	77
Annex I: Diary of activities	82
Annex II: Technical report (in spanish)	99

Annex III: Report on filming done by ZDF	106
Annex IV: Scripts and configuration parameters	107

1. Introduction and objectives

This report contains exhaustive information on the objectives, activities, instrumentation used and preliminary data acquired during the NEAREST-SEIS cruise, which started in Cartagena (Spain) on Oct 27th, and finished in Cadiz (Spain), in Nov 13th, 2009, and took place onboard the Spanish R/V BIO-Hesperides. It was mainly devoted to the acquisition of Wide-Angle Reflection and Refraction Seismic (WAS) data, using a set of 36 Ocean Bottom Seismometers (OBS), as well as complementary acoustic (swath bathymetry, sediment profiler) and gravity data. A total of 27 persons conformed the scientific and technical crew that shared the tasks of instrumentation setup, deployment and recovery, data acquisition, processing and archiving.

This cruise was part of the European Union, FP-6 funded, NEAREST project, concretely of its WP2 "Tsunami Source Characterisation". It is the successor project to a collaborative effort begun by the ESF EuroMargins projects SWIM (PI Nevio Zitellini, Bologna), which coordinated numerous oceanographic expeditions in the Gulf of Cadiz and included most of the NEAREST partners. The primary objective of the NEAREST project was to advance our understanding of active tectonic deformation in the Gulf of Cadiz area (Southwestern Margin of Iberia), and in particular to help identifying the source of past and future tsunamis in the region (Figure 1). The great Lisbon earthquake and tsunami of 1755 that occurred in this area are thus a major focus of interest.

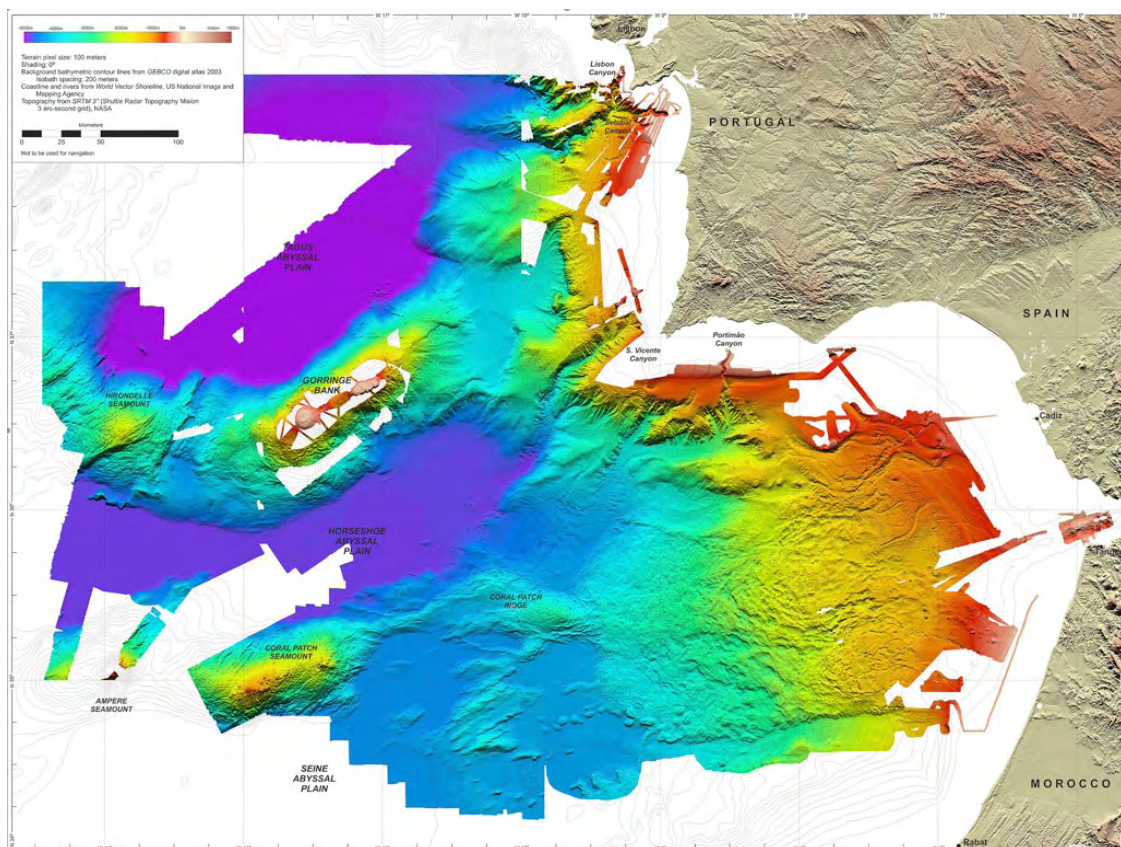


Figure 1.- Map showing bathymetric coverage in the Gulf of Cadiz region (SWIM compilation) (Zitellini et al., in press). Bathymetric compilation carried out at UTM-

CSIC (S. Díez & E. Gràcia).

In the framework of the NEAREST project, the specific objectives of the NEAREST-SEIS survey were the following ones:

- 1) to provide information on the physical properties of the crust as well as the crust-mantle boundary geometry,
- 2) to identify the nature of the crust (eg. oceanic, continental or other) and the limits of the different crustal domains in the region,
- 3) to obtain information to construct a 3-D P-wave velocity model to be used for improving earthquake locations along this complex plate boundary region between NW Africa and SW Iberia (Figure 1).

This report is structured as follows: first, we present the list of participants and participating institutions, second, we present the vessel (BIO Hespérides), then we make an overview of the geologic and tectonic setting of the NW Iberian margin (chapter 4) and present the plan and case for a Wide-Angle seismic study in the area (chapter 5). In chapters 6 to 9 we present the different instrumentation used and several samples of the data acquired. Chapter 6 is devoted to swath bathymetry and acoustic backscatter, chapter 7 to the parametric sub-bottom profiler, and chapter 8 to the gravimeter. Since Wide-Angle seismic data acquisition was the main objective of the cruise, we have devoted two chapters to describe the instrumentation used (chapter 9) and the data acquired (chapter 10). Finally, we have included a summary with the general conclusions concerning the outcomes of the survey, references, and four annexes including the diary of activities, a technical report, another report on filming done on board, and finally the main scripts made to process the seismic data.

2. Participants

2.1. Scientific and technical team

<i>Valentí Sallarès</i>	Marine Geophysicist UTM-CSIC (Barcelona)	Lead scientist vsallares@cmima.csic.es
<i>Rafael Bartolomé</i>	Marine Geophysicist UTM-CSIC (Barcelona)	OBS data processing rafael@cmima.csic.es
<i>Joao Duarte</i>	Marine Geologist U. de Lisboa (Portugal)	Navigation, acoustics, gravity joao_moedas@hotmail.com
<i>Marcel·lí Farran</i>	Marine Geologist ICM-CSIC (Barcelona)	Swath bathymetry, acoustics mfarran@icm.csic.es
<i>Francesco Frugoni</i>	Seismologist INGV (Italy)	Swath bathymetry, acoustics frugoni@ingv.it
<i>Audrey Gailler</i>	Marine Geologist UBO-IUEM	OBS data processing audrey.gailler@univ-brest.fr
<i>David Graindorge</i>	Marine Geophysicist UBO-IUEM (France)	OBS data processing David.Graindorge@univ-brest.fr
<i>Marc-André Gutscher</i>	Structural Geologist UBO-IUEM (France)	Swath bathymetry, acoustics gutscher@univ-brest.fr
<i>Boris Marcaillou</i>	Structural Geologist U. des Antilles et Guyanne (France)	Navigation, acoustics, gravity boris.marcaillou@gmail.com
<i>Sara Martínez</i>	Marine Geologist UTM-CSIC (Barcelona)	Navigation, acoustics, gravity smartinez@utm.csic.es
<i>Adrià Meléndez</i>	Marine Geophysicist UTM-CSIC (Barcelona)	OBS data processing amelendez@cmima.csic.es
<i>Gemma Muñoz</i>	Undergraduate student U. de Granada (Granada)	Navigation, acoustics, gravity yhem80@hotmail.com
<i>Ramon Ametller</i>	Mechanical technician UTM-CSIC	Lead technician, guns ametller@cmima.csic.es
<i>Manuel J. Alpiste</i>	Geologist UTM-CSIC (Barcelona)	Gun controller mjroman@ugr.es
<i>Marc Ambrós</i>	Electronic engineer UTM-CSIC (Barcelona)	UTM OBS ambros@utm.csic.es
<i>Stephen Dockter</i>	Electronic technician Scripps-SIO (USA)	UTM OBS sdockter@ucsd.edu
<i>Thomas Carson</i>	Mechanical technician Canada	Gun array
<i>Jacques Crozon</i>	Mechanical engineer Ifremer (France)	Ifremer OBS Jacques.Crozon@ifremer.fr
<i>Oscar García</i>	Computer technician UTM-CSIC (Barcelona)	System manager ogarcia@utm.csic.es
<i>Roberto González</i>	Mechanical technician UTM-CSIC (Vigo)	Gun array
<i>Igor Mazepa</i>	Mechanical technician	Gun array

	Russia	
<i>Marcus Packard</i>	Electronic technician UTM-CSIC (Barcelona)	Gun controller
<i>David Pina</i>	Electronic technician UTM-CSIC (Barcelona)	UTM OBS
<i>José Luis Pozo</i>	Electronic technician UTM-CSIC (Barcelona)	Bathymery, acoustics, gravity jlpozo@utm.csic.es
<i>Mickael Roudaut</i>	Mechanical engineer Ifremer (France)	Ifremer OBS
<i>Heike Schmidt</i>	Journalist ZDF TV Channel	Documentary film schmidt.hc@zdf.de
<i>Bertram Kropac</i>	Cameraman ZDF TV Channel	Documentary film
<i>Thomas Mailander</i>	Sound technician ZDF TV Channel	Documentary film

2.2. Participating institutions

UTM-CSIC

Unitat de Tecnologia Marina - CSIC
Centre Mediterrani d'Investigacions Marines i Ambientals
Passeig Marítim de la Barceloneta, 37-49
08003 Barcelona (Spain)



UBO-IUEM

Universite de Bretagne Occidentale
Institut Universitaire Europeen de la Mer
UMR 6538 Domaines oceaniques
Place N. Copernic
29280 Plouzané (France)



IFREMER

Institut français de recherche pour l'exploitation de la mer
Place N. Copernic
29280 Plouzané (France)



INETI

Instituto Nacional de Engenharia, Tecnologia e Inovação
Estrada da Portela, Zambujal
2721-866 Alfragide (Portugal)



Universidade de Lisboa

Fundacao da Faculdade de Ciencias da Univ. de Lisboa
Centro de Geofisica da Universidade de Lisboa
Campo Grande, Ed. C8, piso 6
1749-016 Lisboa (Portugal)



ICM-CSIC

Institut de Ciències del Mar - CSIC
Centre Mediterrani d'Investigacions Marines i Ambientals
Departament de Geologia Marina
Passeig Marítim de la Barceloneta, 37-49
08003 Barcelona (Spain)



Universidad de Granada

Instituto Andaluz de Geofísica
Campus Universitario de Cartuja s/n
18071 Granada (Spain)



Université des Antilles et de la Guyanne

Dept. des Sciences de la Terre et de l'Univers
Géologie des domaines océaniques
Fouillole BP 250
97157 Pointe-à-Pitre cédex (France)



INGV

Istituto Nazionale Geofisica e Vulcanologia
Roma 2 section – Marine Unit RIDGE
via di Vigna Murata, 605
00143 Roma (Italy)



ICTJA-CSIC

Institute of Earth Sciences Jaume Almera- CSIC
Lluís Solé i Sabarís, s/n
08028 Barcelona (Spain)



SIO

Scripps Institution of Oceanography
UC San Diego
9500 Gilman Drive
La Jolla, CA 92093 (USA)



ZDF

Zweites Deutsches Fernsehen
SZ 2 Raum 3109
55100 Mainz (Germany)





Figure 2.- Picture of the scientific and technical team that participated in the NEAREST-SEIS cruise.

3. The Vessel (BIO Hespérides)

Research vessel (R/V) Hesperides, a vessel belonging to the Spanish Navy, is based upon the Port of Cartagena (Spain), where it was built and launched on March 12, 1990. The research that is carried out on this vessel is directed and funded mainly by the National R+D+I Plan. Since it is a Great Facility, the Ministry of Science and Technology, through the Committee for the Coordination and Follow-up of Oceanographic Vessels' Activities, undertake the responsibility for the scientific management of the vessel. UTM is accountable for the maintenance of the scientific equipment of the vessel and provides the necessary supporting technical staff for oceanographic expeditions.

Over its existence (over ten years now), R/V Hesperides has carried out many research expeditions, travelled over 300,000 nautical miles and welcome over a thousand researchers and Spanish and foreign technicians.

Characteristics:

<i>Length</i>	82,5 m
<i>Arm</i>	14,30 m
<i>Draw</i>	4,42 m
<i>Weight</i>	2.665,6 Tm
<i>Speed</i>	14,7 nudos (5,0 nudos entre hielo de 40 cm)
<i>Authonomy</i>	12.000 millas nauticas (a 12 nudos)
<i>Engines</i>	2 x electric 1400 kW at 220 rpm Four Diesel groups (2 a 1300 kW and 2 a 750 kW) One emergency Diesel
<i>Crew</i>	58
<i>Scientists</i>	29
<i>Navigation</i>	2 x radars ARPA ECDIS.
<i>Positioning</i>	2 x DGPS
<i>Communication</i>	GMDSS / Fleet 77

Equipment:

<i>Acoustics</i>	EA 600 Echosounder Simrad EM1002S (Shallow water multibeam) Simrad EM 120 (Deep water multibeam) Topas sub-bottom sediment profiler
<i>Seismics</i>	Bolt and Sleeve guns array (max 8 positions) 4 Hamworthy 4TH 190 W 70 compressors

Navigation: KonMAP HYDAQ Mk4,
Gun controller: model LRS-100
17 OBS LC2000 model (Scripps - SIO)
Gravimeter BGM-3 model

Gravimeter



Figure 3. The BIO Hesperides at port in Cartagena.



Figure 4.- The BIO Hesperides sailing in the Gulf of Cadiz during the NEAREST-SEIS survey.

4. Geological setting of the Gulf of Cadiz

4.1. Generalities of the SW Iberian Margin

The study area for the NEAREST-SEIS survey is located off the SW Iberian margin along the plate boundary between the African and Eurasian plates. The region is characterized by moderate to strong earthquakes (1964 Huelva earthquake M6.5; 1969 Cape St. Vincent earthquake M7.9, and 2007 Horseshoe earthquake M6.1), with mostly compressional and strike-slip focal mechanisms (Stich et al., 2003; 2006) (Figure 5 left). Plate kinematic models and GPS observations are in good agreement that NW Africa (Nubia) is moving in a NW to WNW direction with respect to Iberia at a velocity of approximately 4mm/yr (Argus et al., 1989; DeMets et al., 1994, McClusky et al., 2003, Nocquet and Calais, 2004).

The region is also characterized by strong historical seismicity, best expressed by the catastrophic Great Lisbon earthquake of 1 November 1755. This event with an estimated magnitude 8.7, and its associated tsunami (Abe, 1989), struck Portugal, destroying the city of Lisbon, and cities along the Algarve coast, and the coasts of SW Spain (Cadiz, Huelva) and NW Morocco, causing an estimated 60,000 deaths (Martinez-Solares et al., 1979; Johnston, 1996; Baptista et al., 1998a). This earthquake is the greatest recorded in European history and was felt as far away as Hamburg and the Azores (Figure 5 right). However, the complex regional tectonics and the diffuse nature of the plate boundary, makes it difficult to identify the principal faults which store and release the greatest seismic moment over the long term. Therefore, the source region of the 1755 earthquake remains a subject of lively debate, and numerous candidate fault zones have been proposed by different authors (Figure 5 left).

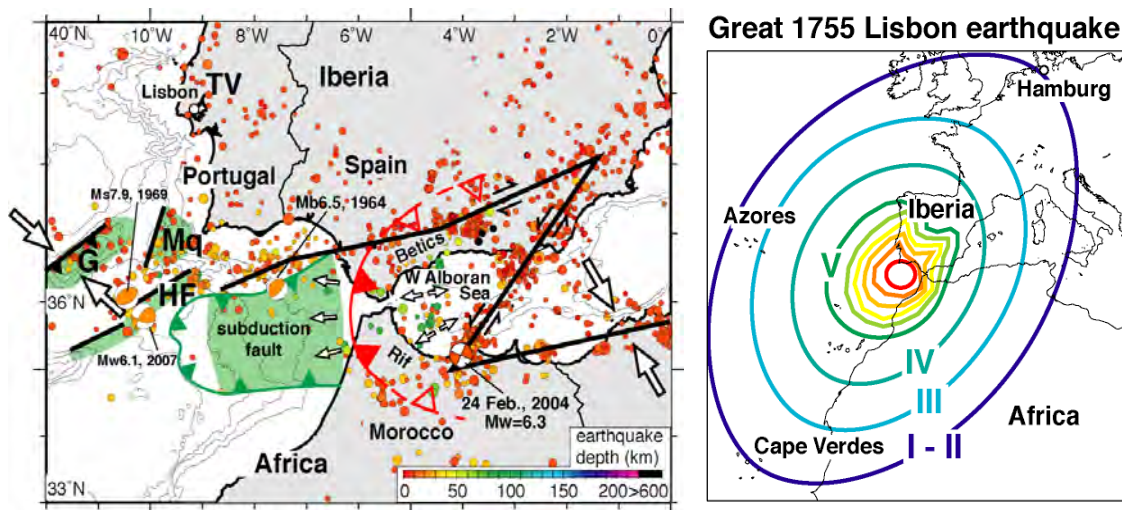


Figure 5.- (left) Location map of the study area, with major faults, earthquake hypocenters and proposed source regions for the 1755 earthquake (shaded green) (after Gutscher, 2004) Mq = Marques de Pombal fault, G = Gorringe Bank, HF = Horseshoe Fault. Focal mechanisms of M>6 earthquakes since 1960 are also shown (Stich et al., 2006; 2007) (right). Isoseismals of the great Lisbon earthquake of 1755 (Johnston, 1996).

Tortella et al. (1997) subdivided the SW Iberian Margin into two main morphotectonic domains: (a) the region between the Goringe Bank and Cape San Vicente to the west, and (b) the Gulf of Cadiz, between the Cape San Vicente and the Straits of Gibraltar to the east (Figure 6). The first area is characterized by a complex and irregular topography, dominated by large seamounts, deep abyssal plains, and massive rises (e.g. Bergeron and Bonnin, 1991; Gràcia et al., 2003a, Terrinha et al., 2003; Zitellini et al., 2004) (Figure 6), such as the Goringe Bank. The oceanic convergence occurring in this area results in a continental collision as the plate boundary crosses towards the Straits of Gibraltar (Grimison and Chen, 1986), although the location of the ocean-continent boundary is still a matter of debate (i.e. Hayward et al., 1999). The second area, the Gulf of Cadiz, is underlain by Hercynian continental crust (González et al., 1998) and is characterized by a smoother topography and by a prominent NE-SW trending positive free-air gravity anomaly (Roberts, 1970; Dañobeitia et al., 1999; Gràcia et al., 2003b). The whole region has experienced a complex history since the Mesozoic in response to the changes in motion and location of the EUR-AFR plate boundary, jumping across the Iberian Peninsula (Srivastava et al., 1990).

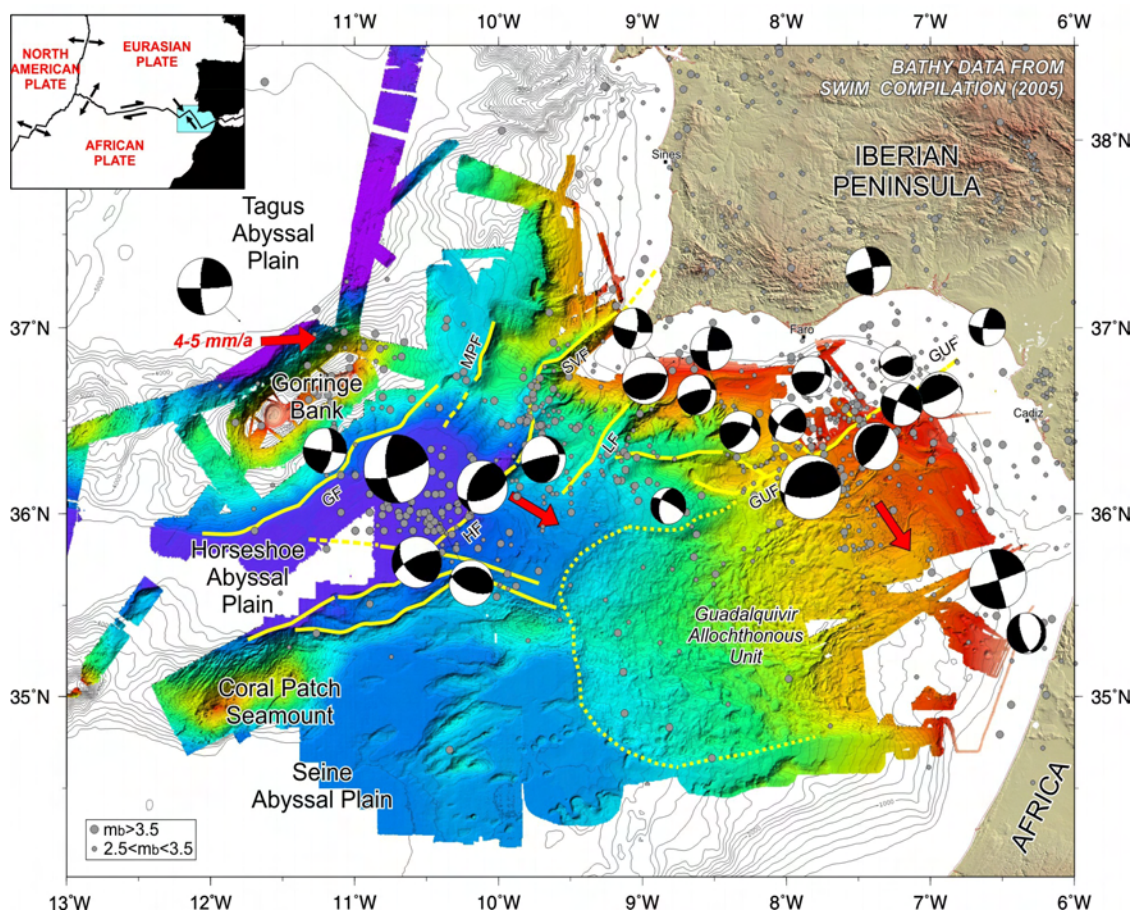


Figure 6.- Inset: Plate tectonic setting of the SW Iberian Margin along the boundary between the Eurasian and African Plates. Detailed swath-bathymetric map of the Gulf of Cadiz from the EuroMargins SWIM compilation (Zitellini et al., in press). Seismicity from the "Instituto Geográfico Nacional" catalog for the period between 1965 and 2000 is depicted (I.G.N., 1999). Small grey dots are epicentres of earthquakes for $2.5 < mb < 3.5$, and large grey dots for earthquakes of $mb > 3.5$. Fault plane solutions are

from Stich et al. (2005). Red arrows show the direction of plate convergence from NUVEL1 model (Argus et al., 1989). Physiographic domains of Gulf of Cadiz and main active faults (thick yellow lines) are located. GF: Gorringer Fault; MPF: Marques de Pombal Fault; HF: Horseshoe Fault; SVF: Sao Vicente Canyon Fault; LF: Lagos Fault; GUF: Guadalquivir Fault.

The structure of the Gulf of Cadiz is a product of the interaction of the southern end of the Iberian rifted margin, the displacement of the Gibraltar Arc, and the convergence of the African and Eurasian Plates (Banda et al., 1995). The original pattern of the Mesozoic Iberian rifted margin was partly obliterated during the successive deformation phases in the region (e.g. Olivet, 1996). The Gibraltar Arc integrates the Betic and Rif mountain belts of Alpine Orogeny, characterized by north, south and west vergent low-angle thrust systems with a radial tectonic transport (Sanz de Galdeano, 1990). The offshore extension of the Western Betics, comprising the Guadalquivir Basin, the Betic External zones and the Campo de Gibraltar Flysch was first identified in the Gulf of Cadiz by Lajat et al. (1975). As a result of the Neogene convergence between the African and Eurasian Plates, a number of allochthonous units were emplaced, and these have been identified from the Gulf of Cadiz to the Horseshoe Abyssal Plain (Bonnin et al., 1975; Torelli et al., 1994; Flinch et al., 1996; Maldonado et al., 1999; Gràcia et al., 2003b; Medialdea et al., 2004; Iribarren et al., 2007) (Figure 6).

4.2. Potential sources of large earthquakes

Several surface ruptures slightly oblique to the N-S trending Mesozoic Iberian Margin (Malod and Mauffret, 1990; Alves et al., 2003), which correspond to NE-W oriented active folds and thrusts, have been recognized within the Gulf of Cadiz area (e.g. Marques de Pombal, Sao Vicente and Horseshoe Faults, e.g. Zitellini et al., 2001; Gràcia et al., 2003a, 2003b, Terrinha et al., 2003; Vizcaino et al., 2004) (Fig. 3). Anticline folding began during the middle-late Miocene, together with the emplacement of the large allochthonous bodies of the Gibraltar Arc (Torelli et al., 1997; Maldonado et al., 1999; Gràcia et al., 2003b; Somoza et al., 2003; Medialdea et al., 2004). The recognition of deformed Quaternary units together with the shallow seismicity swarm associated with the ruptures (e.g. Gràcia et al., 2003a; Buforn et al., 2004; Stich et al., 2005) suggests that the thrusts located beneath these ruptures are active and that they could increase the seismic hazard of SW Iberia.

In this context, four main candidates have emerged for the most likely source of the 1755 earthquake; the Marques de Pombal fault (Zitellini et al., 2001; 2004; Gracia et al., 2003a), Gorringer Bank (Johnston, 1996), the Horseshoe fault (Stich et al., 2007) and an east-dipping subduction fault plane, suggested to be related to the Cadiz accretionary wedge (Gutscher et al., 2002; Gutscher, 2004; Thiebot and Gutscher, 2006; Gutscher et al., 2006). Empirical fault length - earthquake magnitude scaling laws (Wells and Coppersmith, 1994) require at least a 200 km long fault to generate such a strong earthquake. Gorringer, an extended Horseshoe fault and the subduction fault plane can satisfy this condition. The Marques de Pombal fault alone is too small. Thus combinations of sources have also been proposed (Zitellini et al., 2004; Stich et al., 2007), such as, for example, the Marques de Pombal and Horseshoe Faults (Gràcia

et al., 2003a; Zitellini et al., 2004), the Marques de Pombal and Pereira da Souza Faults (Terrinha et al., 2003), an active subduction zone of the Gulf of Cadiz (Gutscher et al., 2002; Gutscher, 2004) (Figure 2), or the combination of a submarine fault with the Lower Tejo Fault (Vilanova et al., 2003). While each of these source faults can explain some of the historical tsunami observations, tsunami modeling has shown that no single source is able to successfully explain all of the arrival times and amplitudes (Baptista et al., 1998a; 1998b; 2003; Gutscher et al., 2006) This is the reason to concentrate on the faults that caused earthquakes ($M_w < 6$) in the Gulf of Cádiz during the instrumental period, such as the 1969 earthquake ($M_w 8$) in the Horseshoe Plain. A detailed study of these faults could provide key interpretations and constraints to be used in the determination of the source of the 1755 Lisbon earthquake.

4.3. Long-term geodynamic evolution of the NW Iberian margin

The NW Iberian margin is also marked by the continental margins of SW Iberia and NW Africa and by other structures, which deform the underlying basement. The NW African margin developed during Triassic-Jurassic times as the Central Atlantic formed by the rifting of Africa from North America. The NW Moroccan margin was situated at the southern end of the modern day Grand Banks of Newfoundland and formed by sub-normal extension along a N60 trending fault and by transcurrent motion along the Southern Grand Banks fault (today oriented N120) (Stampfli et al., 2003; Sahabi et al., 2004) (Figure 7). The NEAREST study area is thus at the modern day juncture between the NW corner of the continental domain of the African plate and the SW corner of the Iberian continental domain.

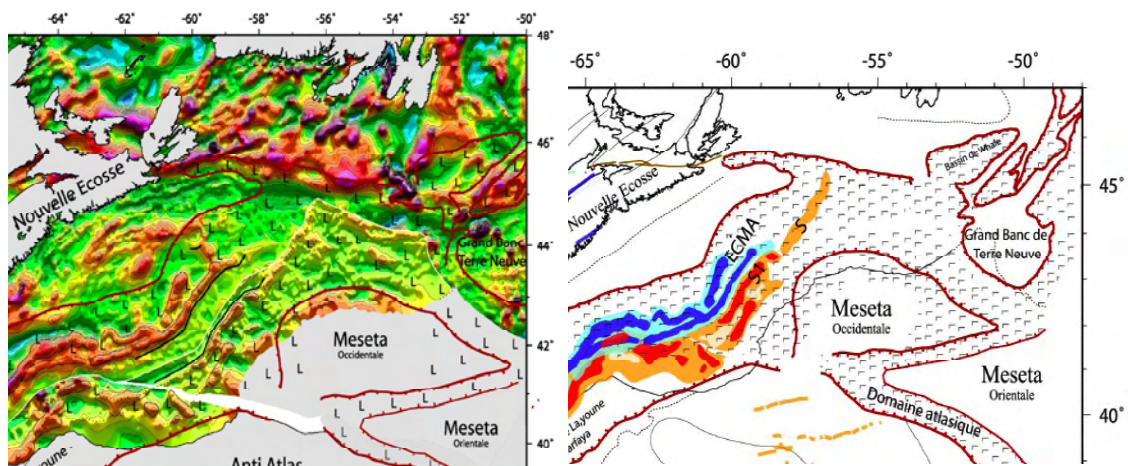


Figure 7.- Magnetic anomaly map of NW Africa and NE North America in their reconstructed position at the time of Jurassic rifting around 200 Ma (Sahabi et al., 2004, Verhoef et al., 1991). Note there is a “western” African margin and a “northern” African margin whose trace exists today in the SW Gulf of Cadiz

The SW Iberia margin was first structured by this transcurrent motion, and later by minor amounts of seafloor spreading (possibly SE-NW) which opened a narrow oceanic corridor between southern Iberia and Africa. Further east this oceanic domain widens to become the Tethys separating Gondwana from Eurasia (Figure 8).

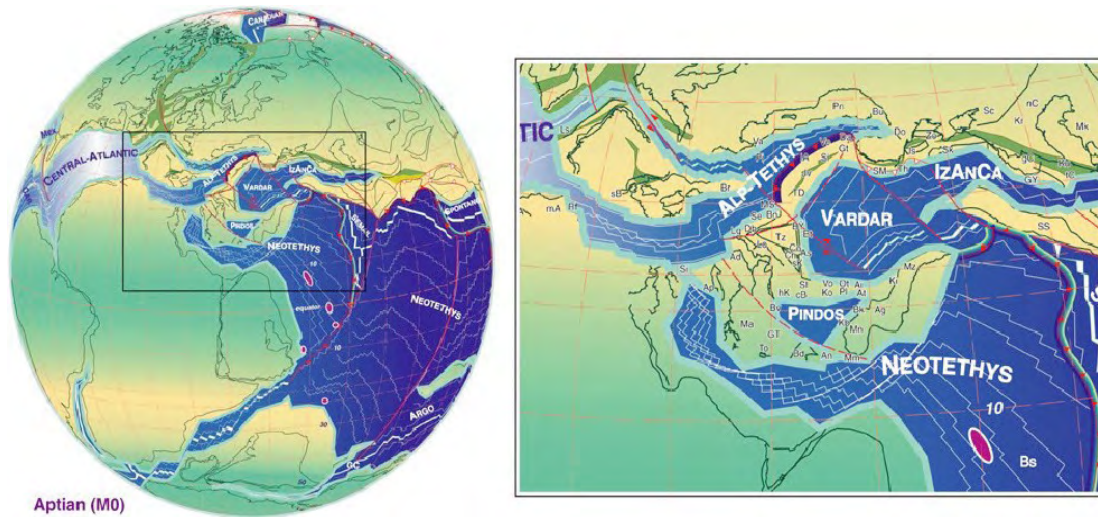


Figure 8.- Paleogeographic reconstruction of the Central Atlantic and Tethyan domains around anomaly M0 (Stampfli et al., 2002)

More recently, the Atlantic basement off NW Africa and Iberia has been deformed by the current 4 mm/yr NW-SE convergence between the Africa (Nubia) and Iberia (Eurasia) plates, to form a series of E-S to NE-SW trending compressive ridges such as the Goringe bank or the Coreal Patch Seamount (Figure 6). Along the SW Iberia margin these basement highs are the site of moderate seismicity (Figure 6) (Gracia et al., 2003a, Zitellini et al., 2004).

5. Cruise plan

5.1. The case for a Wide-Angle Seismic Experiment

The exact nature of the crust in the deep oceanic domains offshore SW Iberia (Tagus Abyssal Plain, Horseshoe Abyssal Plain, Seine Abyssal Plain) is unknown and difficult to determine for two reasons: 1) There are few recognizable magnetic anomaly patterns (Figure 7), and 2) the seafloor is covered by a roughly 2-3 km thick layer of Mesozoic to recent sediments (see section 4.1.- Generalities of the NW Iberian margin). Thus basement samples are not easy to obtain. The only deep sea drilling in the region which penetrated to basement were; DSDP site 120 on Goringe Bank, where serpentinized mantle has also been recovered directly at the seafloor during deep-sea submersible expeditions and off the western Moroccan margin (at the foot of the Mazagan plateau - near present day El Jadida) at ODP site 546 during Leg XX drilling (Hinz et al., 1982). DSDP hole 135 penetrated Jurassic sediments but did not reach basement.

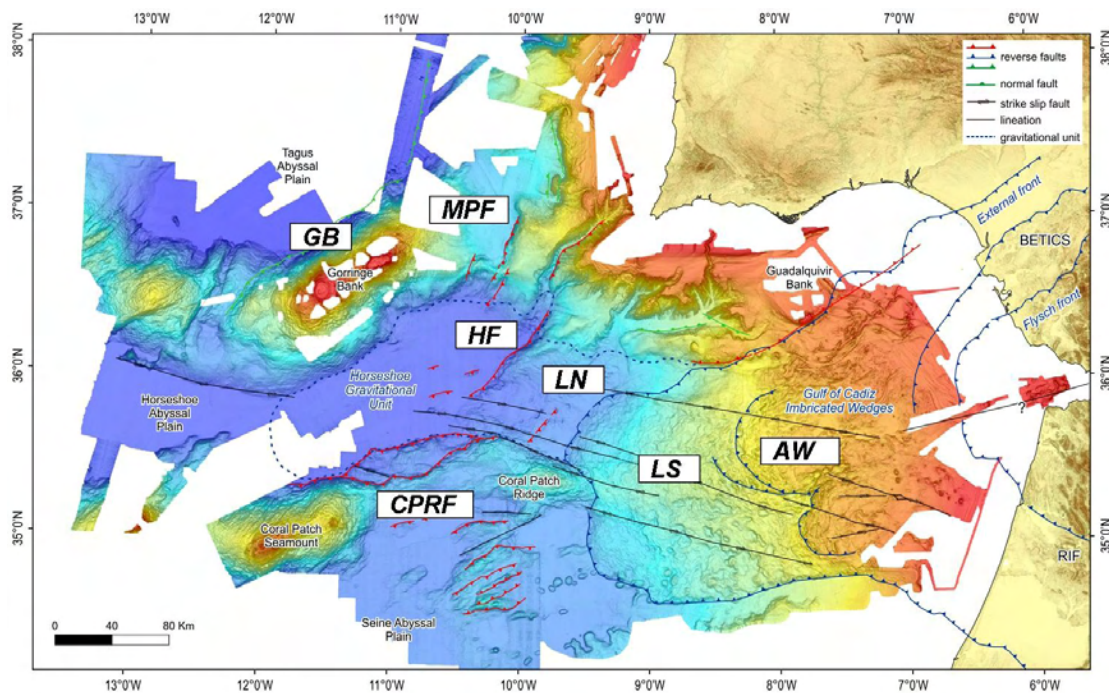


Figure 9.- Tectonic map of the Gulf of Cadiz. See legend for further explanation. AW: Accretionary Wedge; HF: Horseshoe fault; CPRF: Coral patch ridge fault; MPF: Marques de Pombal fault; GB: Goringe bank; LN/LS: North and South WNW-ESE lineations

Because of the lack of basement samples, current knowledge of the crustal domains in the NEAREST study area is based almost exclusively on seismic data and digital terrain models (multibeam bathymetry, backscatter). The recent work of compilation made in the framework of the Nearest project, summarized in the form of a new tectonic map (Figure 9), has helped to update all the information relative to the main tectonic structures of the area and to shed some light into its history, functioning, and relative significance (Terrinha et al., 2008). Multichannel seismic (MCS) reflection data used in this work have been acquired during successive National and EU funded projects (Figure 10) (e.g.

Sartori et al, 1994; Banda et al., 1995; Mendes-Victor et al., 1998) with the aim to characterize the shallow structure, and to identify active tectonic sources in the region (e.g. Dañoibeitia et al., 1999; Gutscher et al., 2002; Gràcia et al., 2003a,b; Maldonado et al., 1999; Medialdea et al., 2004; Terrinha et al., 2003, Zitellini et al., 2001, 2004). As can be seen in figure 10, the MCS data set almost completely covers the region of interest. With the exception of Rovere et al. (2004) and Thiebot and Gutscher (2006), however, MCS profiles have been processed using standard seismic techniques. This means that most of the available MCS profiles have not been depth-migrated, so they do not provide realistic information on the depth and geometry of tectonic structures.

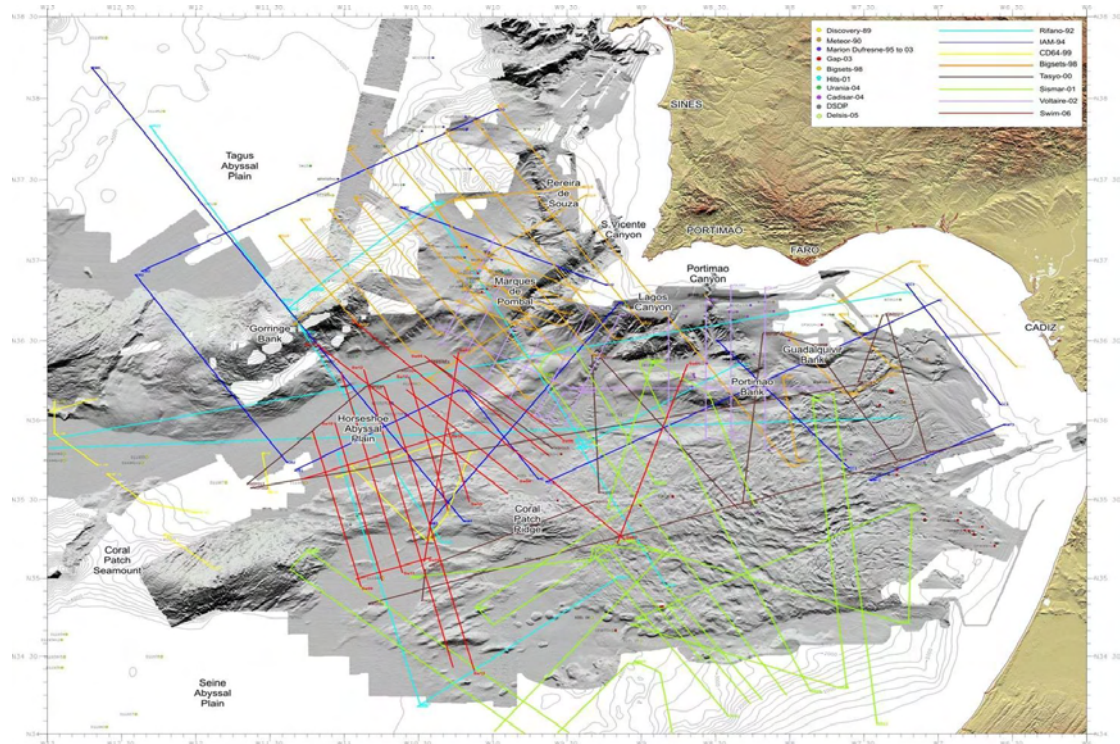


Figure 10.- Compilation of all the scientific MCS data acquired in the Gulf of Cadiz during successive cruises since 1992. See legend for cruise identification. Background shaded relief map in grey corresponds to the EuroMargins SWIM bathymetric compilation map (Zitellini et al., in press).

One of the key goals of WP2 within NEAREST project, was thus to provide accurate images of the tectonic structure as MCS depth sections across the most significant tectonic features, rather than time sections as seismic images are usually interpreted. The purpose was two-fold: on one hand, provide in-depth information about the functioning of the main structures identified in the recent tectonic compilation (Terrinha et al., 2008). On the other hand, provide complementary information to design the best possible location for the OBS-wide-angle seismic profiles to be shot during the NEAREST-SEIS survey based on the general objectives stated in section 1. A total of 10 long MCS profiles crossing the most relevant tectonic structures, were compiled, reprocessed and presented in NEAREST Deliverable D4: Depth-migrated multichannel seismic profiles (Sallarès et al., 2008).

Recent related work performed within the NEAREST project in the area includes an 11 month long deployment of a network of 24 Broad-Band Ocean

Bottom Seismometers (OBS-BB). The objectives were to observe local seismicity and micro-seismicity in order to identify seismically active faults offshore and help select the optimum location for a future seafloor observatory as part of a tsunami warning system. In order to relocate the earthquakes recorded by this OBS-BB network (Figure 11), as well as to precisely locate future earthquakes that may occur here, a good 3-D seismic velocity model of the region is required. One of the main objectives of the current OBS survey is to obtain the necessary regional seismic velocity information to construct such a model.

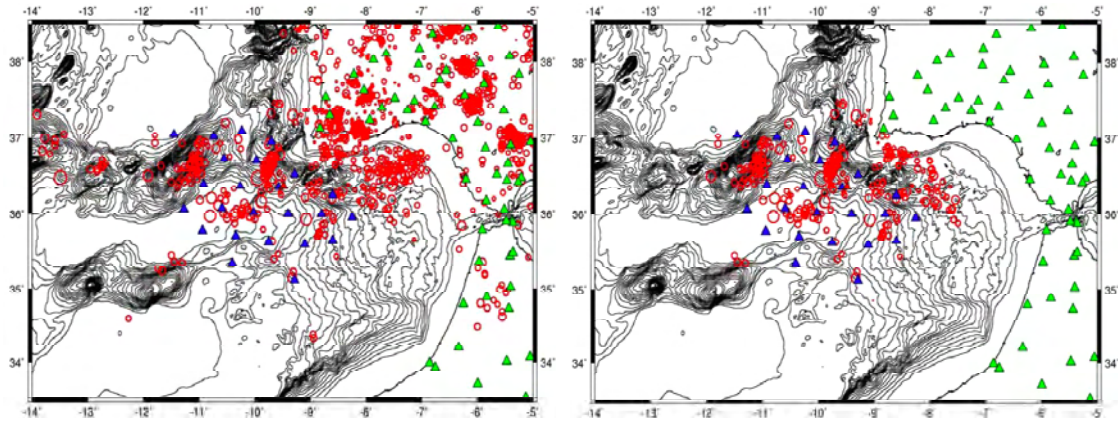


Figure 11.- Map of OBS broad-band network deployed by AWI (blue triangles) from Aug 2007 - July 2008, (left) with all earthquakes (red circles) recorded by landstations (green triangles) during this period. (right) Same map showing the 276 known earthquakes located within 75 km of the network.

Based on the active tectonic map shown in figure 9, three major types of faults can be observed; N60-70°E trending thrust faults, which commonly bound the uplifted basement ridges described above, N110-N120°E trending lineaments interpreted as dextral strike-slip faults, and the horseshoe shaped deformation front of the accretionary wedge. This information, together with the analysis of the data quality and structures observed on the reprocessed MCS profiles (Sallarès et al., 2008), was used to select the most appropriate transects to accomplish the objectives listed in section 1.

5.2. Wide-Angle seismic transects

These Wide Angle seismic profiles selected and shot during the NEAREST-SEIS (OBS) cruise are shown in figure 12. Together, these two profiles cut across most of the major structures identified in figure 9. One of the primary objectives of the OBS survey was to obtain information on the crustal nature and overall geometry (thickness, dip, etc.) across these major structures and tectonic boundaries.

- P1 extends from the Tagus Abyssal Plain, over Gorrington Bank, across the Horseshoe Abyssal Plain and the Horseshoe fault, up onto Coral Patch Ridge and finally to the small fold and thrust belt in the Seine Abyssal Plain beyond the NW Moroccan continental margin. It roughly coincides in its southern half with one of the PSDM MCS profiles included in D4 (SWIM-13, Figure 13), and in the northern half with IAM4.

- P2 crosses from the Easternmost Seine Abyssal Plain (just beyond the NW Moroccan margin) crosses the accretionary wedge and several of the “SWIM” lineaments (including the buried prolongation of Coral Patch Ridge), then the Guadalquivir Ridge/Portimao Bank structure, the Portimao Canyon and all the way up onto the S. Portuguese continental shelf. It coincides in its northern half with another of the PSDM lines (SWIM-01, Figure 14) and in the southern half with SISMAR-23.

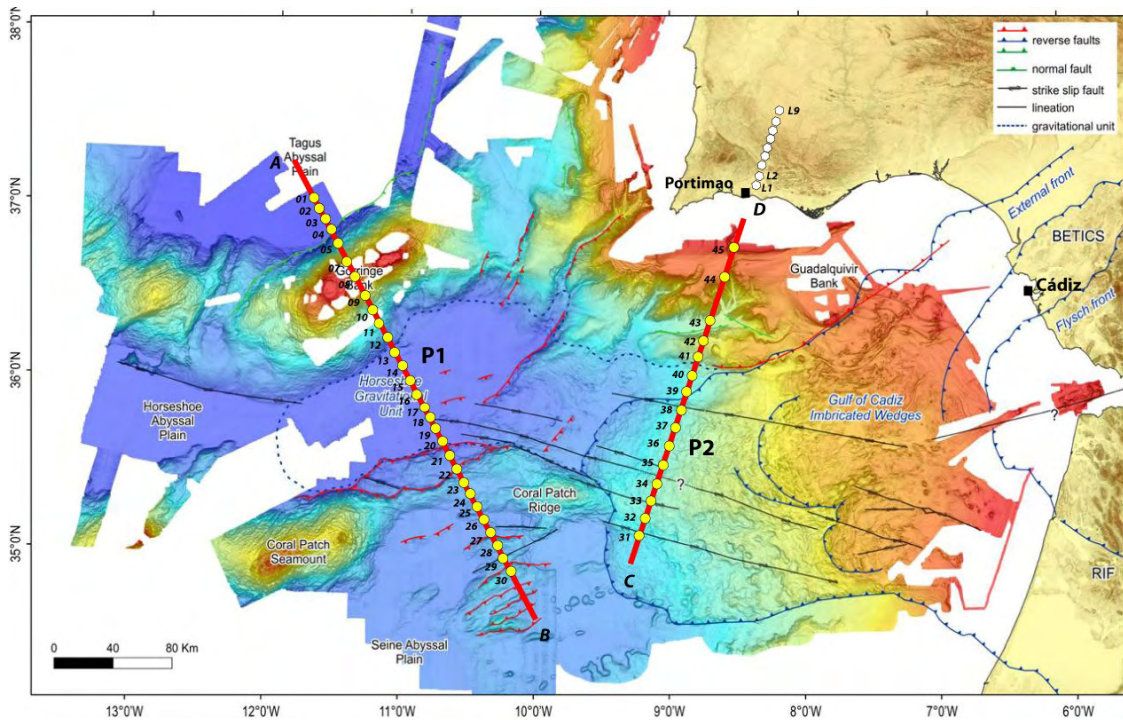


Figure 12.- Bathymetric map of the study area (data from SWIM compilation) with the cruise plan. Red lines show the Wide-Angle seismic profiles that were shot (P1 and P2). Yellow dots labelled 01 to 45 indicate the OBS location along both profiles. White hexagons labelled L1 to L9 show landstations deployed during shooting along P2.

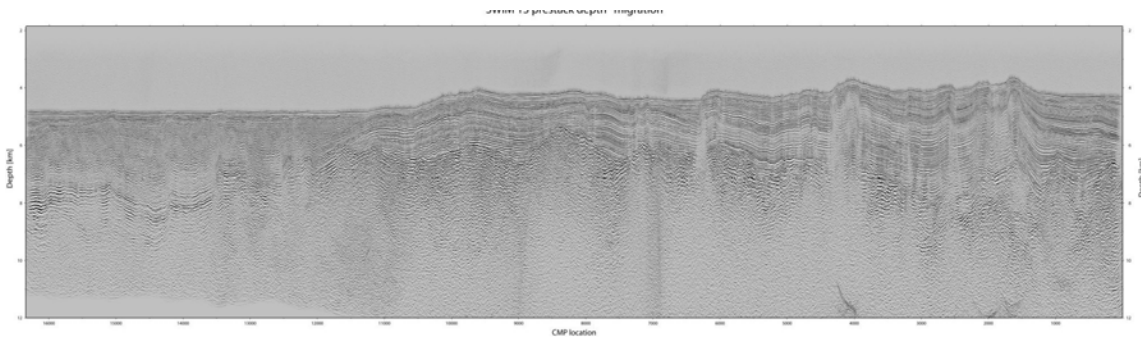


Figure 13.- Pre-stack depth migrated section of multichannel seismic profile SW-13 (SWIM-06 cruise, PI E. Gràcia), unpublished data.

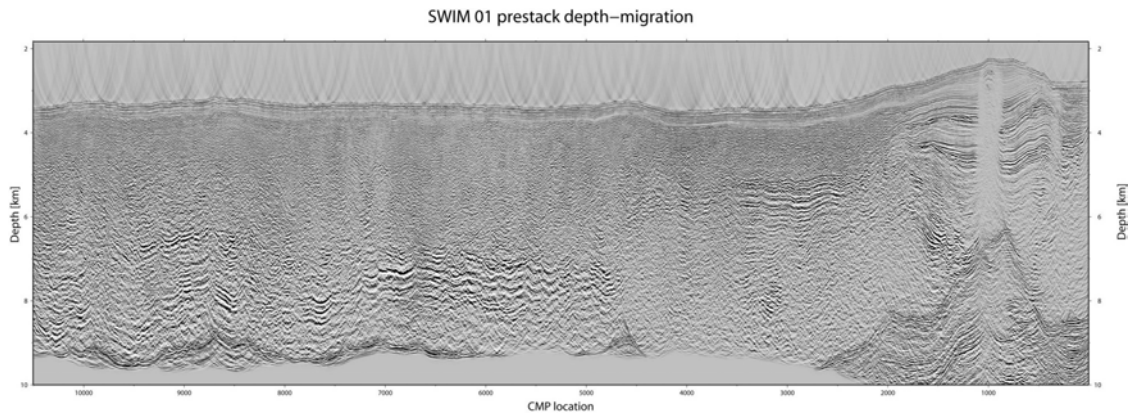


Figure 14.- Pre-stack depth migrated section of multichannel seismic profile SW-01 (SWIM-06 cruise, PI E. Gràcia), unpublished data.

The overall strategy of the survey consisted on (1) heading from Cartagena to the westernmost point (A in Figure 12), (2) deploying a total of 30 OBS (finally 29) along profile P1, (3) deploying the airgun array and shooting P1 from B to A, (4) recovering the OBS along P1, (5) heading to point C and deploying 24 OBS (finally 15) along profile P2, (6) shooting P2 from D to C, (7) recovering the OBS along P2, and (8) going back to Cadiz and finish the survey. Along with the acquisition of the seismic data (the main objective of the cruise), swath bathymetry, 3.5 KHz sediment profiler, and gravity data were also collected along the profiles and during transits. The shooting along profile P2 was also recorded onshore by a landstation array (Figure 12).

6. Swath bathymetry and acoustic backscatter

6.1. Technical description

The swath bathymetry system used in the NEAREST-SEIS survey is the Simrad model EM120. The system is designed to perform seabed mapping to full ocean depth with a high resolution, coverage and accuracy and follows the IHO S44 normative for bathymetric surveying. It operates between 20 to 11000 metres, with a vertical resolution of 10 to 40 cm. The nominal sonar frequency is 12 kHz with an angular coverage sector of up to 150 degrees and 191 beams per ping of $1^\circ \times 2^\circ$. The length of the pulse is 2, 5, 15 ms, with a sampling frequency of 2 KHz. It includes information from attitude sensor Seapath 200 / MRU 5 and Hydaq navigation system (Figure 15). Achievable swath width on a flat bottom is approximately six times the water depth. The angular coverage sector and beam pointing angles may be set to vary automatically with depth according to achievable coverage. This maximizes the number of usable beams. The beam spacing is normally equidistant with equiangle available. The system is reliable, and easily operated on workstations with familiar operating systems.

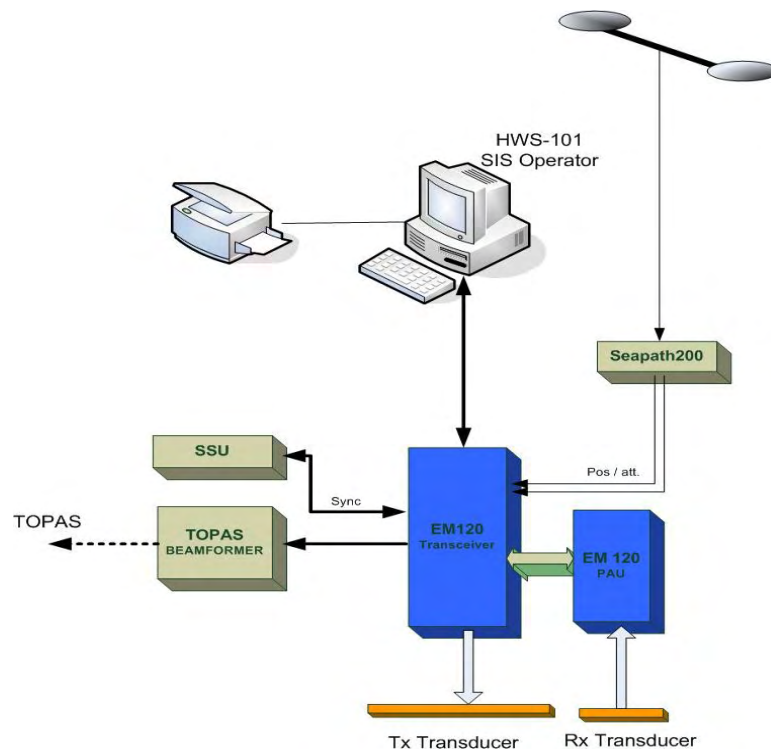


Figure 15.- Functioning diagram of the Simrad EM120 system.

The transmit fan is split in several individual sectors with independent active steering according to vessel roll, pitch and yaw. The sectors are frequency coded (11.25 to 12.60 kHz), and they are all transmitted sequentially at each ping. The sector steering is fully taken into account when the position and depth of each sounding is calculated, as is the refraction due to the sound speed profile, vessel attitude and installation angles. Pulse length and range sampling rate are variable with depth for best resolution. The ping rate is mainly limited by the round trip travel time in the water up to a ping rate of 5 Hz.

The transducers are linear arrays in a Mills cross configuration with separate

units for transmit and receive. The arrays are divided into modules. The number used (and hence the beamwidth) may be adjusted according to particular installation requirements ($1^\circ \times 2^\circ$ in the case of NEAREST-SEIS), resulting in an array length are between 2 and 8 m. A combination of phase and amplitude detection is used, resulting in instrument measurement accuracy practically independent of beam pointing angle.

From the EM120 system we recorded swath bathymetric and acoustic backscatter data. The swath-bathymetric and acoustic backscatter data have been processed onboard using the NEPTUNE system, a submarine mapping software developed by SIMRAD to process data from multibeam echosounders. During all the cruise a Simrad Synchronization unit was used to synchronize Hydrographic echo sounder, Multibeam echo sounder and Topas in order to avoid interferences between them.

6.2. Bathymetry data

Using the EM120 multibeam echosounder, we mapped at high-resolution an area limited between $36^\circ 37'N$ and $34^\circ 30'N$ latitude, and $11^\circ 15'W$ and $06^\circ 30'W$ longitude and the transit from Cartagena to the strait of Gibraltar. Multibeam data were continuously acquired, although most of it was on areas already mapped in other surveys (Zitellini et al., in press). New data was obtained on the top of Gorringe Bank, filling part of preexisting bathymetric gaps. The quality and resolution of the acquired data is variable since the data were acquired at 3.5 knots during shooting, 8 to 10 knots during deployment of the OBS's and around 13 knots on transits.

During the transit from Cartagena to the study area and back to Cadiz, new swath-bathymetry data was also acquired in alboran Sea and the northern part of the Gulf of Cadiz to fill some bathymetric gaps in the EuroMargins SWIM compilation (Figure 16).

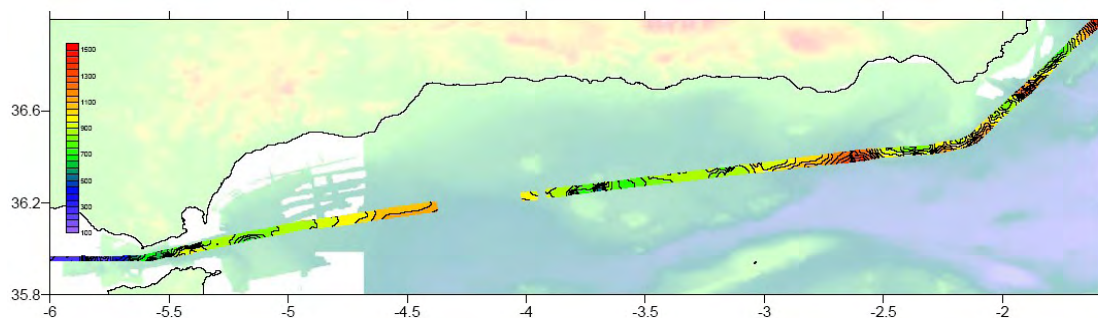


Figure 16.- Swath bathymetry acquired during the transit in the Alboran sea.

The main steps during data pre-processing included at first import of the raw data, search of possible errors due to the variations in water column sound velocity profiles and motions of the vessel (roll, pitch, yaw and heave), and elimination of the noisy external beams. Once these corrections were made, data was filtered and cleaned up using different methods, most specially raw data automatic cleaning by comparison with a reference DTM using a band-pass filter. A last manual cleaning with the ping graphical editor allowed us to get more accuracy on the depth data control. After filtering, bathymetric data

was interpolated at nodes of regular-spacing grid of 90 meters in order to get a final DTM.

The raw file numbers of the multibeam profiles acquired are the following ones:

Fist file name: 0000_20081027_210231_Hesperides

Transit Cartagena-Tarifa: file numbers 0000 to 0018

TransitTarifa to P1: file numbers 0018 to 0042

Line P1: file numbers 0046-0145

Transit P1 to P2: file numbers 0146-0158

Line P2 file numbers: 0159-0211

Guadalquivir lines and mosaic: file numbers over 0211

The resulting maps obtain along profiles P1 and P2 are shown in Figure 17, and the complete set of data acquired during the full survey is shown in Figure 18.

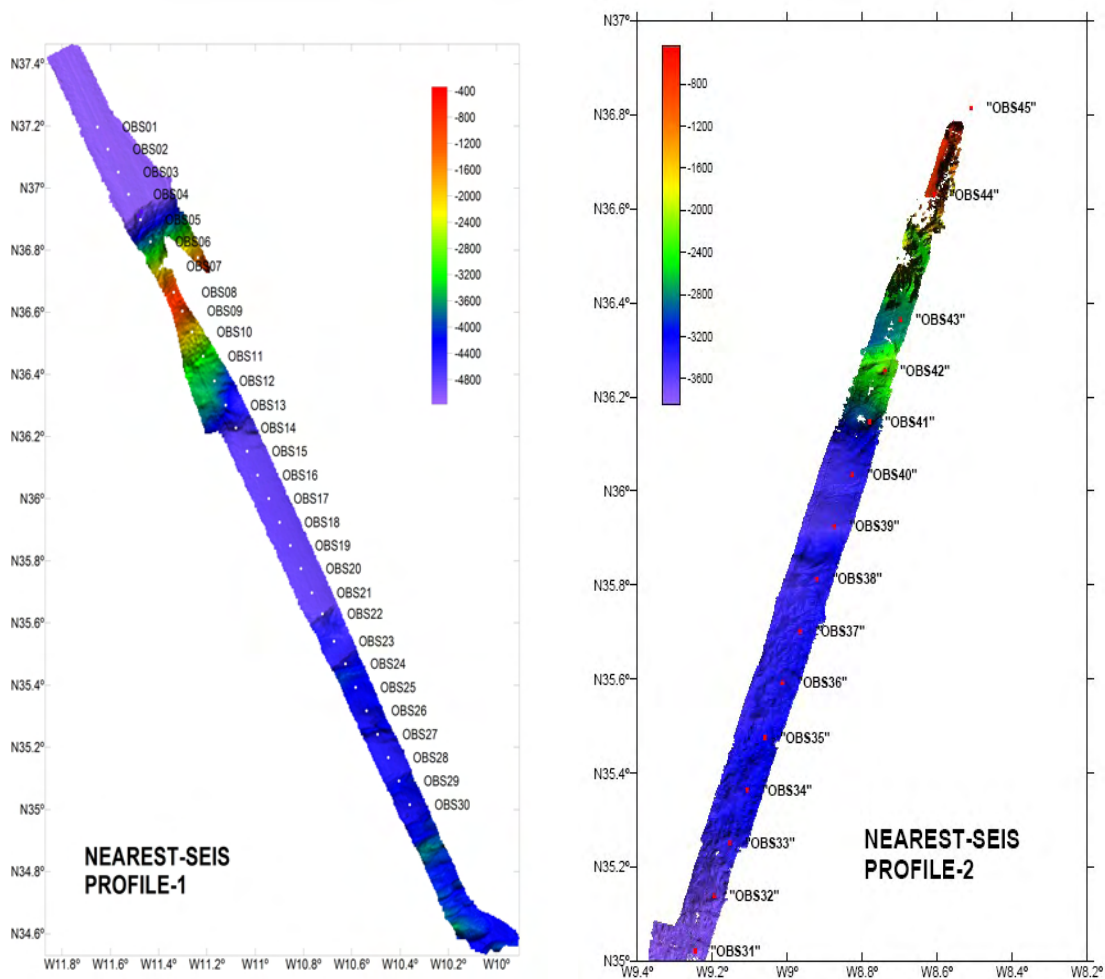


Figure 17.- Coloured relief map of line P1 with OBS locations along profiles P1 (left) and P2 (right) (Illumination from NW corner).

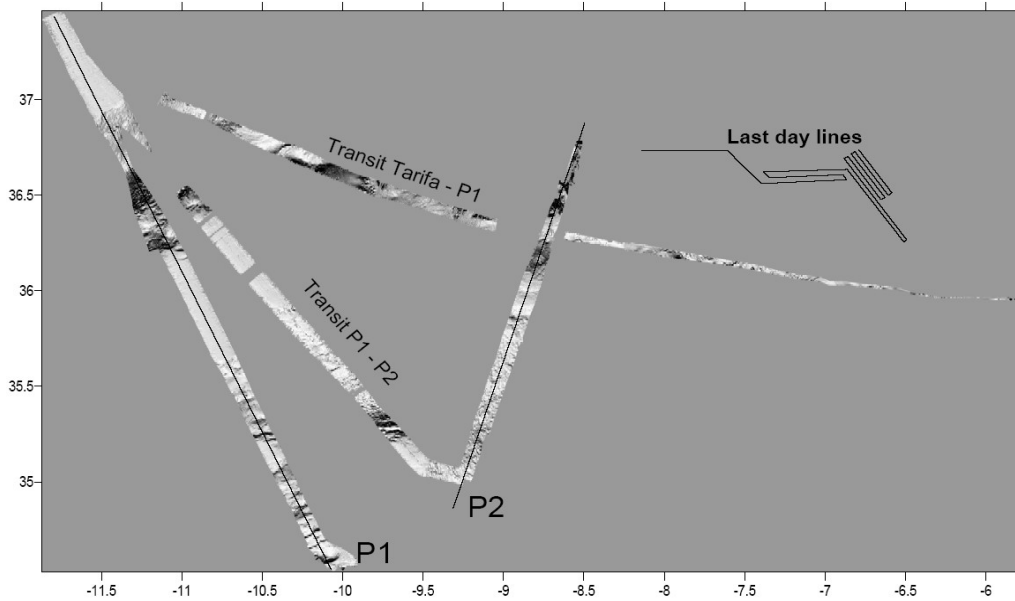


Figure 18.- Shaded relief map (at 90 m grid) acquired during the Nearest-Seis cruise. Illumination from NW corner.

6.3. Acoustic backscatter

Acoustic backscatter data was extracted from the EM120 multibeam echosounder from all navigation lines. Most of it corresponds to an area where backscatter data had not been previously acquired. A backscatter map of the lines is presented in Figure 19. Image mosaic from backscattered acoustic energy of Simrad EM-120 multibeam sounder was also generated and operations of filtering and interpolation were performed in order to get the final backscatter image.

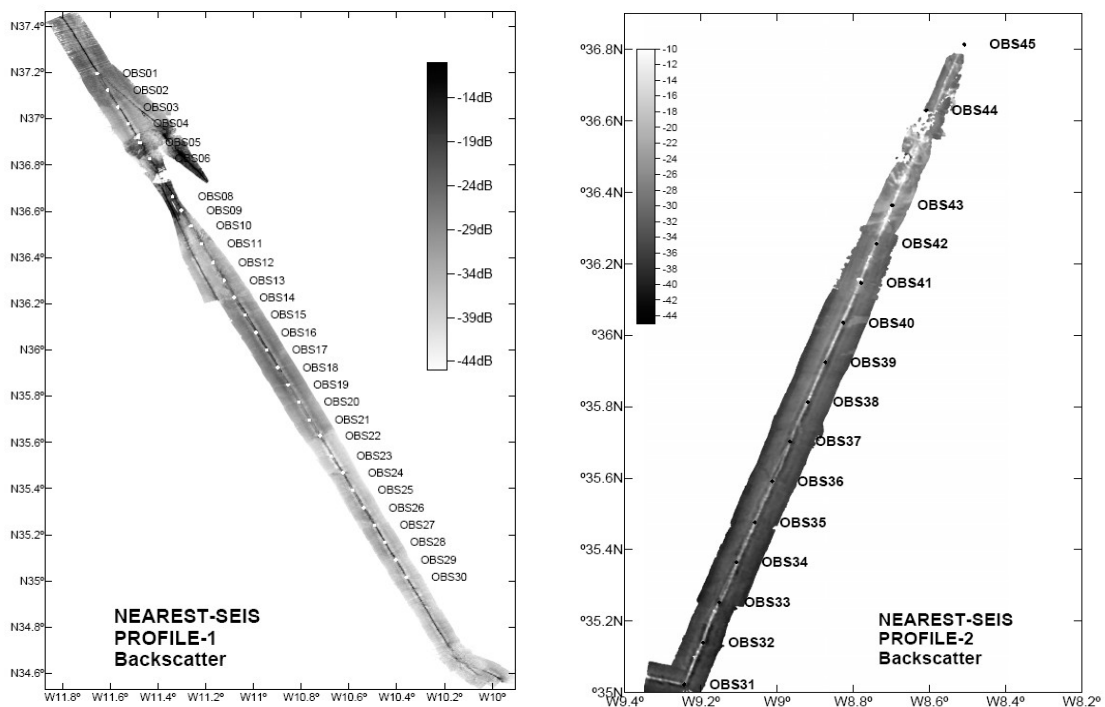


Figure 19 (previous page).- Mosaics of acoustic backscatter data (90 m grid) acquired along lines P1 (left) and P2 (right). High reflective areas (pale grey) correspond to steep slopes and/or rock outcrops at the ridges. Low reflectivity areas (dark grey) correspond to hemi pelagic sediments.

7. Parametric sub-bottom profiler

7.1. Technical description

The TOPAS (TOPographic PArametric Sonar) PS18 is a high-resolution sub-bottom profiler with parametric effect. The system comprises of a transducer unit of 8x 16 channels, a linear transceiver unit switched mode power amplifier and built in T/R-switch, an operator console MMI, Real-time processing, and PC- based platform (W2K, Linux etc.). A scheme of the implementation in the BIO Hesperides is shown in Figure 20.

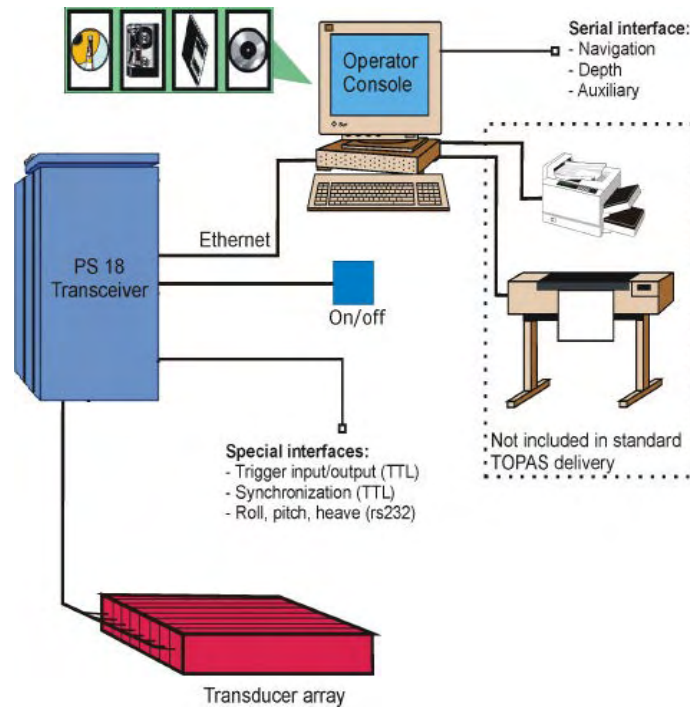


Figure 20.- Scheme of the implementation of the TOPAS PS18 system in BIO Hesperides.

The system is designed for very high spatial resolution sub-bottom profiling in water depths from less than 20 meter to full ocean depth. The +/-80% relative bandwidth, low frequency signal is generated in the water column as a difference frequency signal by non-linear interaction between two high frequency signals. It uses a primary frequency of 18 kHz, and a secondary frequency of 1 to 6 kHz. Maximum vertical resolution is of 0.2 ms, and bandwidth of 4° - 6°. The parametric sources have the advantage of generating a low frequency signal beam with no distinct sidelobe structure. The beam tapers off smoothly, which reduces the possibility of spurious signals due to sidelobes. The transducer is hull mounted.

The system can operate with various signal waveforms for optimum performance: Typically Ricker pulses are used for very high resolution work; Chirp pulses are used for deep water, high penetration work and CW pulses are used for narrow band, frequency sensitive work. The transmitted beam is electronically stabilised in both roll, pitch and heave (requires input from a vertical reference unit) ensuring that the insonified area on the sea floor is accurately positioned. The transmitter can be used in a sequentially beam

steering mode covering a larger sector. This is of particular importance in object detection / location applications. Penetration performance depends on sediment characteristics, water depth, transmitted signature etc. Penetration of more than 150 meters has been achieved in water depths of 1000 meters with a range resolution of typically 30 cm or better.

During the NEAREST-SEIS cruise a Chirp pulse wavelet was used, with frequencies of 1.5 – 5 kHz. The pulse length was 20 ms with a triggering rate of 1.5 seconds. Trace length was 300 ms with a sampling frequency of 16000 kHz and a pass band filter of 2 kHz. Data has been recorded in digital raw format and printed on film using Octopus thermal printer.

7.2. TOPAS data samples

High-resolution Simrad TOPAS data have been acquired during the NEAREST-SEIS cruise simultaneously to the seismic survey at a variable speed between 3 and 13 knots with good quality data. During the transit from Cartagena to line P1 the system was affected by a problem in the power supply electronic board (see Annex III: Technical report). TOPAS profiles have also been acquired during all lines except during the OBS deployment and recovering to avoid interferences with the transducer that sends commands to OBS.

The TOPAS data gives us detailed stratigraphic information on the uppermost tens of metres below the seafloor (80 to 100 m at an assumed sediment velocity of 1.5 km/s). These data provide insights into the control of neotectonic structures over the Plio-Quaternary sedimentary architecture of the external part of the Gulf of Cadiz, as well as subsurface tectonic geometry of the active structures. The best results have been achieved in flat areas with highly penetrative sediments, while abrupt slope areas and rock outcrops display very low penetration. Acquisition is sometimes difficult due to the complex topography of the area, with scarps over 500 m high. In those cases, signal is lost and side echoes were obtained at the foot of the scarps.

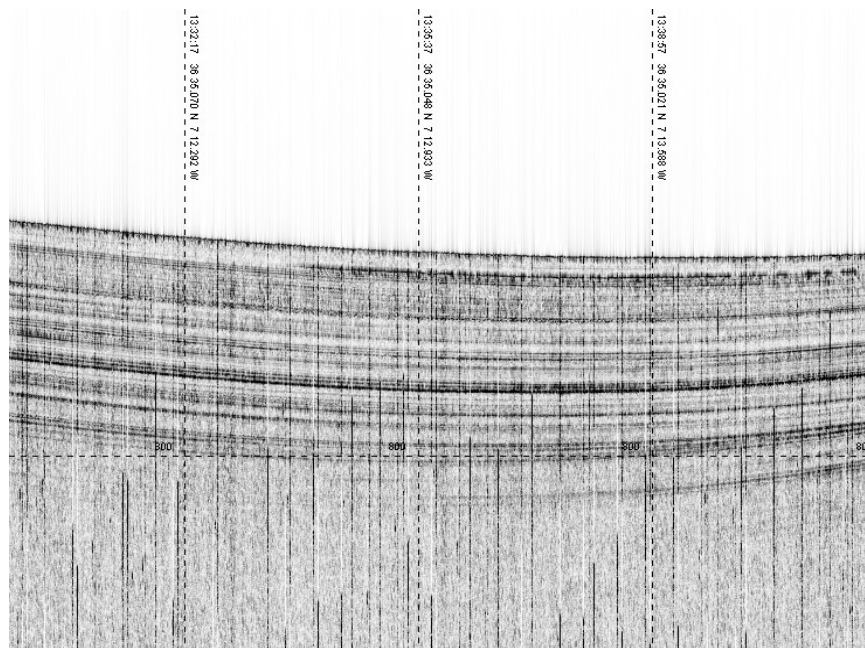


Figure 21.- Detail of TOPAS profile showing highly penetrative and

continuously well-stratified facies.

Different seismic facies can be identified in the area: highly penetrative and continuously well-stratified facies (Figure 21), which is the most common facies in the area; discontinuously to broken stratified and hyperbolic, corresponding to unstable areas located near rock outcrops or high slope areas; faulted stratified facies (Figure 22) low penetration chaotic to transparent facies on top or embedded into the sedimentary sequence, corresponding to mass wasting deposits.

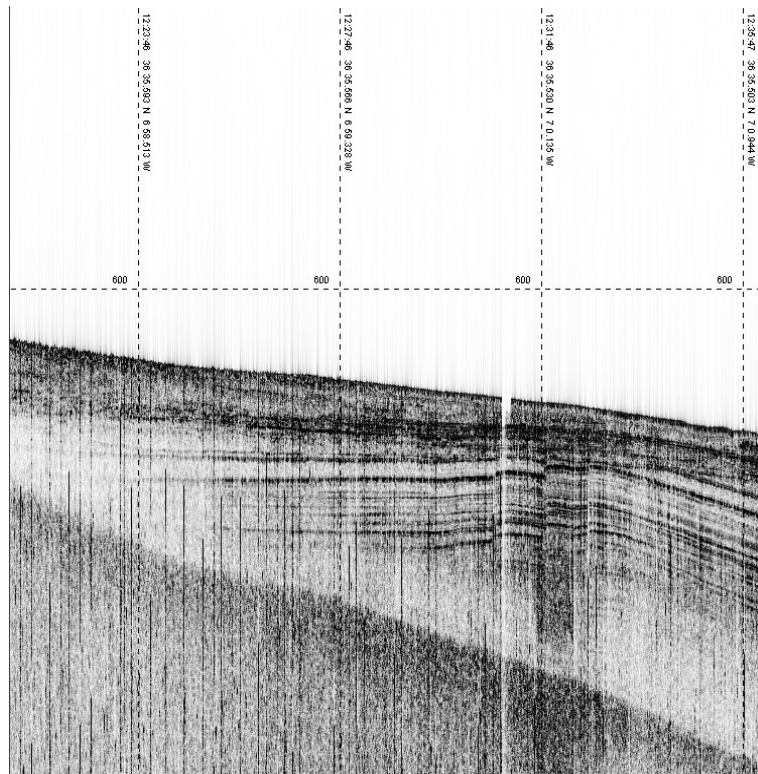


Figure 22.- Detail of TOPAS profile faulted stratified facies with discontinuous sediments limited by an unconformity.

8. Gravimetry

8.1. Technical description

The BGM-3 gravimeter is a data acquisition system of marine and aero-transported gravimetry. The system has a sensor mounted on a platform spin-stabilized, the raw data are processed, filtered and climb on a computer which in turn stores data in hard disk and sent by the Ethernet network to be captured by the data integrator.

It is composed of the following elements:

Sensor subsystem: The sensor subsystem generates a pulse train whose frequency is proportional to the gravity in the range of the instrument and a reference signal for counting. They also generate the bits of status for a badly functioning.

Stabilized platform: It isolates the sensor severity of the possible influences of the movements of the ship and it aligns with the vertical (Figure 23).



Figure 23.- Sensor subsystem front panel (left) and stabilized platform box (right).

Acquisition subsystem: It consists of a PC HP-486/50.

Calibration: The gravimeter is calibrated at the factory, but it is periodically checked, to adjust any deviation is carried out with a portable gravimeter.

For additional technical details about the system see Annex II: Technical report.

8.2. Gravity data samples

Figures 24 and 25 show examples of gravity data, as well as other parameters used to correct them (e.g. vessel speed, etc) along the two profiles P1 and P2. The most relevant feature is the presence of several striking anomalies such as the Gorrige Bank, but also the the presence of intervals in which the gravity records are bad due to different effects. The most relevant effects to distort the acquired data are related to sudden variations on the heading or in the velocity of the vessel.

Summary of observations along Profile P1:

About the heading: from 31/10/2008 at 22:33:30 with heading: 333.71°, until 02/11/2008, at 21:05:00 with heading: 339.47° the gravity data are correct (Figure 24).

About ship velocity: when the velocity is constant (between 4 – 4.5 nm) the gravity data are good for to be interpreted, from 31/10/2008 at 19:36:29, until 02/11/2008 at 20:45:09 (Figure 25).

A point of interest is the anomaly over Gorringe Bank, shown as a prominent bulge in the graphic. In this point the gravity anomaly grows up to 980.126 mGal. The measure corresponds to the day 02/11/2008 at 07:06:29 (Figure 24).

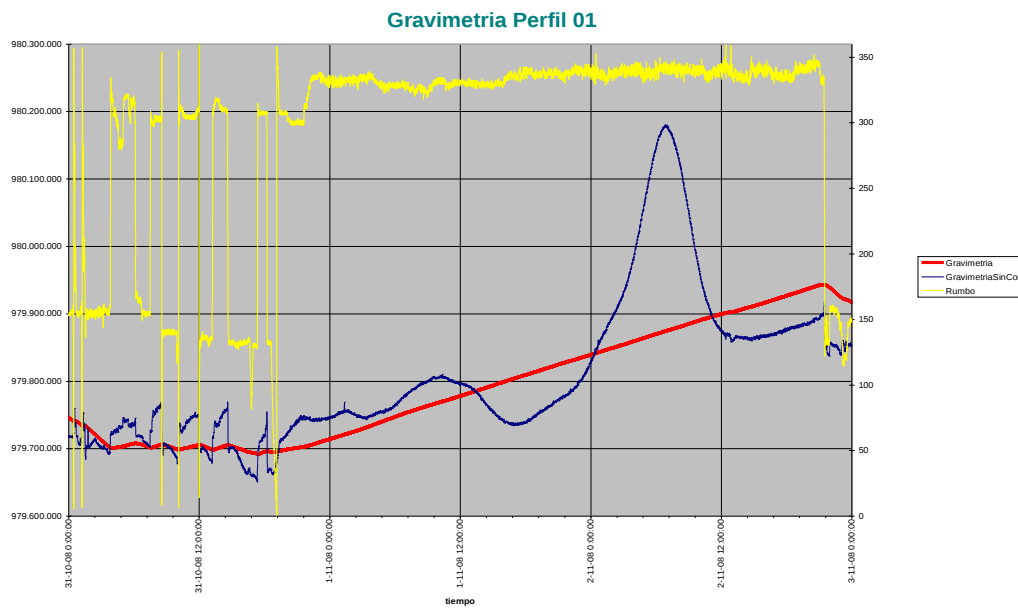


Figure 24.- Gravity anomaly recorded along profile P1 (blue line), filtered gravity (red line), and ship heading (yellow line). Note the bulge associated to the Gorringe Bank.

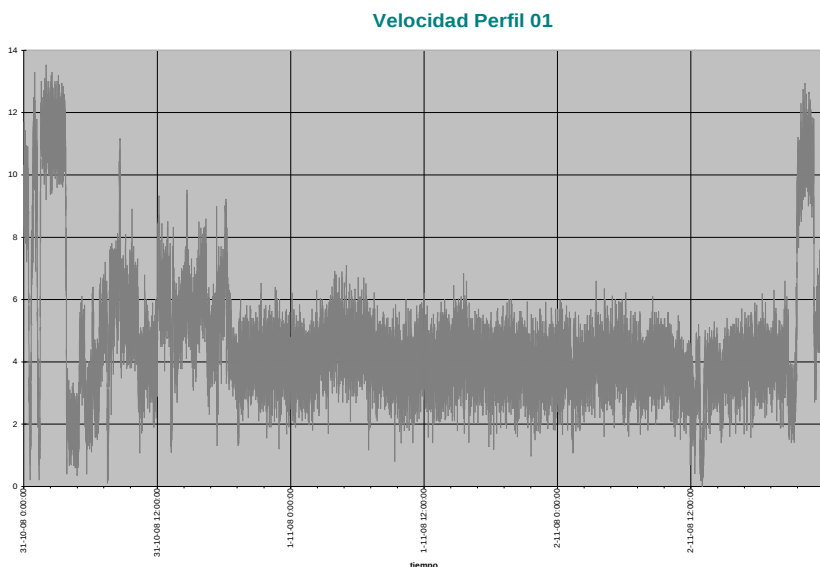


Figure 25.- Ship velocity during transect along P1. Note the major influence of speed on the gravity anomaly (left side of this figure and figure 24). A detail of this influence during OBS deployment is given in figure 26.

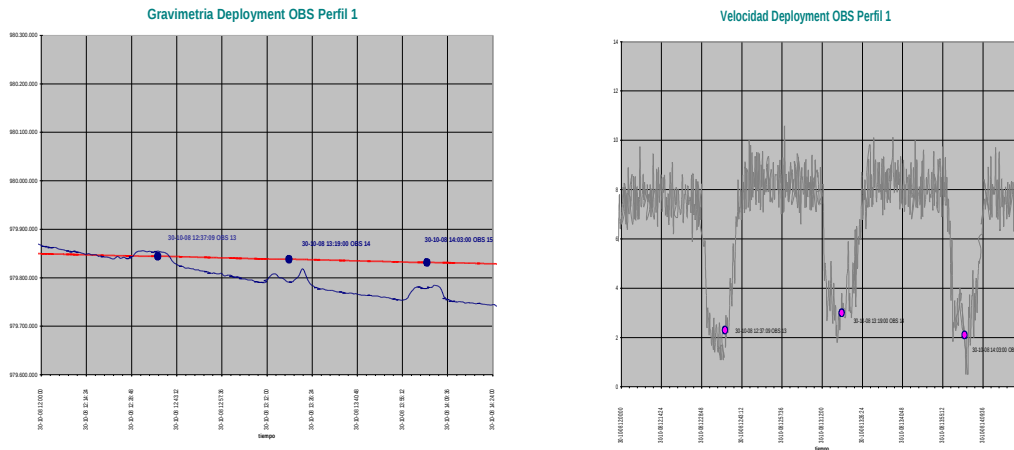
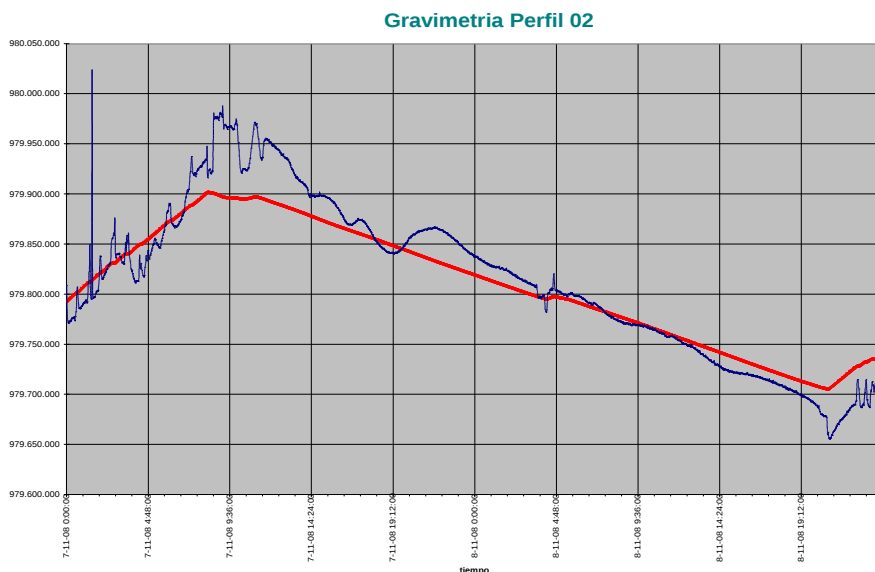


Figure 26.- Detail of gravity anomaly recorded during OBS deployment along P1 (blue line, left panel). Ship velocity during the same phase of deployment.

Summary of observations along Profile P2:

As in profile P1, a most relevant feature is the big influence of ship velocity on gravity data: the gravity data are fine only when the speed is constant (between 4 – 4.5 nm, from 07/11/2008 at 10:19:00, until 08/11/2008 at 20:15:09) (Figure 27).

In this profile, the highest point of the graphic, Portimao Canyon, in which, the gravity data is 979.985 mGal, that correspond to the day 07/11/2008 at 09:11:20. The lowest anomaly corresponds to the East of Coral Patch Ridge, in which the gravity data is 979.657 mGal, that correspond to the day 08/11/2008 at 20:57:30 (Figure 27).



Velocidad Perfil 02

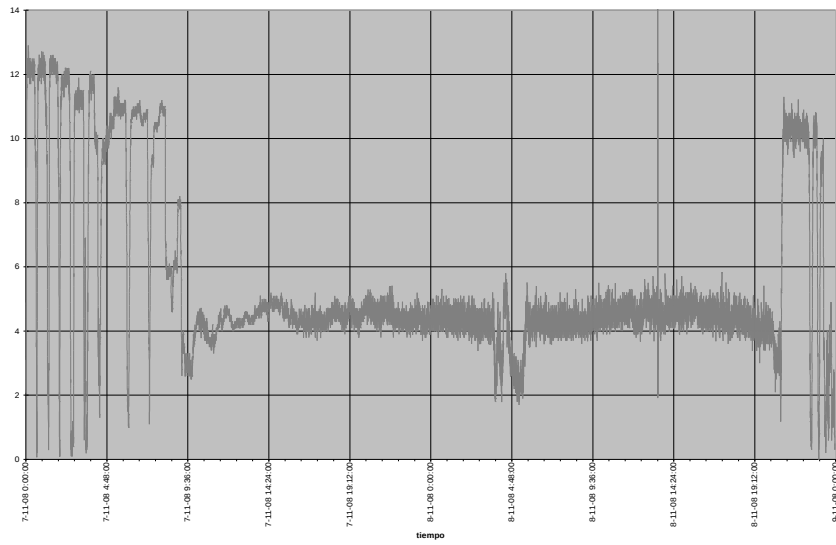


Figure 27.- Gravity anomaly recorded along profile P2 (blue line), filtered gravity (red line) (up), and ship velocity along this line (bottom).

9. Instrumentation for Wide-Angle Seismic data acquisition

The instrumentation for Wide-Angle Reflection and Refraction Seismic (WAS) acquisition was constituted by a pool of 36 Ocean Bottom Seismometers (OBS). A total of 19 OBS corresponded to the model microOBS, designed and owned by IFREMER. The other 17 corresponded to the model LC2000, built by the Scripps Oceanographic Institution and owned by the Unidad de Tecnologia Marina from CSIC. Apart from this, the seismic source was constituted by an array of 8 airguns towed by the ship. In the following sections we briefly describe the characteristics of the different equipment used.

9.1. French OBS (microOBS Model)

In order to increase the number of OBS available for the french geoscientific community, in 2002 IFREMER began designing a new generation of small, low-cost instruments for WAS use, which are easy and fast to deploy and recover, the so-called MicroOBS (Figure 28). During the NEAREST cruise 19 MicroOBS (14 belonging to IFREMER and 5 to IUEM) were deployed and successfully recovered.

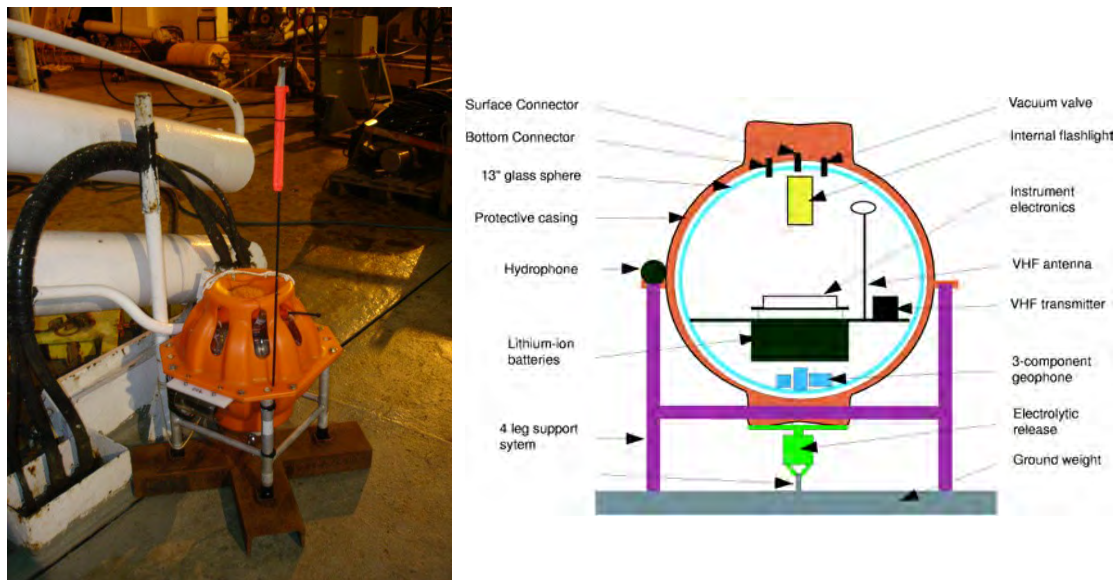


Figure 28.- MicroOBS on deck (left). Schematic diagram of MicroOBS components (right).

Four basic new ideas have emerged during the development of the new generation of MicroOBS as compared to the older OBS:

- Integration of acquisition and instrument release: This integration is possible due to the use of a broadband hydrophone which allows recording of the low frequency signal from airgun shots or earthquakes (from 0.1 Hz up to several 100 Hz) as well as the high frequency release signal (about 10 kHz). This significantly reduces the weight of the instrument and therefore facilitates its handling.

- Rechargeable batteries: To avoid the opening and resealing of the instrument, which remains a delicate operation at sea, a rechargeable battery pack is used in the MicroOBS.
- Data download by USB cable: The data are downloaded from the instrument via a USB 1.1 cable connection, to avoid opening and closing the instrument between successive deployments at sea.
- Size/weight reduction: The substantial size reduction of the MicroOBS compared to the older OBS was possible due to the three points mentioned above, the integration of the electronics with the release, the reduction of the battery weight and the download of the data. Thus, it was possible to fit the complete instrument into a 13" glass sphere. The complete weight of the instrument is only 20 kg in air and additional 20 kg for the ground weight.

The main characteristics of the MicroOBS are the following ones:

Mechanical parameters:

- Glass sphere Vitrovex 13 inches
- Integrated Flashes
- Integrated Gonio VHF
- Weight in air (<15Kg)
- Maximum immersion depth = 6000 m

Acquisition parameters:

- Seismic data acquired by one hydrophone and three geophones (x, y, z)
Hydrophone: LF-3dB, 2 Hz, sensibility: -160 dB ref 1 V/ μ Pa, signal full scale 70 Pa.
Geophones: 3-axis, type: 4,5 Hz (-3 dB), sensivity: 22,4 mV/mm.s⁻¹, full scale: +/- 0,38 mm/s.
- Sampling frequency: 10 Hz to 500 Hz
- 4 channels and 24 bits of resolution
- Capacity 2 Gb
- TCXO clock: 1e⁻⁷
- Programming OBS without opening the sphere
- Download by USB port without opening the sphere (RS232 460kb/s ou USB 2 a 12000kb/s)
- Acoustic release integrated to the electronic of acquisition.
- Synchronisation with GPS clock

Energy:

- Rechargeable batteries (Lithium-Ion)
- Autonomy: 10 days (minimum)
- Recharging batteries without opening the sphere.

Deployment:

- Programming for deployment : 15 minutes

9.2. Spanish OBS (LC2000 Model)

The Marine Technology Unit (UTM) provided 17 short period OBS of the model LC2000s for this experiment. These instruments were designed and built by the Scripps Oceanographic Institution (La Jolla, USA), and the pool was purchased in 2008 and is now managed by the UTM. The sensors on the LC2000s are a High-Tech hydrophone and a three component Sercel L-28 seismometer. Each instrument is comprised of an anchor, a 4 McLane glass float assembly on which the lifting bail is attached, a polyethylene frame holding the sensors, an acoustic release transponder, a 4X4 data logger, and a mechanical release (Figure 29). The float and frame components are stored separately in a custom rack system, and are assembled and tested prior to deployment on a square preparation platform which is bolted to the deck. The complete instrument weights approximately 300 pounds in air. The anchor is a 100-pound iron grate held to the base of the poly frame by a single 2" oval quick-link when the release mechanism is cocked and secured. After the anchor is released for recovery, the four 12" glass balls in the float package, as well as the syntactic foam blocks provide sufficient buoyancy to lift the instrument at about 45 m/min to the sea surface. To increase visibility at the surface, an orange flag on a 48" fibreglass resin staff is attached to the floats. The recovery aids also include a Novatech low-pressure activated strobe beacon and radio. We have radios that operates at four different frequencies, 154.585 MHz, 159.480 MHz, 160.725 MHz, 160.785 MHz.

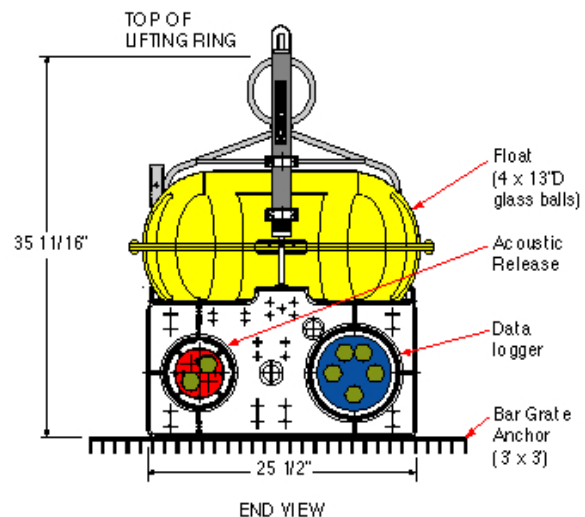
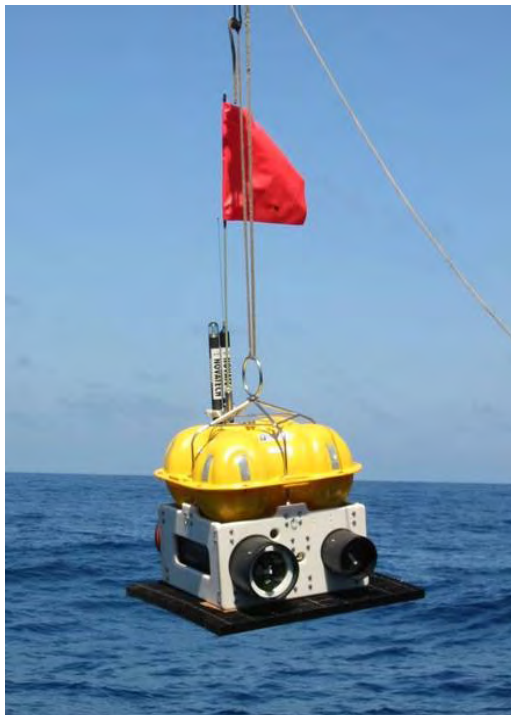


Figure 29.- LC2000 OBS hanging from the ship's crane during a deployment (left). Schematic diagram of LC2000 components (right).

The acoustic release transponder is comprised of a main circuit board, and an ITC-3013 transducer manufactured by International Transducer Corp. These are all installed in and on a 4-5/8" aluminium pressure case. All SIO

transponders interrogate at 11kHz and respond at 12kHz. Alkaline batteries provide 18 volts power the burn, 12 volts power for the transponder, and 9 volts power for the circuit board logic. The release mechanism includes two double wire burn elements. When fresh, two battery strings are combined to provide the 18 volts to burn one of two release wires in an average of 6 minutes for water depths encountered during this experiment.

The main characteristics of the MicroBS are the following ones:

- Dimensions: 914 mm x 660 mm x 965 cubic inches
- Weight (+ ballast): 125 kg
- Consumption: 0.270 – 0.759 W
- Authonomy: Up to 9 months
- Batteries: Alkalines (primary cells), lithium (prim cells)
- Clock: Sea Scan [0.02 - 0.05 ppm]
- ADC: Crystal CS5321 delta-sigma (24 bits)
- Dynamic range: 124-130 dB
- Sampling rate: 1 - 4000 sps
- Memory: Compact flash up to 192 Gb
- Sensors: Geophone (Sercel L-28; 4.5 Hz)
Hydrophone (HighTech HTI 90; 0.05 – 2500 Hz)
- Release system: Two redundant electrolytic systems
- Location aids: Flash, beacon, flag

9.3. Landstations (Hathor LEAS)

The seismic profile P2 was also recorded onshore by an array of 9 landstations (Figure 12). The model used is Hathor 3 from LEAS, an acquisition station which allows data storage on three channels, equipped with a Mark L4-3D seismometer (1 Hz) (Figure 30). The communication with the station is executed by means of a PC equipped with the appropriate software (provided), or by means of a GSM modem (if the option has been held). The equipment falls in with the CE norms and its box is designed to fight a duel (water-tightness, resistance, autonomy...). Its major performances are : large storage, easy programming, use and many applications (seismology, volcanology...). This product is the result of a long collaboration between LEAS and the University (more than 15 years).



Figure 30.- Hathor LEAS seismic landstation (left). Mark L4-3D seismometer (1 Hz) (right).

Its main technical characteristics are the following ones:

General:

- Energy : External 12,6 Volts DC.
- Consumption :
 - Acquisition mode : 50 mA.
 - Data transmission to internal PC : 550 mA during 180 seconds each 1h30 at 100 Hz in continuous mode.
- Auto power off mode in case of low battery (<9,6V).
- Analog input : 3 channels (differential inputs).
- Preamplifier gain : 4 selectable.
- ADC : 24 bits Delta Sigma.
- ADC gain : 1 to 128 software selectable
- Sensor: Mark L4-3D seismometer (1 Hz)
- Dimensions : 300 x 250 x 120 mm.
- Weight : 4,5 kg.
- Temperature range : -5°C / +40°C.
- Box : IP 65.
- Connectors : FRB type.
- Dynamic range : 108 dB at 100Hz.
- 90 dB at 250 Hz.

- Sample rate : Up to 300 sps.

Recorder modes and timing:

- Trigger modes : - Selectable fixed level. ! TCXO 1 ppm (option) : Synchronization made by external
- STA va. LTA. signal DCF-UTC, or LPC \leq (LEAS Position and Clock Code) with a
- External trigger. LOCSAT (GPS receiver internal or external).
- Continuous and trigger modes.

Storage:

- Modem link : Data are stored in the 4 MB Ram. (GSM transmission will be available soon)
OR
- Extractable IDE hard disk 3,2 GB : storage capacity of 2 months at 100 Hz.

Programming and communication:

- Means : Direct cable link or modem link.
- Software provided : - SIS3DIR for local communication.
- SIS3MOD for modem communication at 14 400 Bds.
- SIS3BUS for data local retrieval.
- PICKEV for data proceeding.
- SISMALP format converter to AH or SAC formats.
- Parameters : Time, identification, station name and password, viewing of online data without stopping
- measurements, viewing of parameters, checking of storage capacity, checking of power supply and temperature, online data retrieval without stopping measurements...
- Controlled : Startup, time synchronization, storage...

9.3. Airgun system

The two seismic profiles acquired during NEAREST-SEIS were carried out in two different phases with a group of compressed air guns. In the following the technical specifications of the gun cluster used to run the two seismic profiles is described, as well as the laboratory equipment used for the firing and synchronization of guns.

Seismic source

To carry out the different seismic profiles, a total of 7 Bolt, model 1500LL, guns are used, organized in 2 arrays (Figure 29). The main array was approximately 12 meters long and the secondary consisted of a single gun towed off the stern on amidships. The function of the group of guns is emitting a discrete pulse of acoustic energy in the water after receiving an electric signal from the Seismic Laboratory. The energy emitted is obtained after the release of the compressed air that is constantly supplied by group of compressors and is contained in fixed volume chambers. The energy pulse is generated activating the solenoid valves installed on each gun, this provokes the sudden opening of the piston that hold the air in the gun chamber.

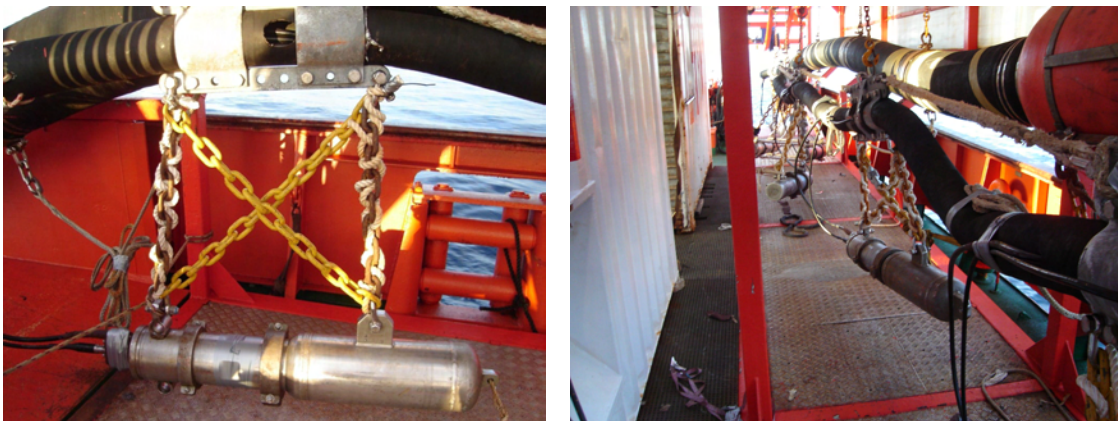


Figure 29.- 1000 c.i. airgun, model Bolt 1500LL used in this experiment (left). Detail of the main airgun array (right).

The capacities of the guns deployed during this survey are the following: 500, 1000, 500, 255, 265 and 1000 cubic inches (cu.in.) in the main group and the other is of 1000 square inches on amidships, for a total volume 4520 c.i. The separation between guns is of 2.5 meters between plates and of 0.8 meters in the case of a cluster that consists of the 255 and 265 cu.in. guns, all of them working at a depth of 12 meters. To supply the air at the work pressure of 140 bars to the guns, 4 Hamworthy, model 4TH190W70, are used. Each has the capacity of supplying 304 m³/h of air at said pressure.

The firing frequency on both lines was 90 seconds to reduce *wrap-around* effects, except for the first two events of calibration, that lasted approximately 20 shots at a rate of one shot every 60 seconds.

Spatial distribution and capacity of the gun array

The source array and firing interval was designed to be the best adapted to this particular experiment (e.g. WAS), for which the key element is to obtain the maximum possible energy concentrated at the lowest possible frequency range.

The design was done using Gundalf commercial software, taking into account the limitations of the BIO Hespérides system. The main characteristics of the signal emitted from the array are the following:

Paramaters of the array	Values obtained with simulation
Number of guns	7
Total volume (cu.in).	4510.0 (74 liters)
Peak to peak pressure in bar-m.	50.4 (5.04 MPa, 254 db re 1 microPascal. at 1m.)
Zero to peak pressure in bar-m.	21.9 (2.19 MPa, 247 db re 1 microPascal. at 1m.)
Primary-bubble	6.42
Period between the bubble and the first peak (s.)	0.207
Maximum spectral ripple(db): 10.0 - 50.0 Hz.	6.62
Maximum spectrum value (db): 10.0 - 50.0 Hz.	210
Middle spectrum value (db): 10.0 - 50.0 Hz.	207

The signature of the source wavelet in the time domain, as well as its frequency spectrum, are shown in figure 30.

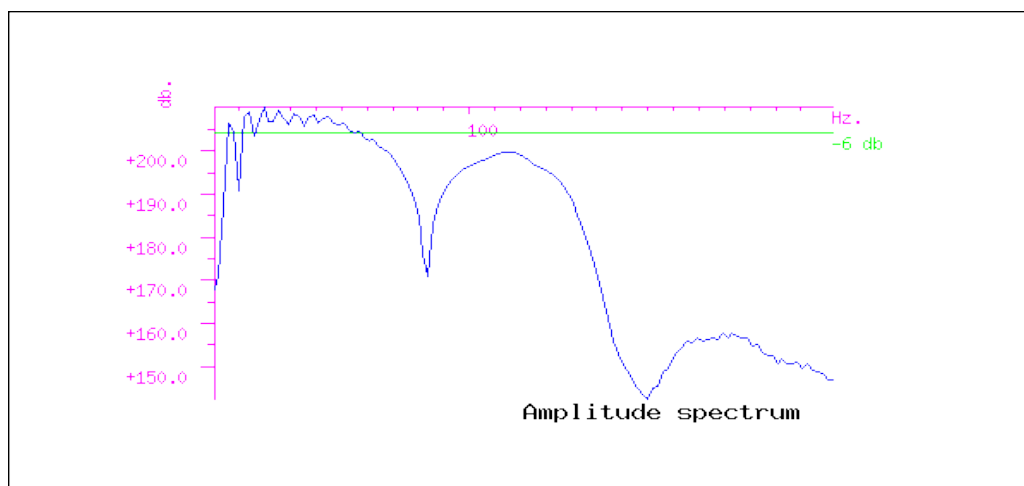
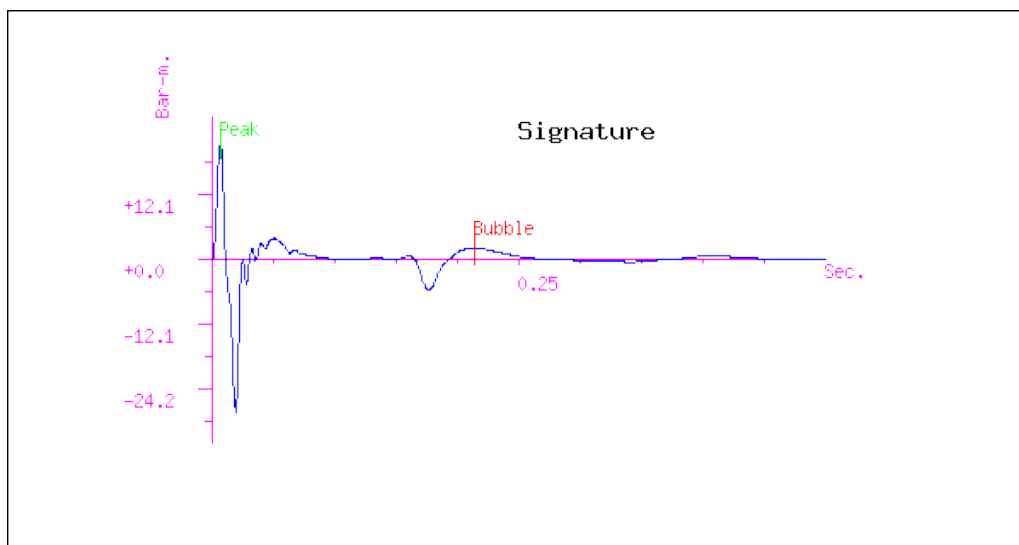


Figure 30.- Signature of the source wavelet used during NEAREST-SEIS cruise (up). Amplitude spectrum of the source wavelet (bottom).

Note that the bandwidth is reduced (10-60 Hz) due to the depth at which the guns are located (12 meters). This is not an issue for WAS, since due to attenuation effects, the energy spectrum recovered at the long distances characteristic of WAS layouts is almost completely <30 Hz. On the other hand, this implies that the energy released, more than 50 bar-m, is being concentrated in this range of the spectrum, accomplishing, in this manner, an adequate signal for studies that require a large displacement between the shot point and the registration.

Some incidents happened with the source array, specially during the first profile, and during most of the experiment one of the 1000 c.i. guns of the main array did not work properly. The array in P1 consisted therefore of six guns with a total volume of 3520 c.i. These incidences are detailed in Annex I.

Laboratory equipment

For the firing and the synchronization of the guns we used a Hydrasystems' gun controller with Minipulse software to operate it (see description below), and a PC to run the software on. Also, a second PC was used to register the navigation telegram coming from the gun controller set up, as well as the EIVA navigation system, in charge of generating the navigation telegram received by the gun controller set up.

The Minipulse gun controller by Hydrasystems is able to fire and synchronize up to a total of 8 guns. The system is composed of a PC that controls the instant of firing and the signal conditioning stage. It is in charge of generating the signals coming from the sensors installed in each gun. These signals are what later are used by the system to calculate the differences in the shot moments and applying the appropriate corrections to so that the shot is executed with a maximum error of one microsecond in respect to the "aim point", therefore assuring a maximum possible amplitude of the signal emitted and that the signal is of minimum phase.

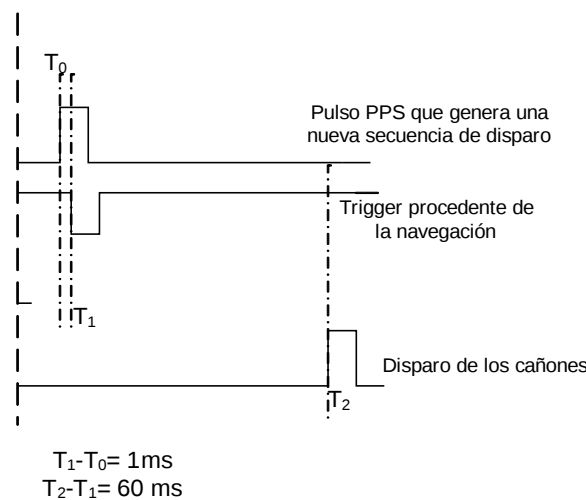


Figure 31.- Sequence of the signals that generate a new firing of the guns.

The gun shot (aim point) is produced 60 ms after the reception of the pulse received from the navigation (fix point). The fix point is 1 ms after the generation of the pulse by the GPS Fei-Zyfer GPS Starplus that indicates the arrival at the second corresponding to the new shot, for which the real firing of the canons is produced 61ms after the UTC time that is indicated in the telegrams generated after every shot. To understand the sequence in more detail see Figure 31.

Along with the navigation pulse, the gun controller receives, through a serial port, all the information corresponding to the fix point: latitude, longitude, date, UTC time, heading, speed, depth, line name, and event of fix point number. Once the guns have fired, the controller emits, through a serial port as well, a telegram that gives the details about how many guns fired, the total capacity, the delays of each gun in reference to the aim point, as well the information about the fix point that describes the telegram that is created after every shot and the meaning of every field (see Annex II). The telegram emitted is registered by a computer in text format so that it can be used later in the processing of the data recorded by the OBS. The position and characteristics of the gun array used are graphically detailed in Annex II. Exactly in the shot instant, on the Field Time Break a pulse is generated and is sent to the GPS that generates the shot trigger, in which a new shot telegram is created, one that is much more finely tuned than that generated by the gun controller. The structure is described in detail in Annex II.

10. Wide-Angle Seismic data samples

In this section we present the record sections of all the data acquired during the NEAREST-SEIS survey. They correspond to the 29 OBS that recorded profile P1 (Figure 33 to 46), the 15 OBS that recorded profile P2 (Figure 48 to 55), as well as the 7 landstations that recorded P2 (Figure 55 to 58). A section showing local earthquakes that occurred during the experiment has been also included.

10.1. Seismic records of airgun shooting along P1

The quality of the seismic data recorded along P1 (Figure 32) is remarkably high, though the distance to which the seismic phases are recorded is notably variable from OBS to OBS. As stated in section 9.3 the source used had reduced capacity for WAS due to the ship limitations, but still we were able to record signal to more than 40 km in most OBS and to more than 75 km in a number of cases (e.g. OBS 27 to 30, Figures 44 and 45). Almost all identified arrivals correspond to refractions (first arrivals), and almost no reflections have been preliminarily identified. It is noteworthy that the maximum offset with identifiable signal highly depends on the location of the instrument, and not on the instrument type, being recordings in both micrOBS and LC2000 models of similar quality. Concerning the location, OBS located in the Tagus Abyssal plain (OBS01-OBS04, Figures 33 and 34), show clear arrivals to some 40 km, enough to reach the upper mantle in oceanic-like crust.

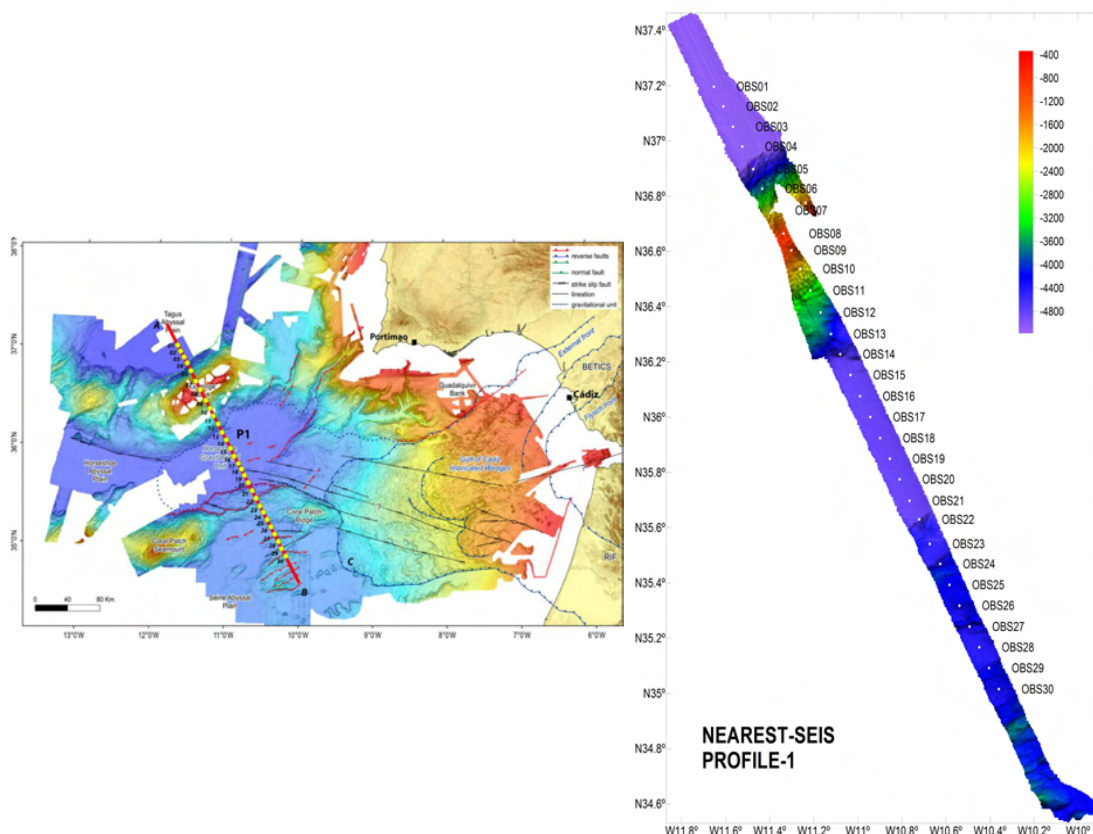


Figure 32.- Bathymetric map of the study area with the location of P1 superimposed (red line) as well as OBS locations along this line (left). Detail of swath bathymetry data acquired along profile P1 with the OBS locations superimposed (OBS01-OBS30) (right). The record sections of these OBS are shown in Figures 33 to 44.

Most recordings in the Gorringe bank are surprisingly good in spite of the prominent topography and steep flanks, with several recordings to more than 50-60 km (e.g. OBS09, OBS10, Figure 36). These recordings should provide useful information on the nature of this striking feature. With the exception of a couple of record sections (e.g. OBS 16, OBS20, Figures 38 and 40), recordings in the Horseshoe abyssal plain are slightly poorer, confirming the attenuative nature of the thick gravitational unit that covers the plain. But signal is still identifiable there up to more than 40 km in most OBS. Finally, the best recordings are obtained in the Seine abyssal plain, where signal can be clearly identified up to more than 70 km from the source in most OBS (e.g. OBS 25-30, Figures 42 to 45). All this information together should allow building a well-constrained crustal model using travelttime tomography methods.

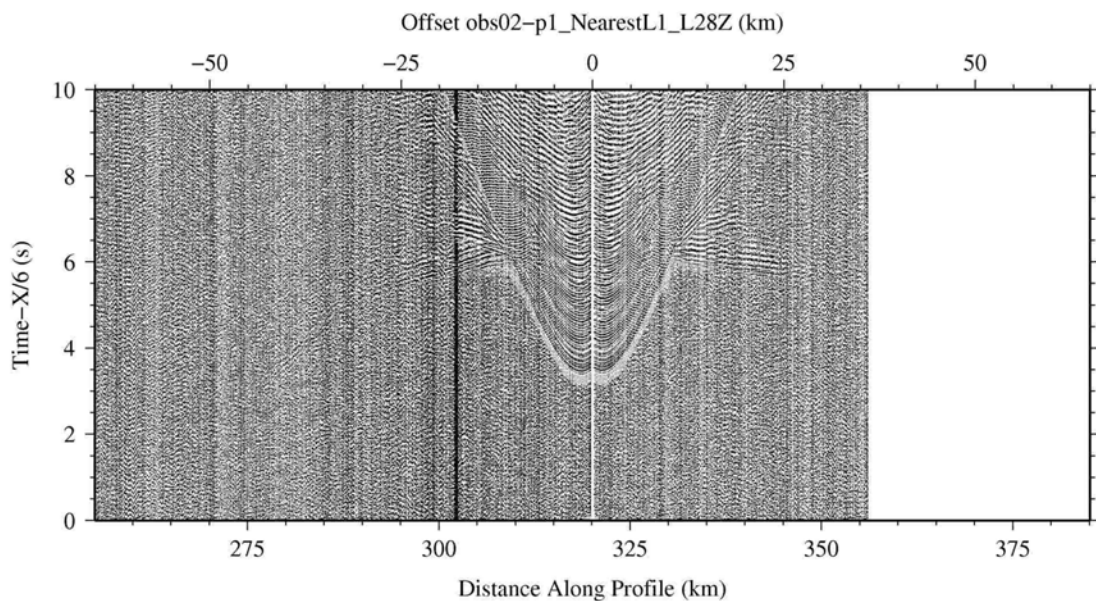
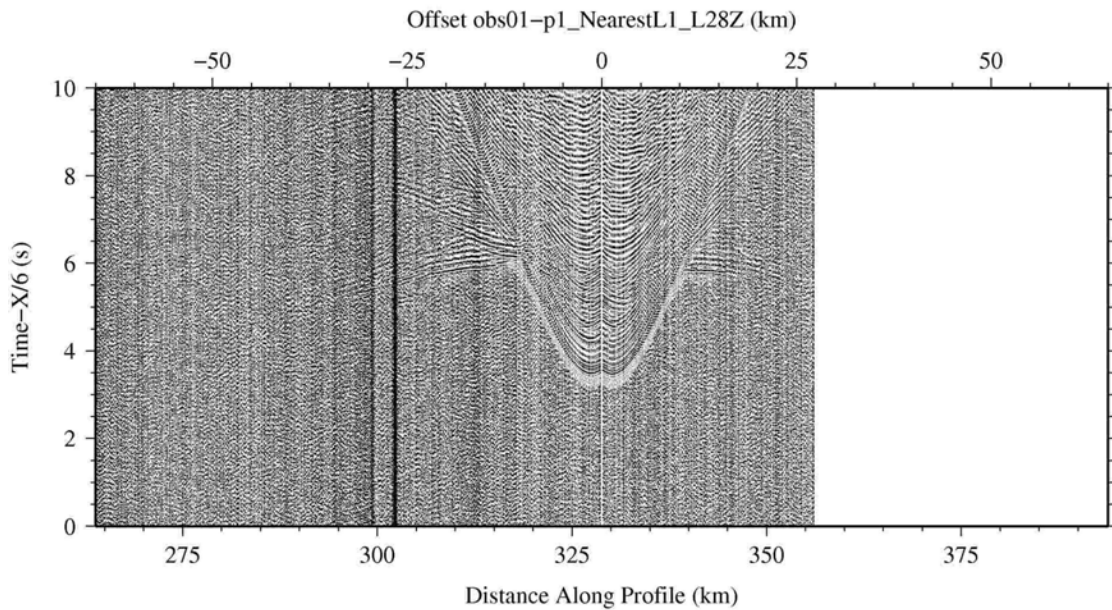


Figure 33 (previous page).- Record section of OBS01 (up) and OBS02 (bottom) along P1 (vertical component). The OBS model is LC2000.

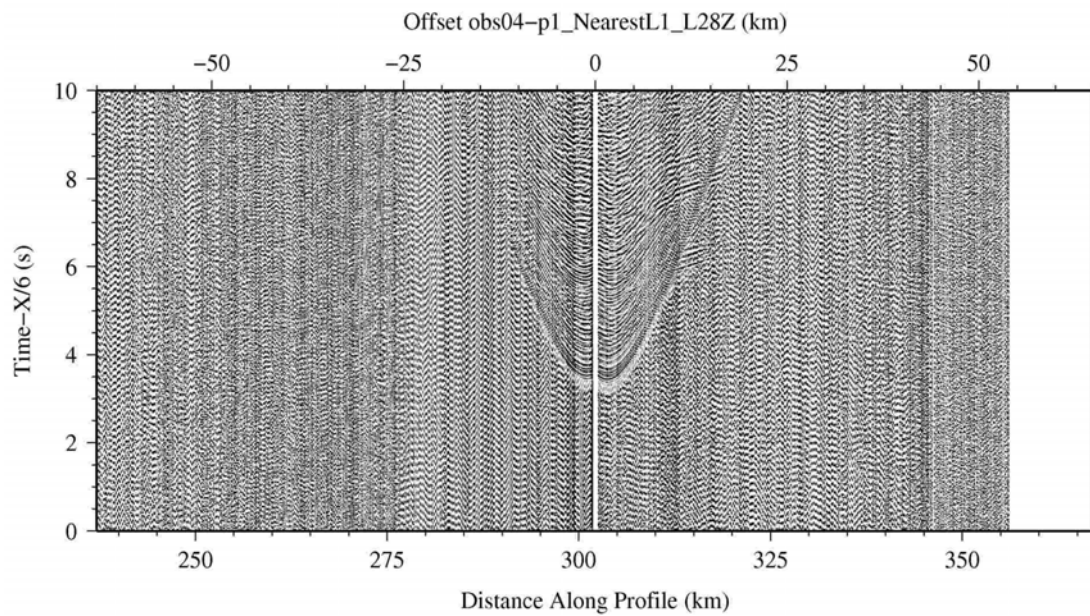
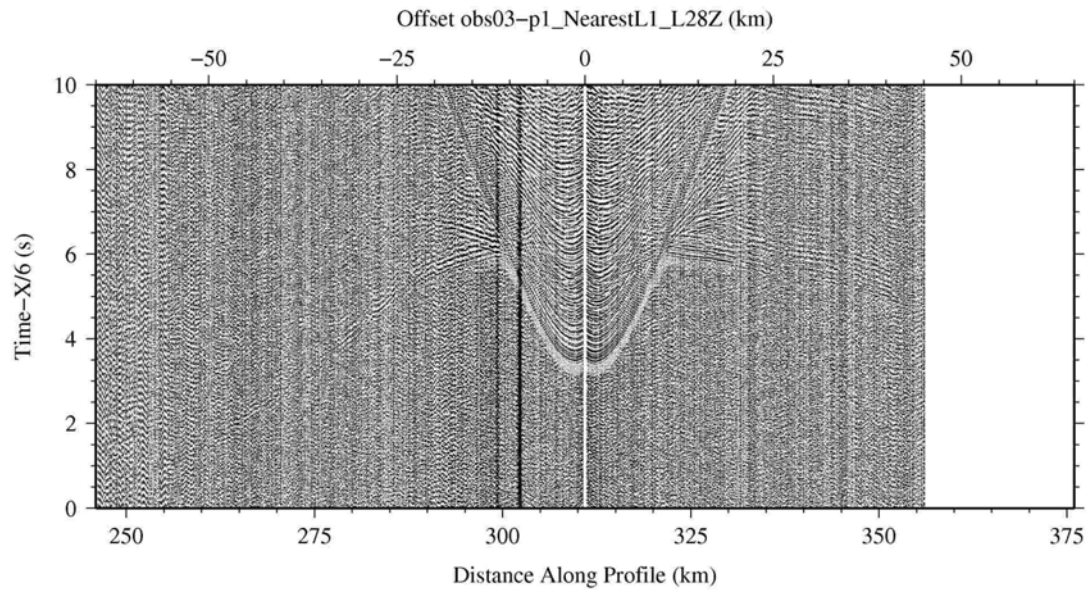


Figure 34.- Record section of OBS03 (up) and OBS04 (bottom) along P1 (vertical component). The OBS model is LC2000.

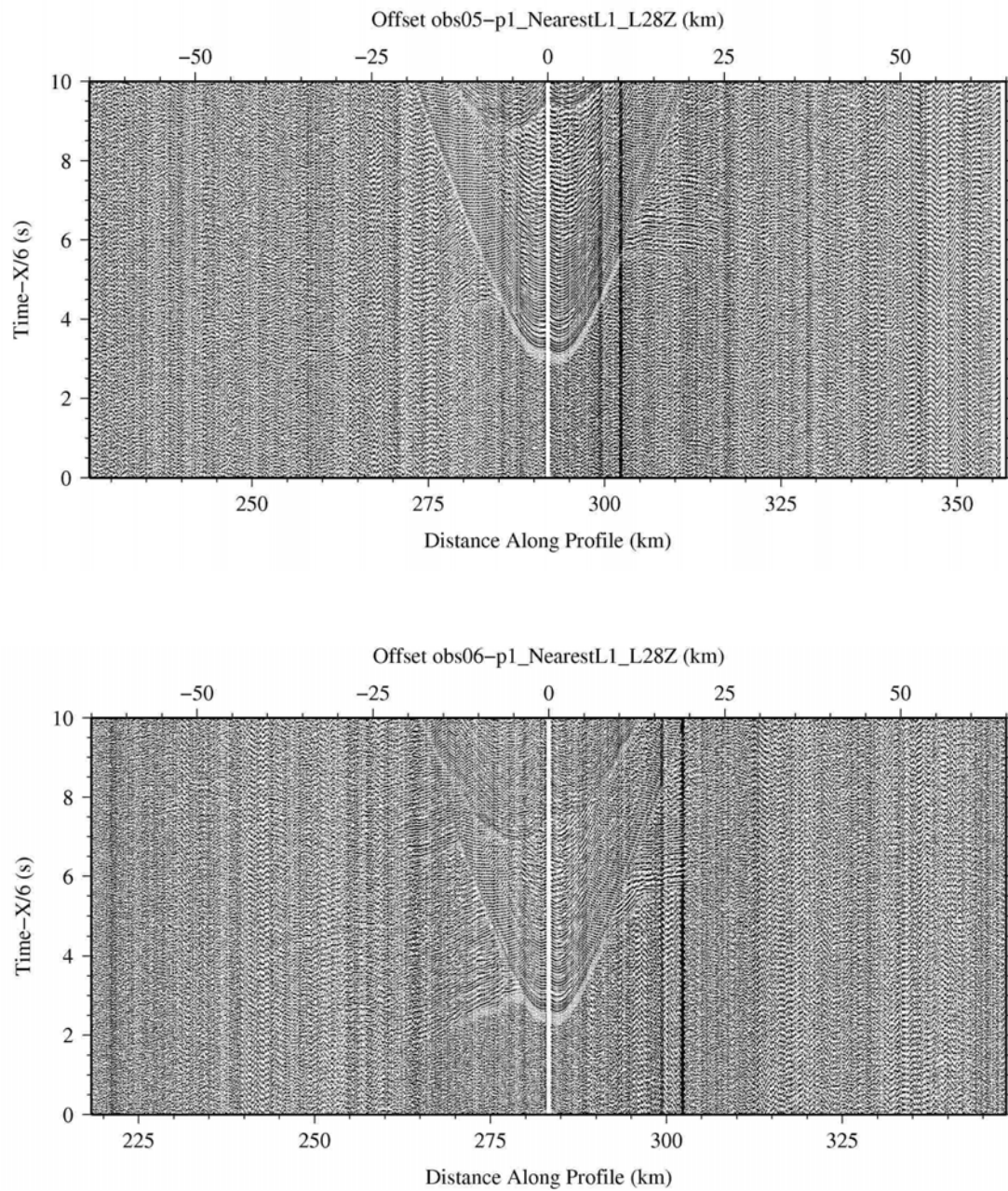


Figure 35.- Record section of OBS05 (up) and OBS06 (bottom) along P1 (vertical component). The OBS model is LC2000.

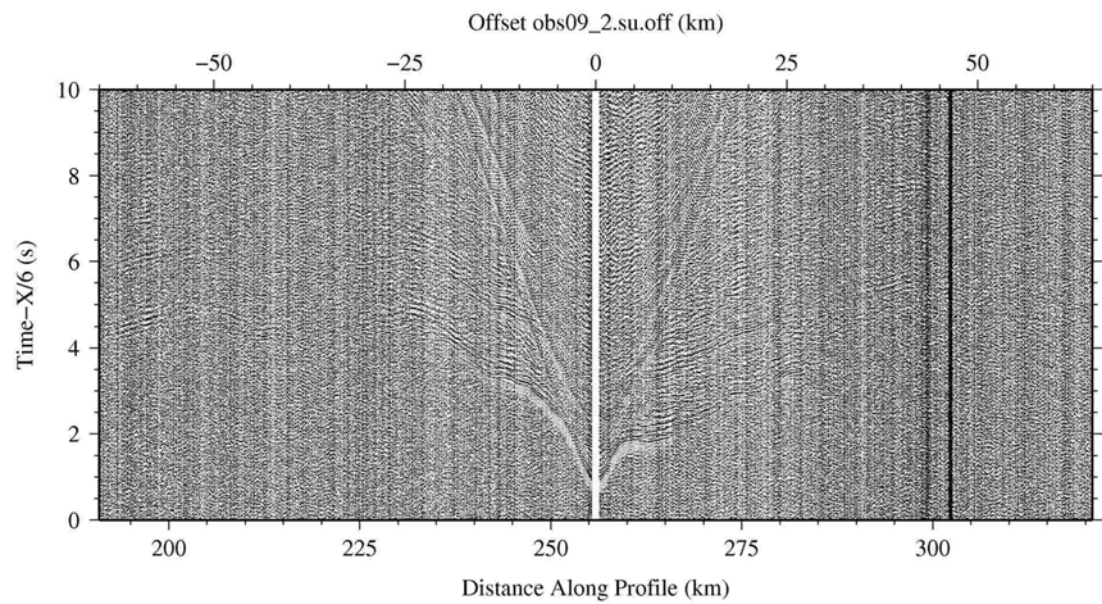
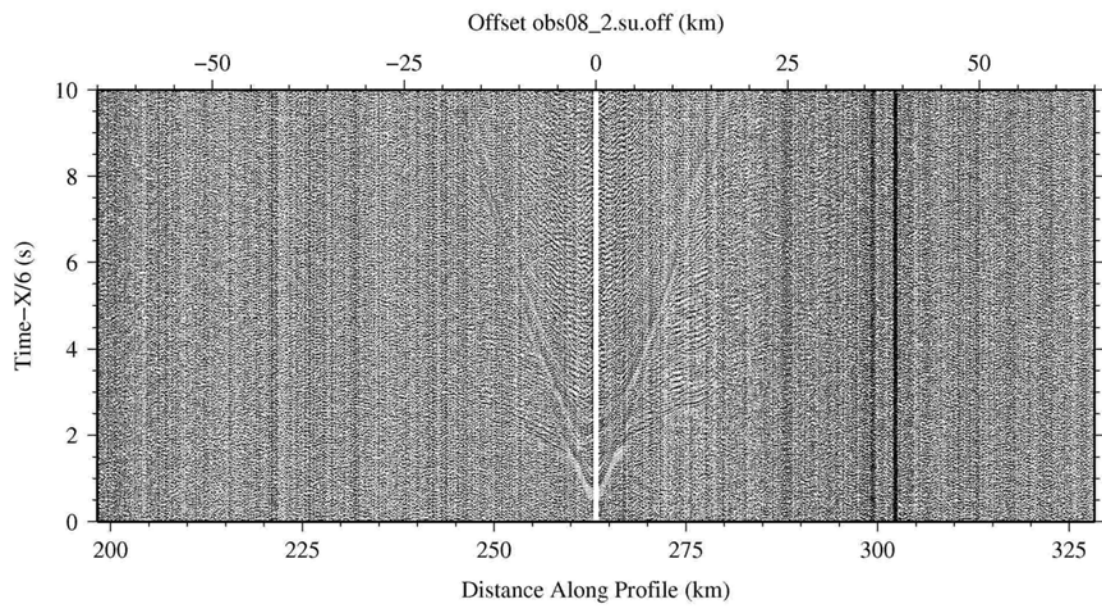


Figure 36.- Record section of OBS08 (up) and OBS09 (bottom) along P1 (vertical component). The OBS model is MicroOBS.

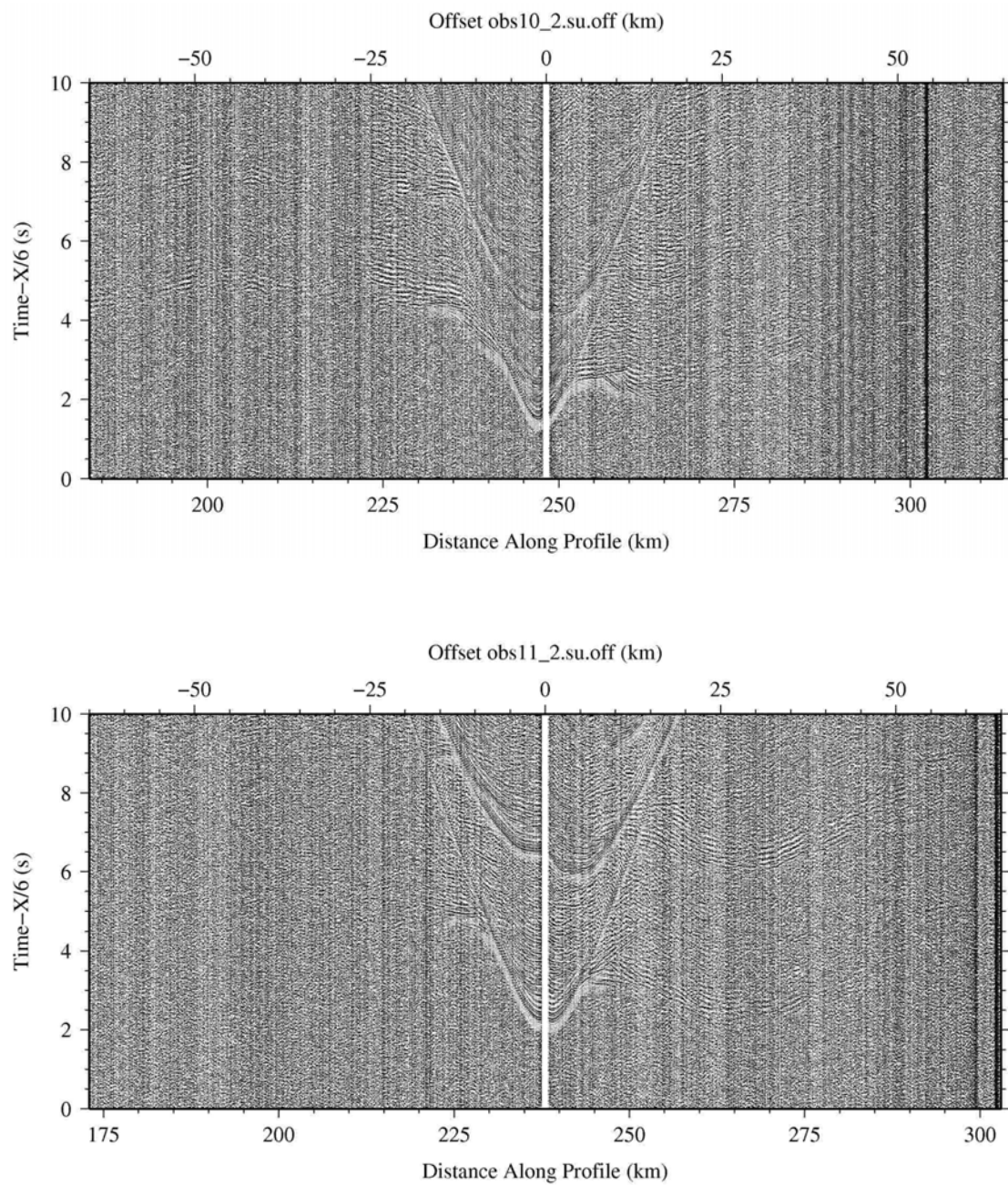


Figure 37.- Record section of OBS10 (up) and OBS11 (bottom) along P1 (vertical component). The OBS model is MicrOBS.

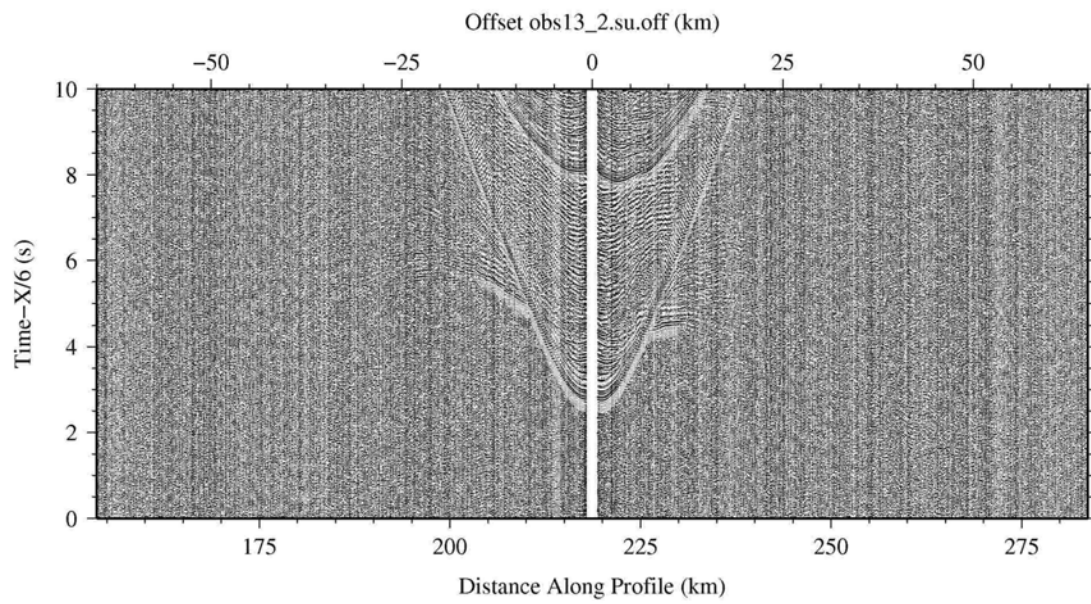
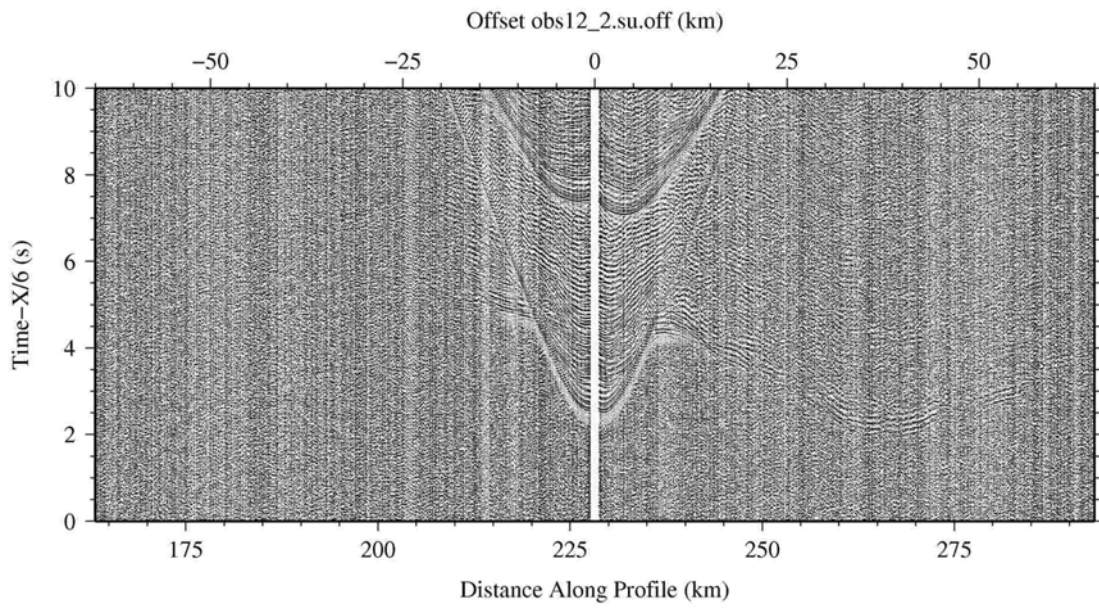


Figure 38.- Record section of OBS12 (up) and OBS13 (bottom) along P1 (vertical component). The OBS model is MicroOBS.

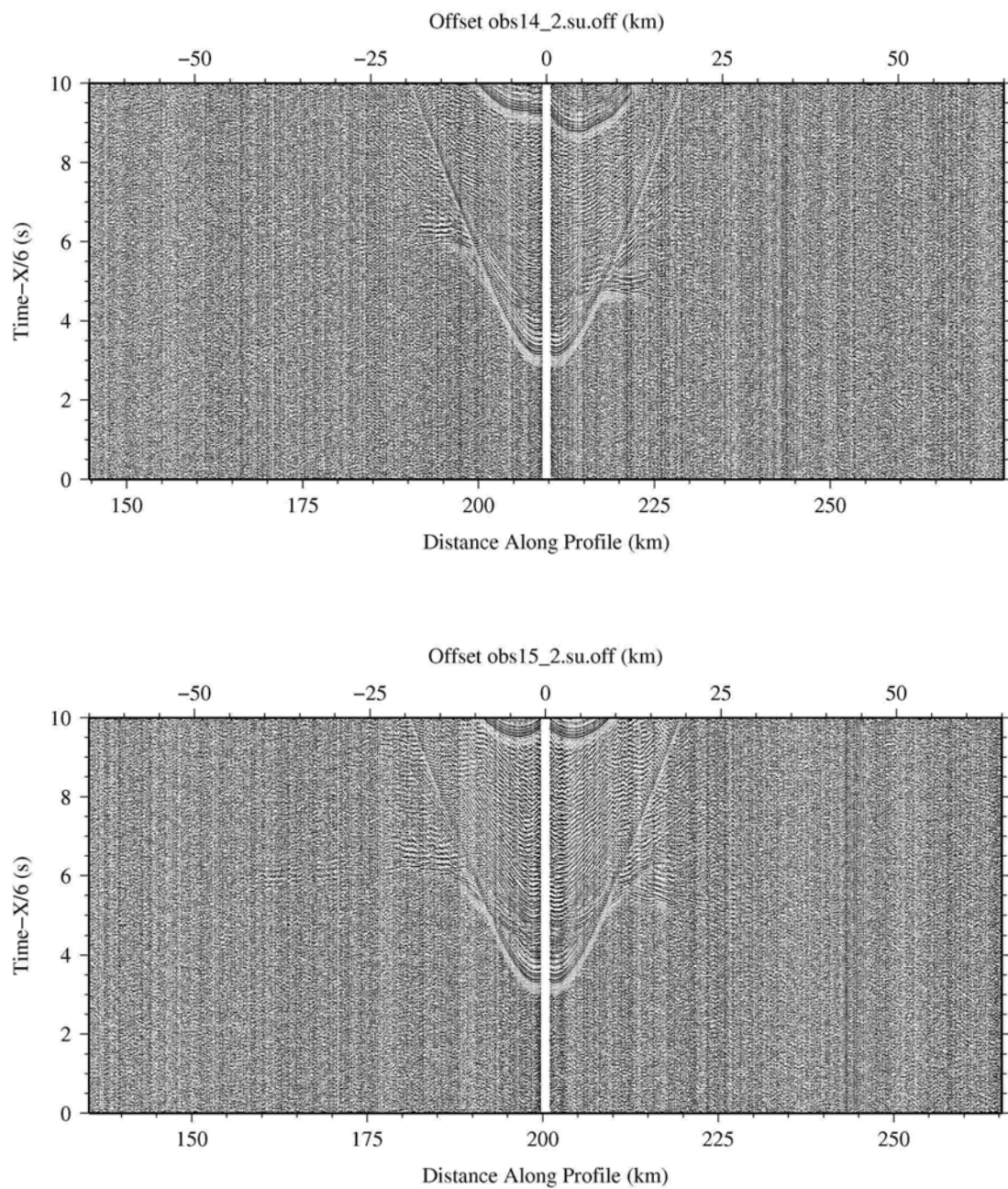


Figure 39.- Record section of OBS14 (up) and OBS15 (bottom) along P1 (vertical component). The OBS model is MicrOBS.

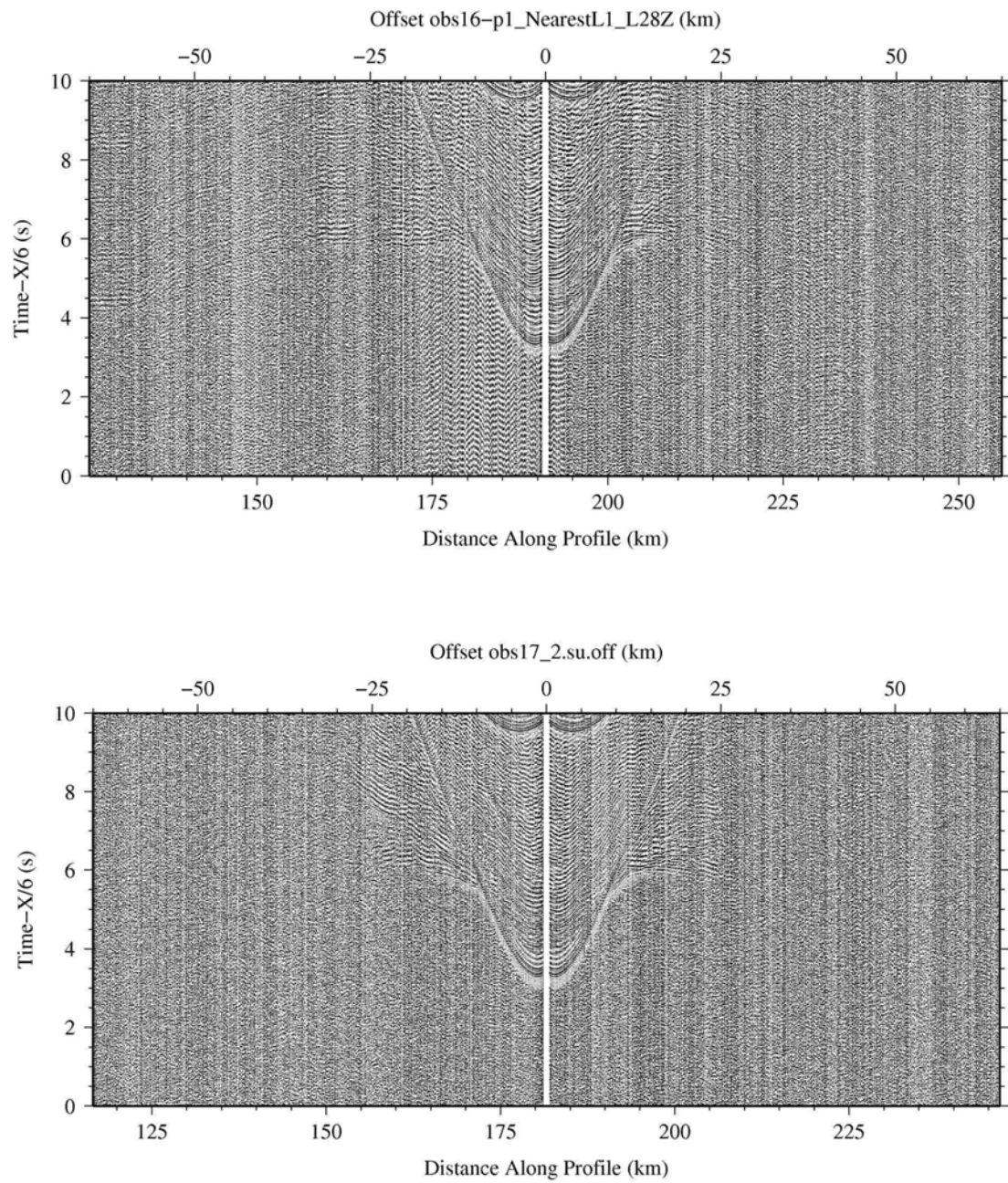


Figure 40.- Record section of OBS16 (up) and OBS17 (bottom) along P1 (vertical component). The OBS model is LC2000 (OBS16) and MicroOBS (OBS17).

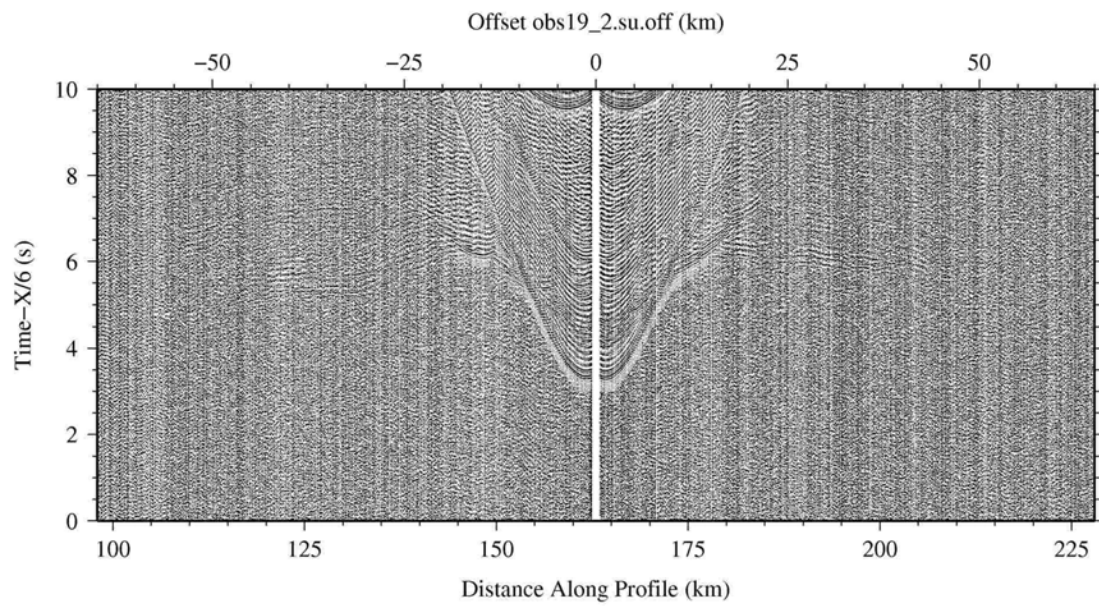
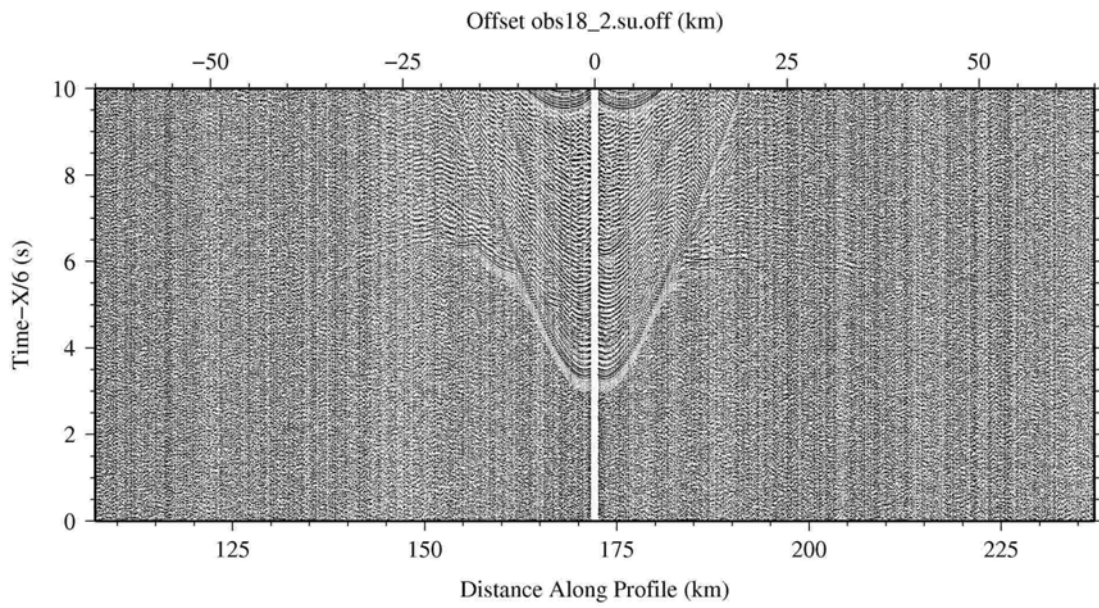


Figure 41.- Record section of OBS18 (up) and OBS19 (bottom) along P1 (vertical component). The OBS model is MicroOBS.

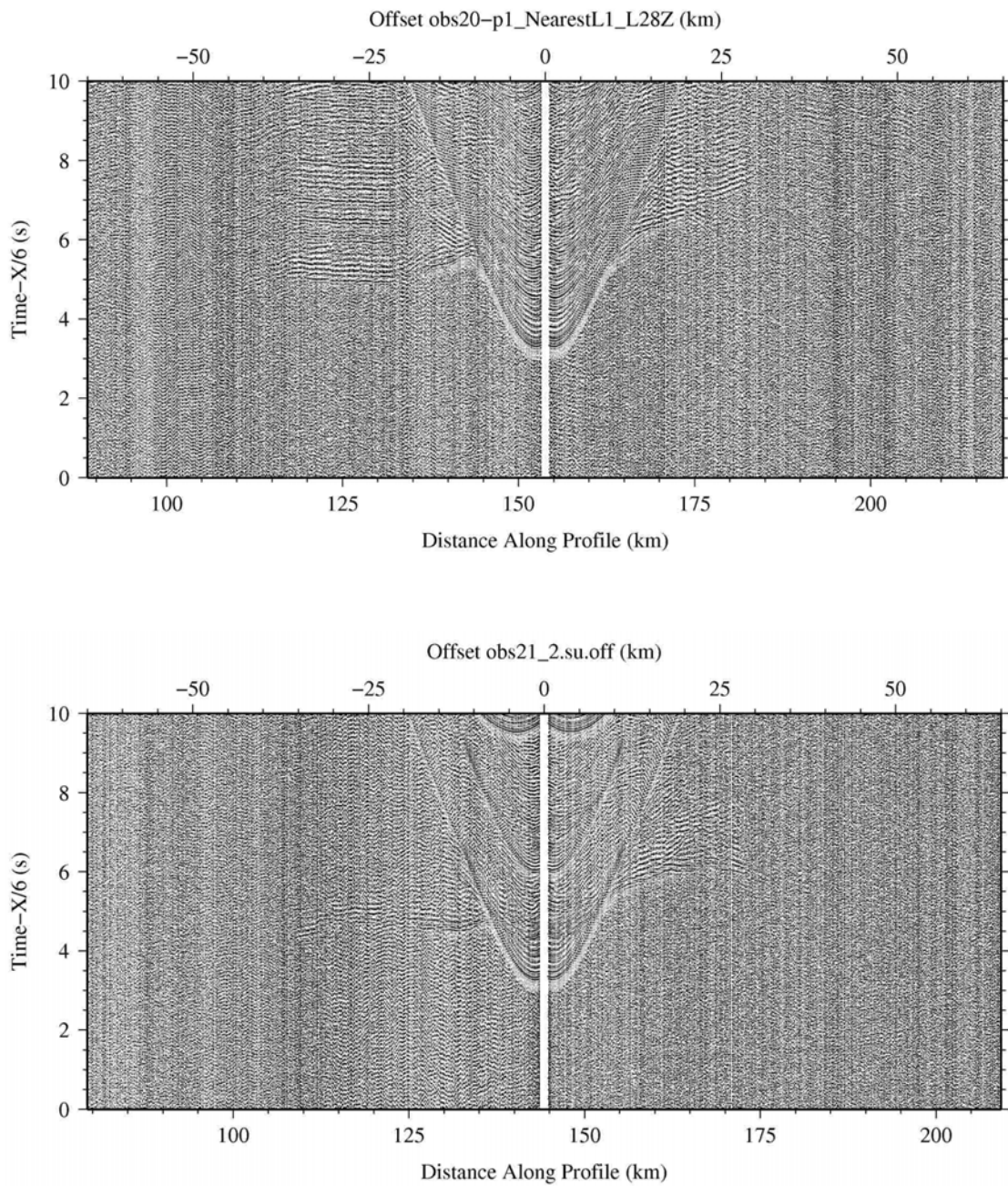


Figure 42.- Record section of OBS20 (up) and OBS21 (bottom) along P1 (vertical component). The OBS model is LC2000 (OBS20) and MicroOBS (OBS21).

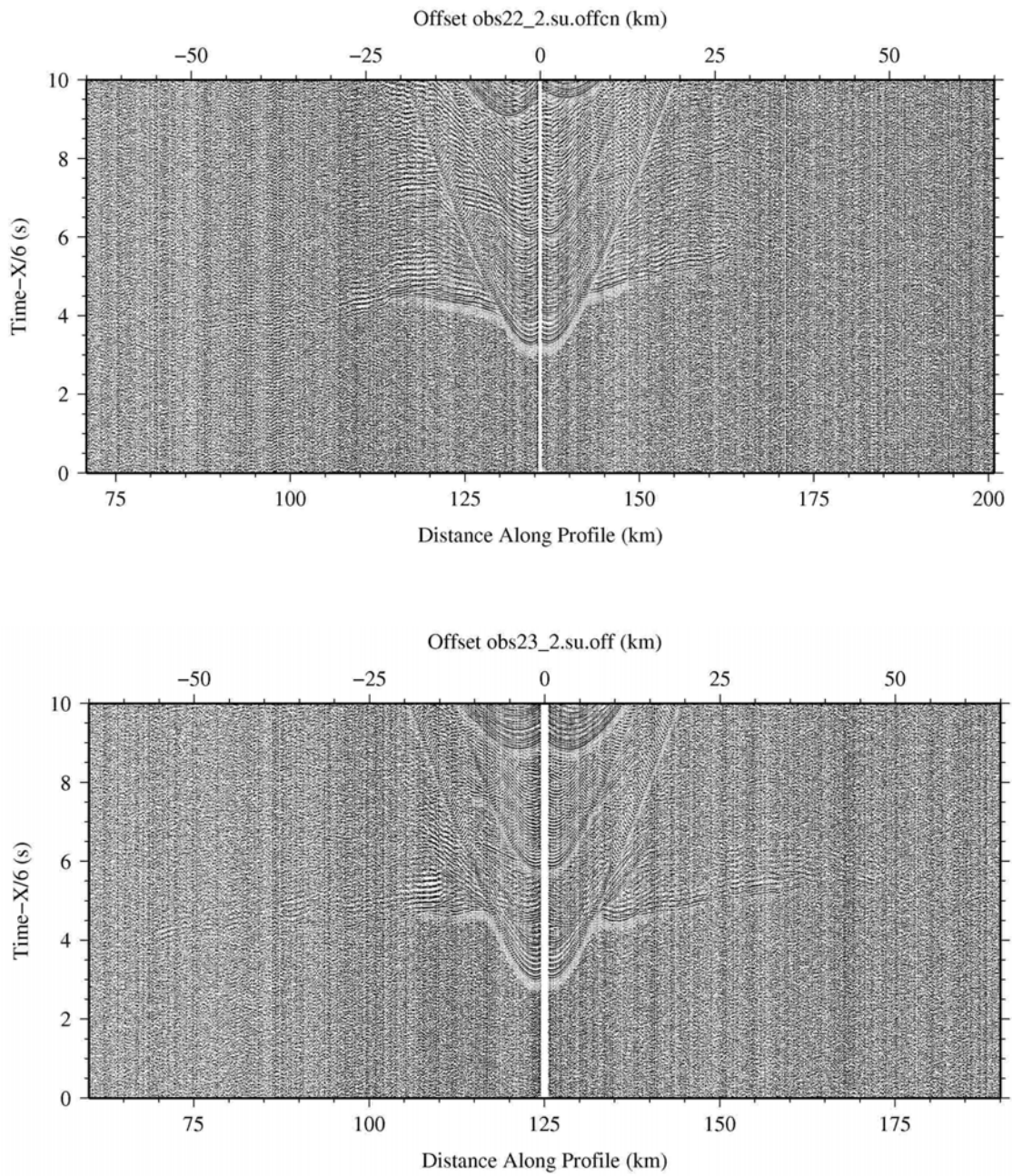


Figure 43.- Record section of OBS22 (up) and OBS23 (bottom) along P1 (vertical component). The OBS model is MicroOBS.

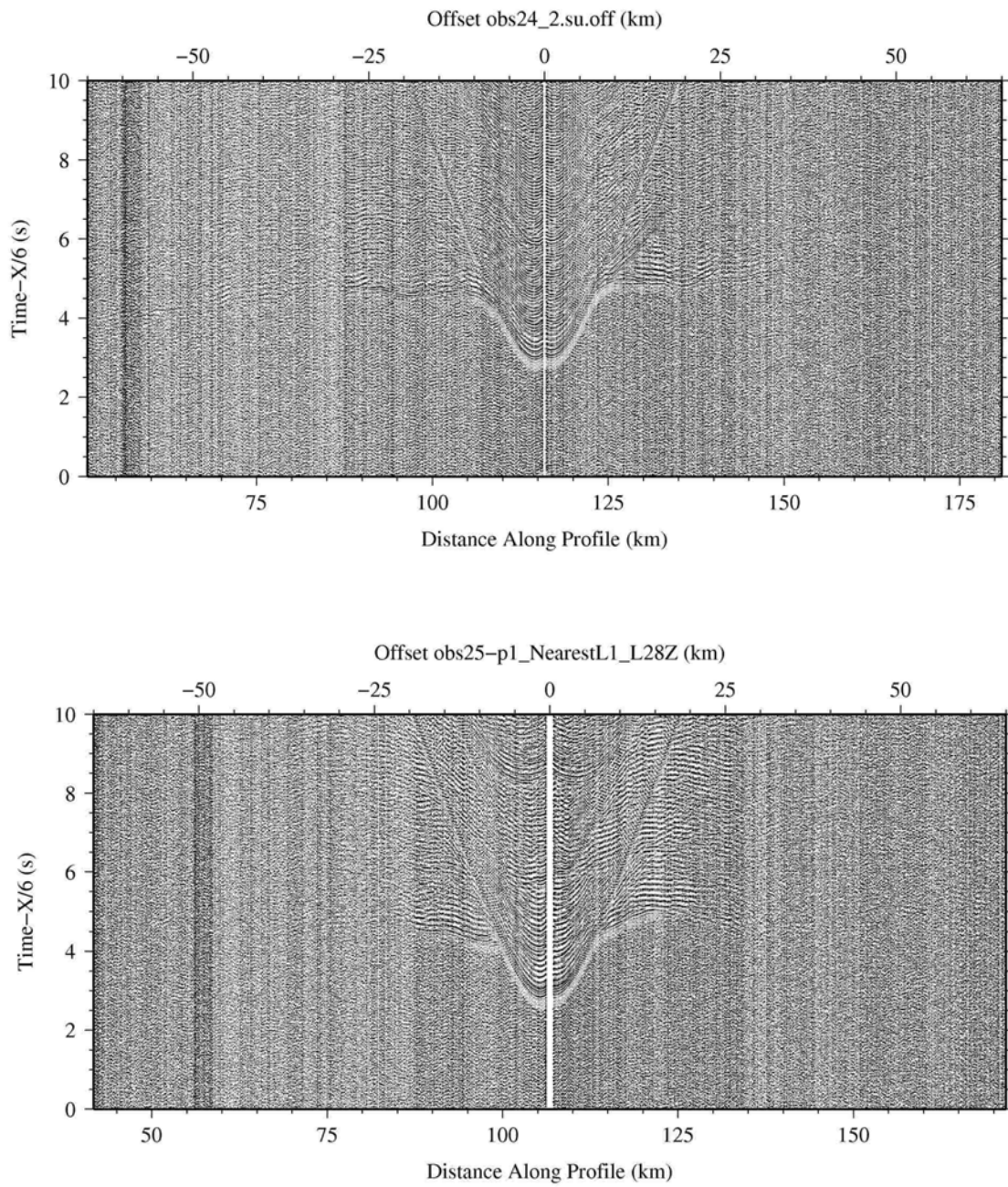


Figure 44.- Record section of OBS24 (up) and OBS25 (bottom) along P1 (vertical component). The OBS model is MicroOBS (OBS24) and LC2000 (OBS25).

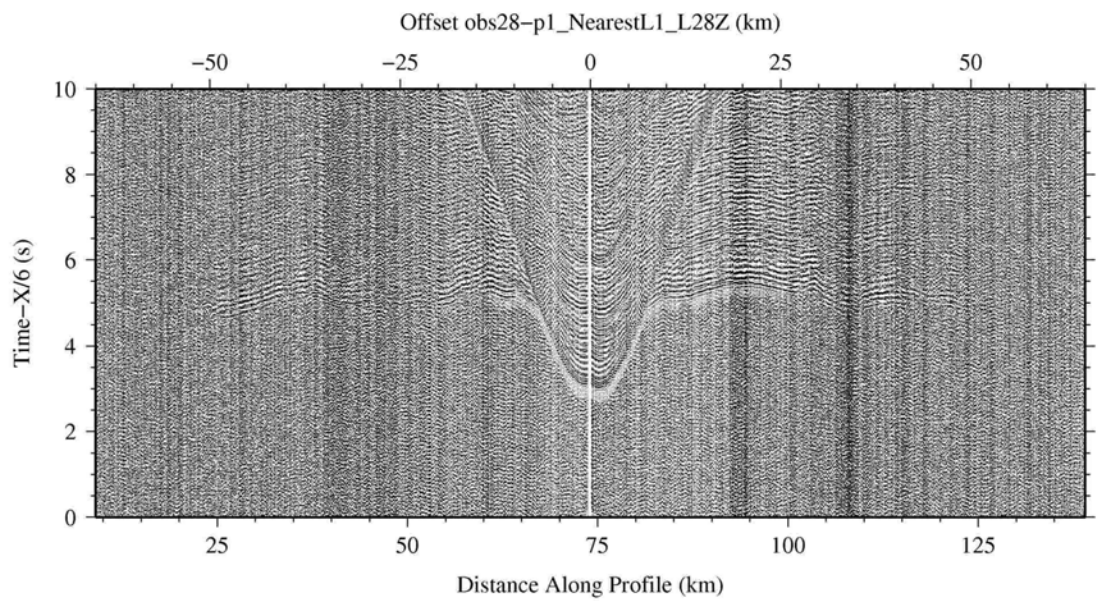
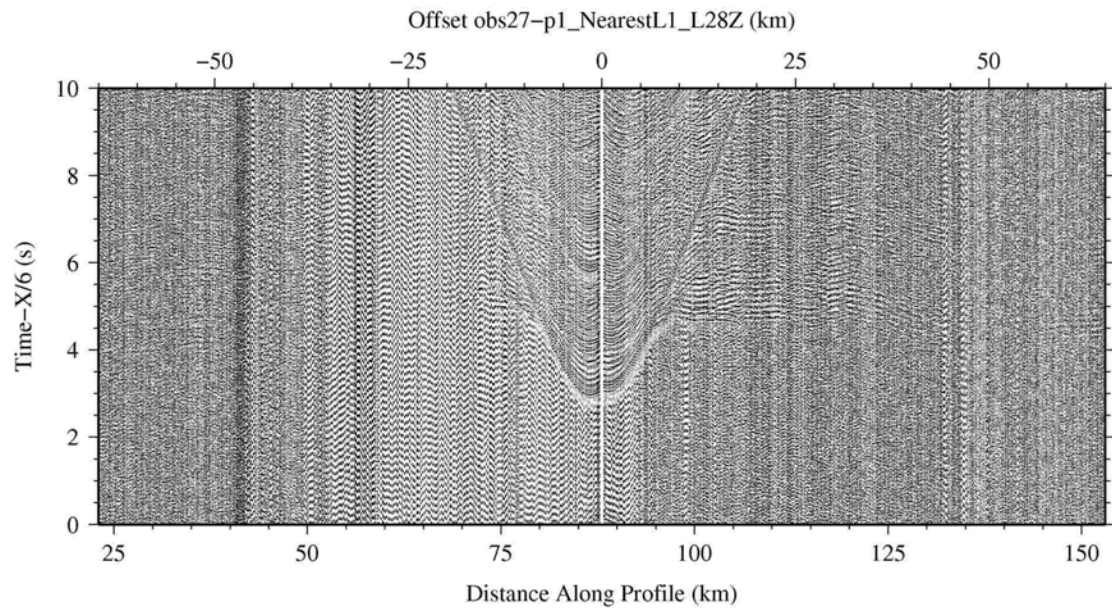


Figure 45.- Record section of OBS27 (up) and OBS28 (bottom) along P1 (vertical component). The OBS model is LC2000 .

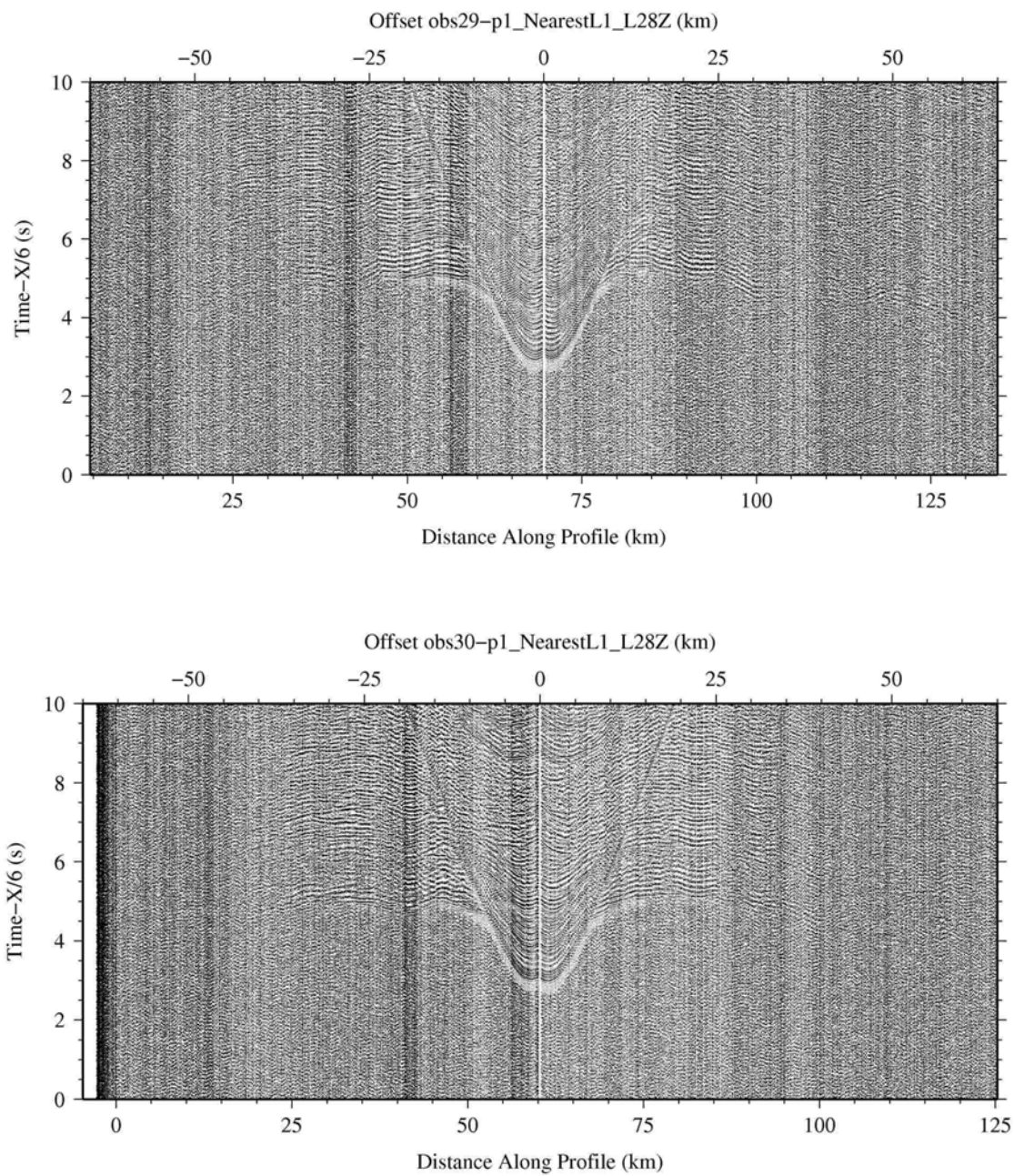


Figure 46.- Record section of OBS29 (up) and OBS30 (bottom) along P1 (vertical component). The OBS model is LC2000 .

10.2. Seismic records of airgun shooting along P2

Profile P2 was recorded by a total of 15 OBS and 9 landstations (Figure 47). The seismic source used was the same as in P1, and thanks to the good sea conditions the array worked fine during most of the line (see Annexes I and II: Diary of activities and Technical report). However, the OBS records have a systematic lower quality than in P1. In fact the signal was not recorded to more than 25-30 km in most of the OBS (Figures 48-55). The main reason is the presence of the accretionary wedge, the chaotic body that fills the eastern half of the Gulf of Cadiz (Figures 9 and 47). This disaggregated body is extremely attenuative, as had been proved in previous seismic experiments in the area (e.g. SISMAR). Conversely, landstation recordings have much higher quality, showing identifiable signal up to more than 150 km (Figures 55 to 58). The reason for the difference in quality between OBS and landstations is probably twofold: on one hand, OBS are deployed, without any control of coupling, on top of a *pile of rubble*, whereas landstations are carefully installed in appropriate locations. On the other hand, at OBS the seismic waves should cross the *pile of rubble* twice, but only once for landstations (roughly half attenuation). The interest of this profile was trying to determine the nature of the crust beneath that body (oceanic vs. other) in order to have additional hints on the tectonic behaviour of the area and on the possible occurrence of active subduction. In order to overcome the limitations related to the high attenuation, the profile was run at the frontal part of the wedge, where it is thinnest. But still, the recordings (given the source limitations), were poor.

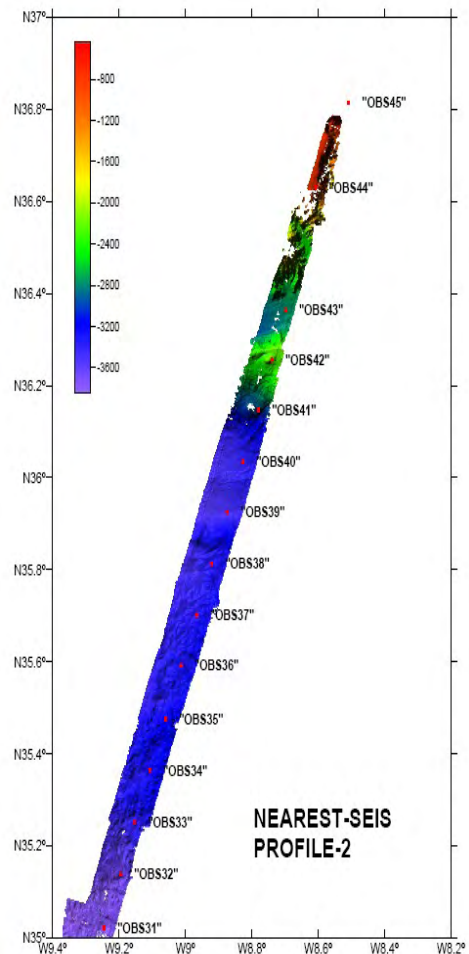
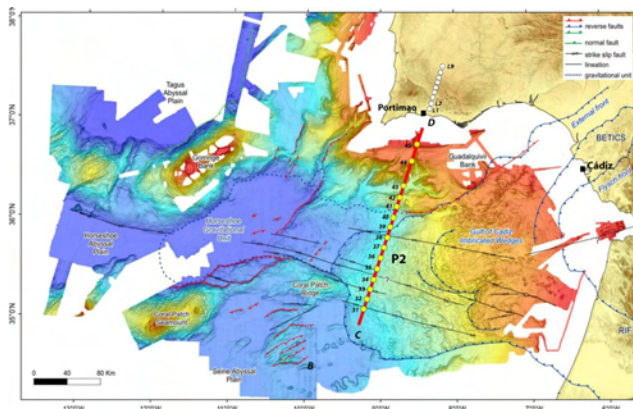


Figure 47 (previous page).- Bathymetric map of the study area with the location of P2 superimposed (red line) as well as OBS locations along this line (left). Detail of swath bathymetry data acquired along profile P2 with the OBS locations superimposed (OBS31-OBS45), as well as landstations (L1-L9) (right). The record sections of these OBS are shown in Figures 46 to 62.

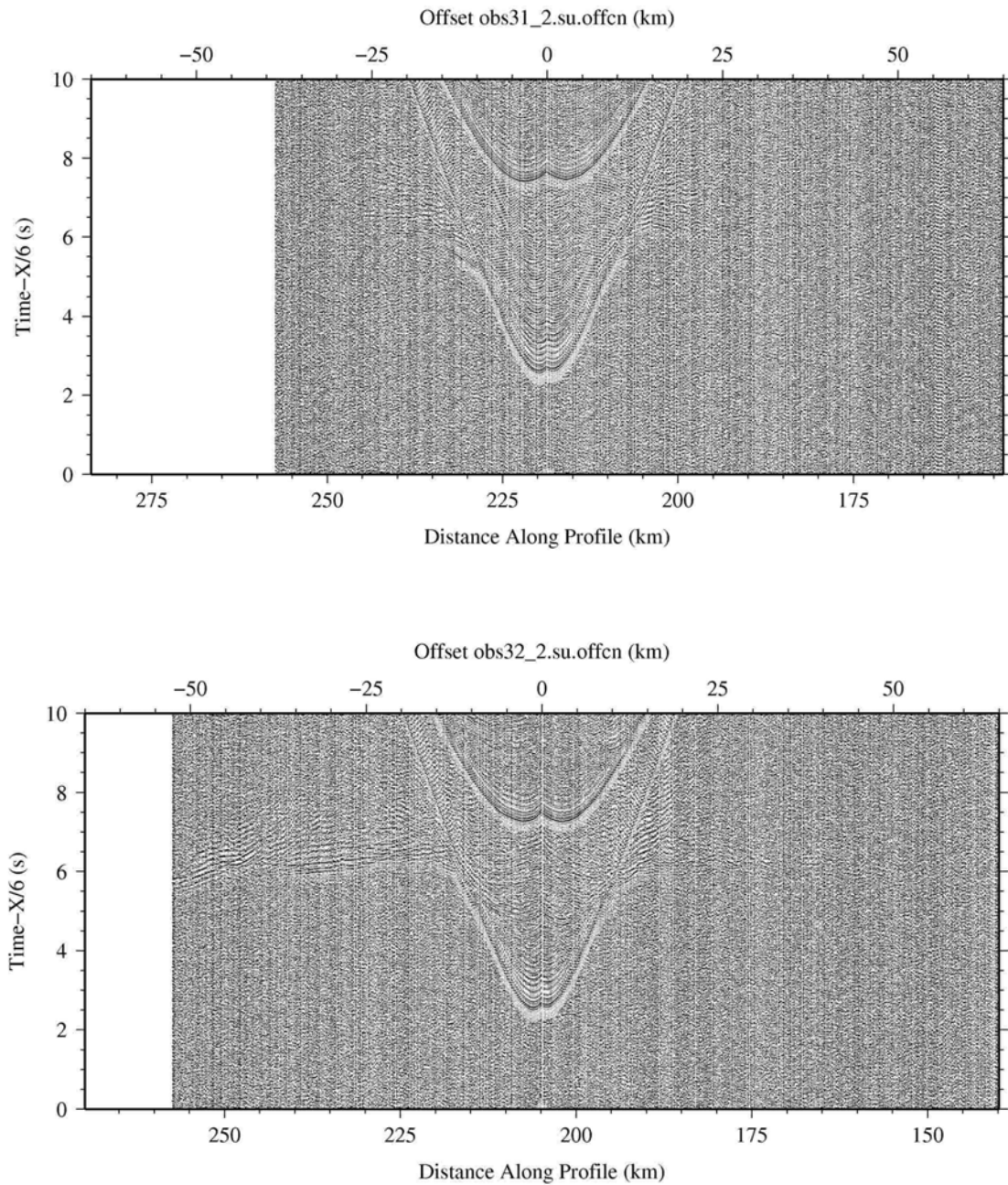


Figure 48.- Record section of OBS31 (up) and OBS32 (bottom) along P2 (vertical component). The OBS model is MicroBS .

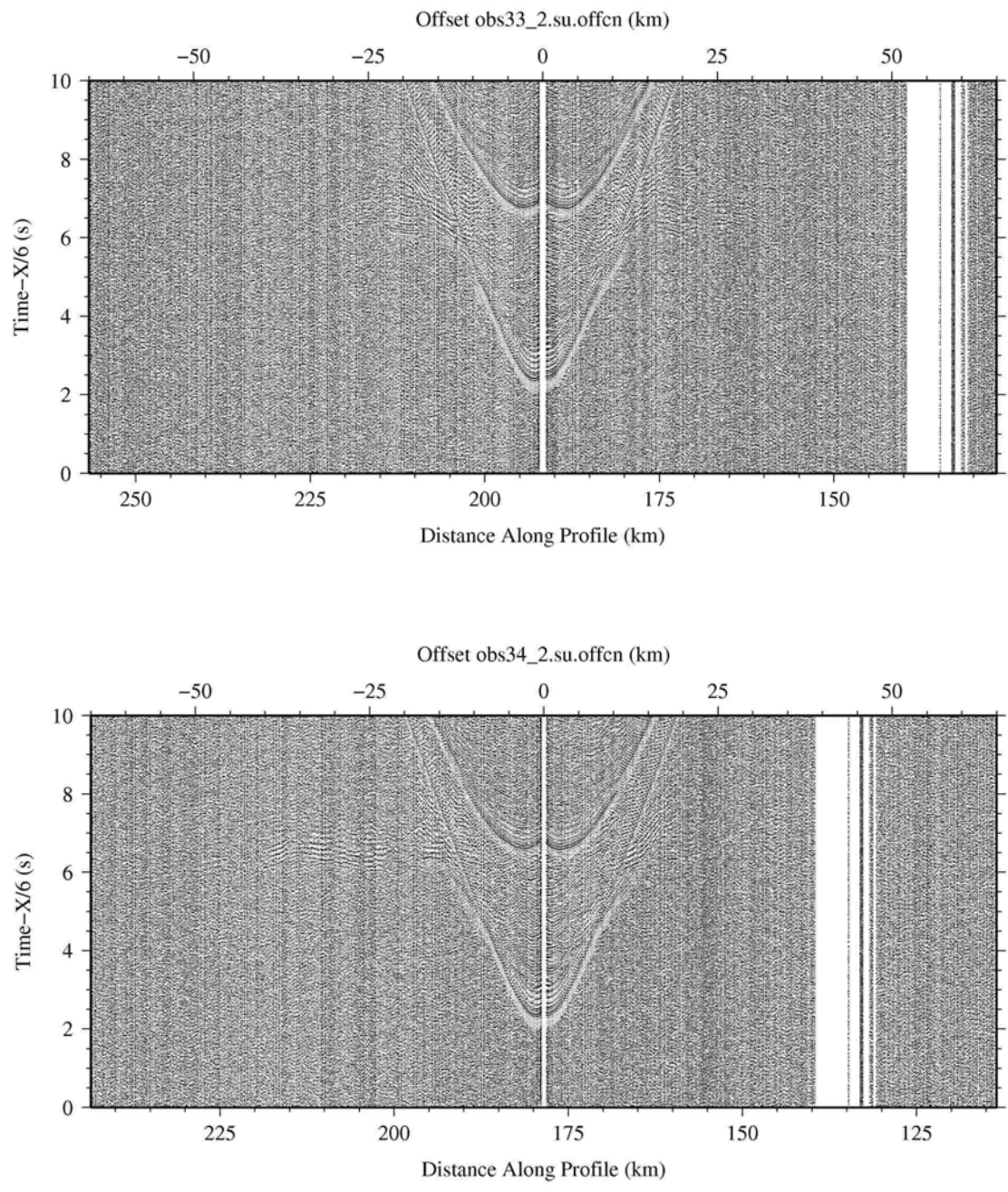


Figure 49.- Record section of OBS33 (up) and OBS34 (bottom) along P2 (vertical component). The OBS model is MicroBS .

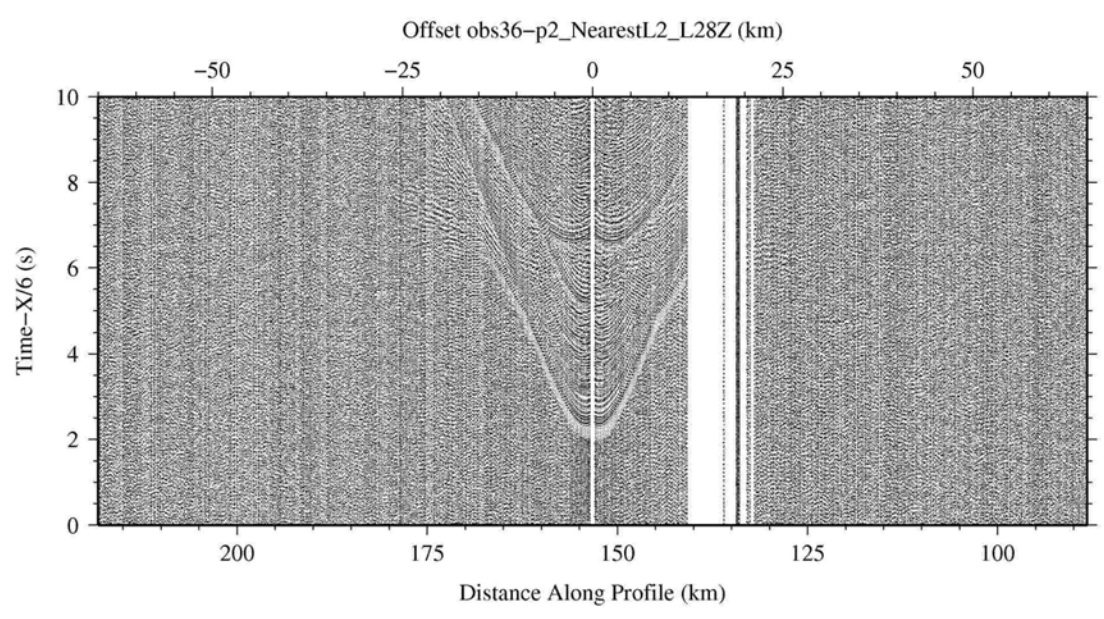
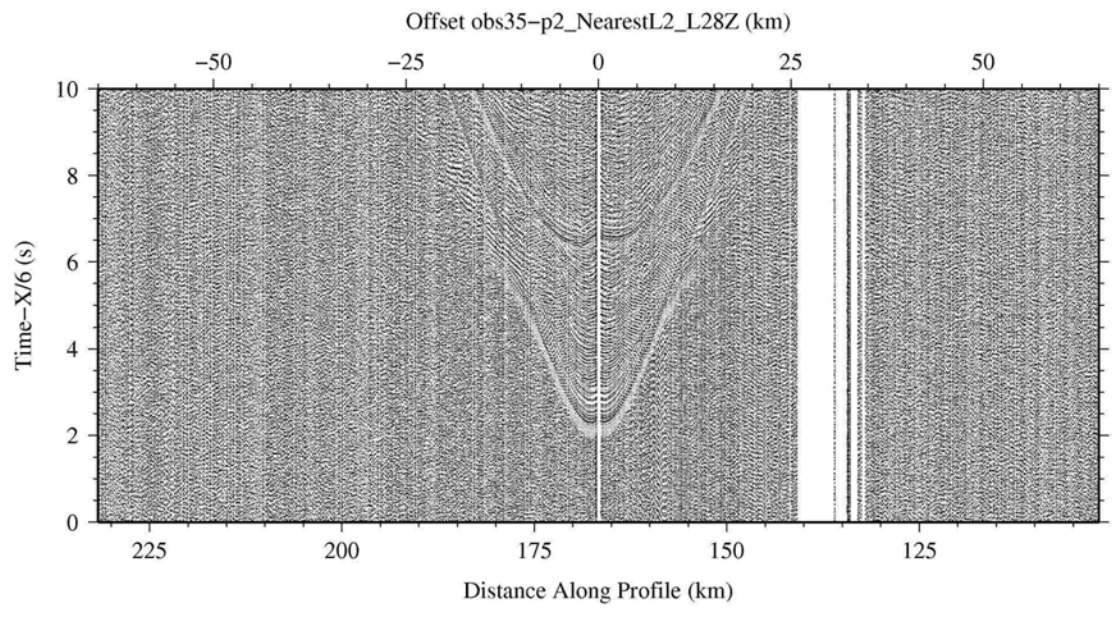


Figure 50.- Record section of OBS35 (up) and OBS36 (bottom) along P2 (vertical component). The OBS model is LC2000.

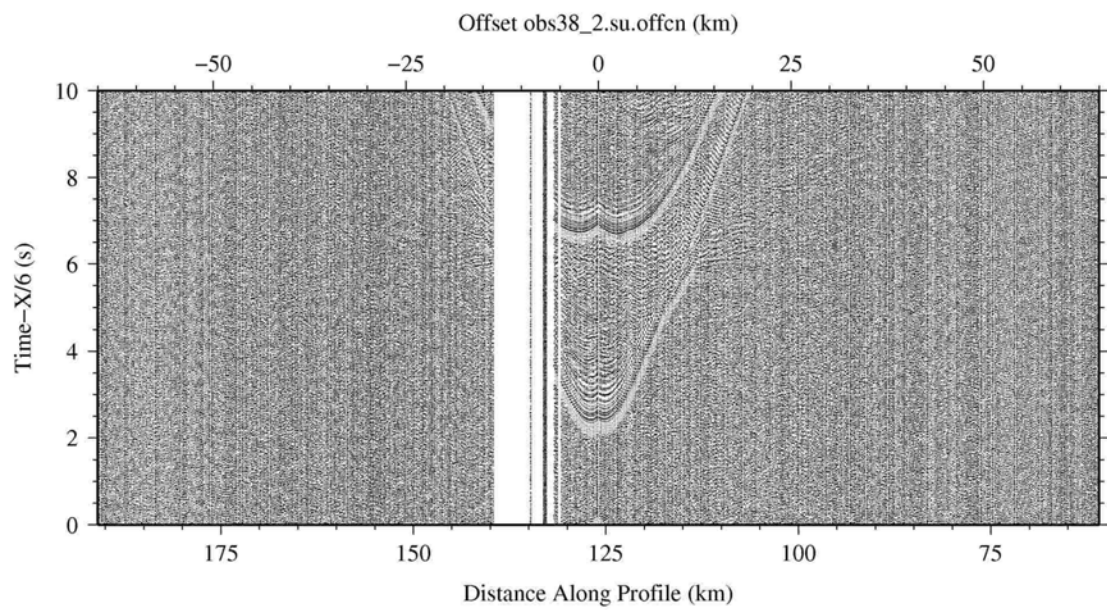
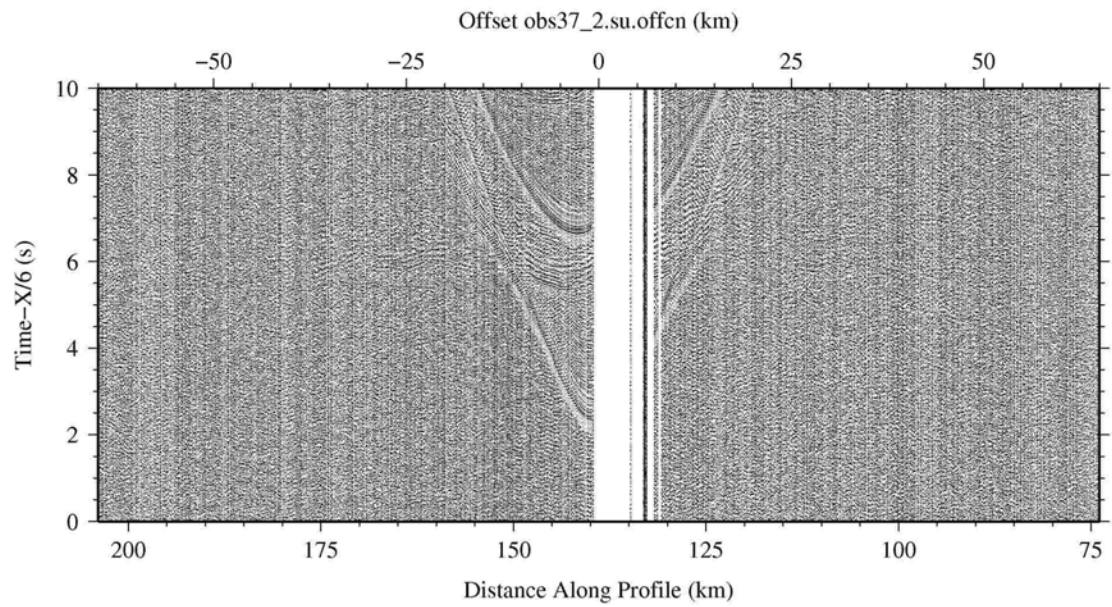


Figure 51.- Record section of OBS37 (up) and OBS38 (bottom) along P2 (vertical component). The OBS model is micrOBS.

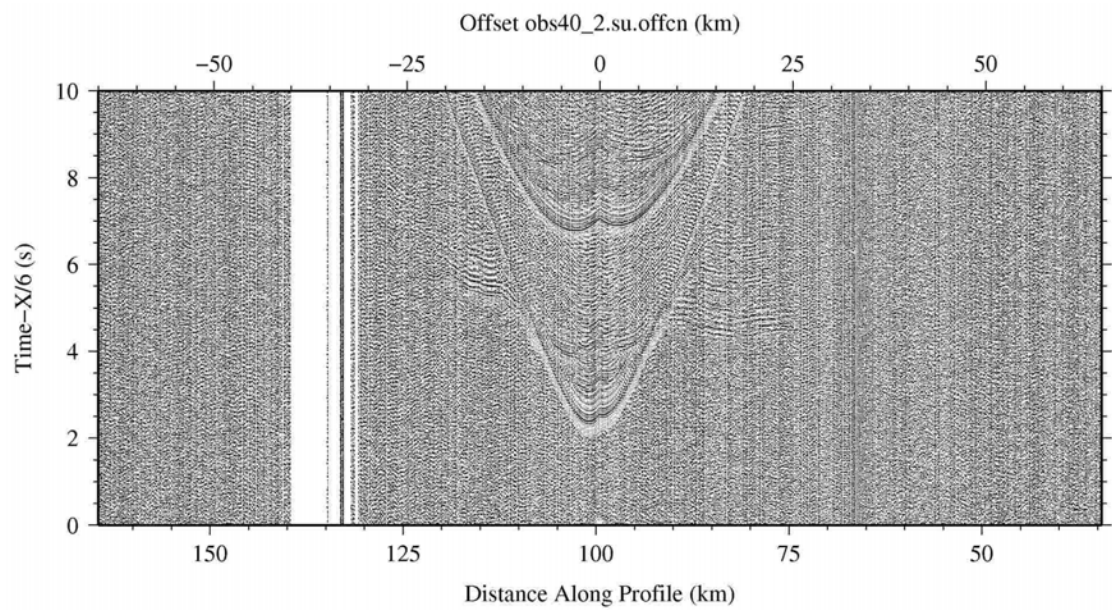
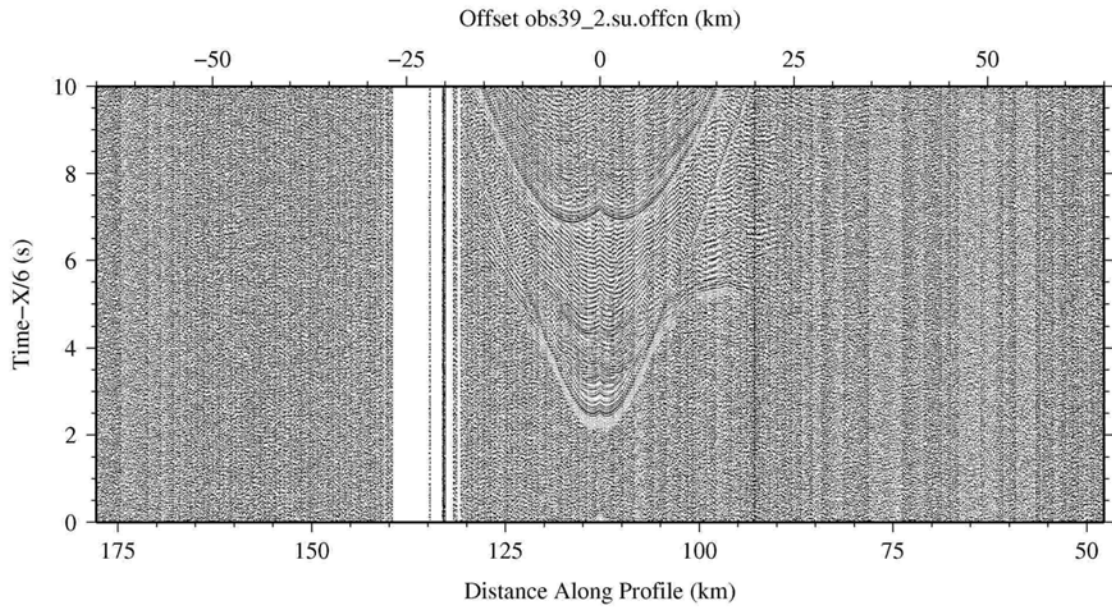


Figure 52.- Record section of OBS39 (up) and OBS40 (bottom) along P2 (vertical component). The OBS model is microOBS.

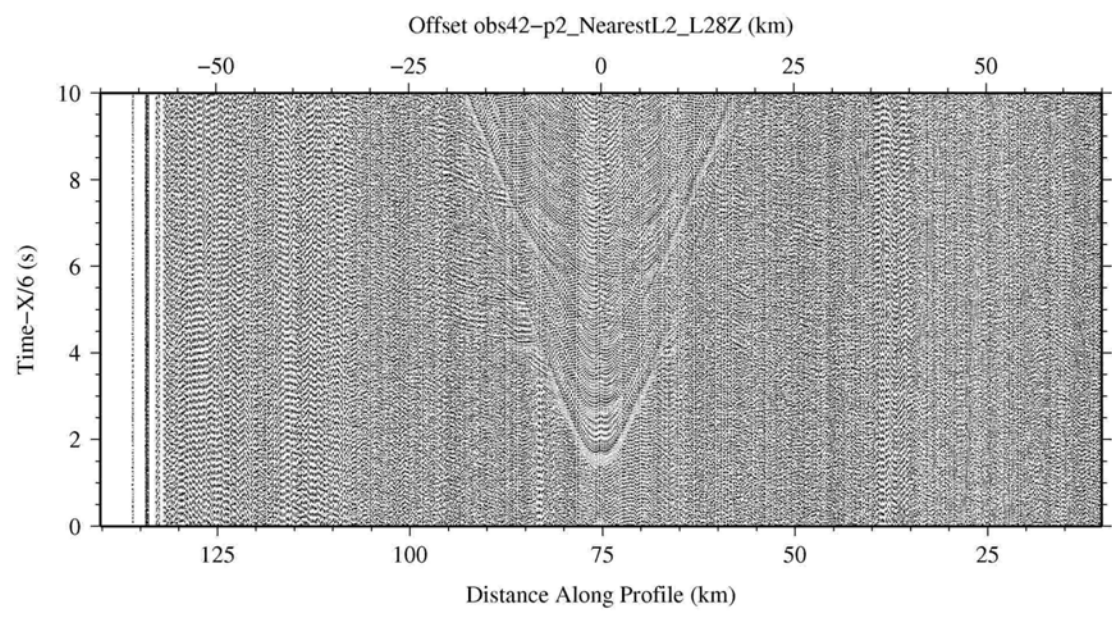
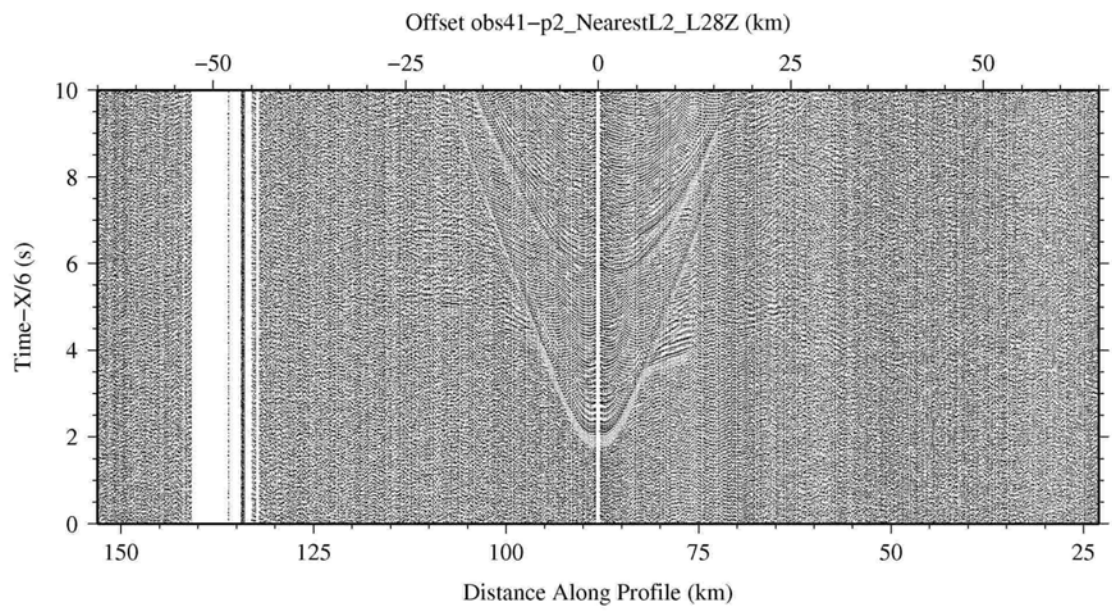


Figure 53.- Record section of OBS41 (up) and OBS42 (bottom) along P2 (vertical component). The OBS model is LC2000.

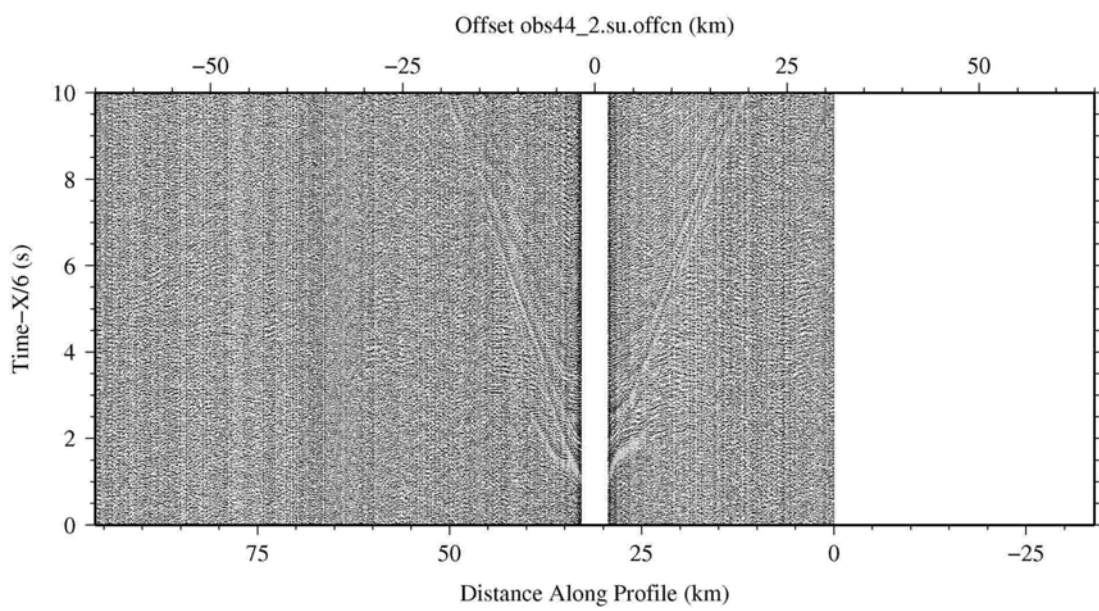
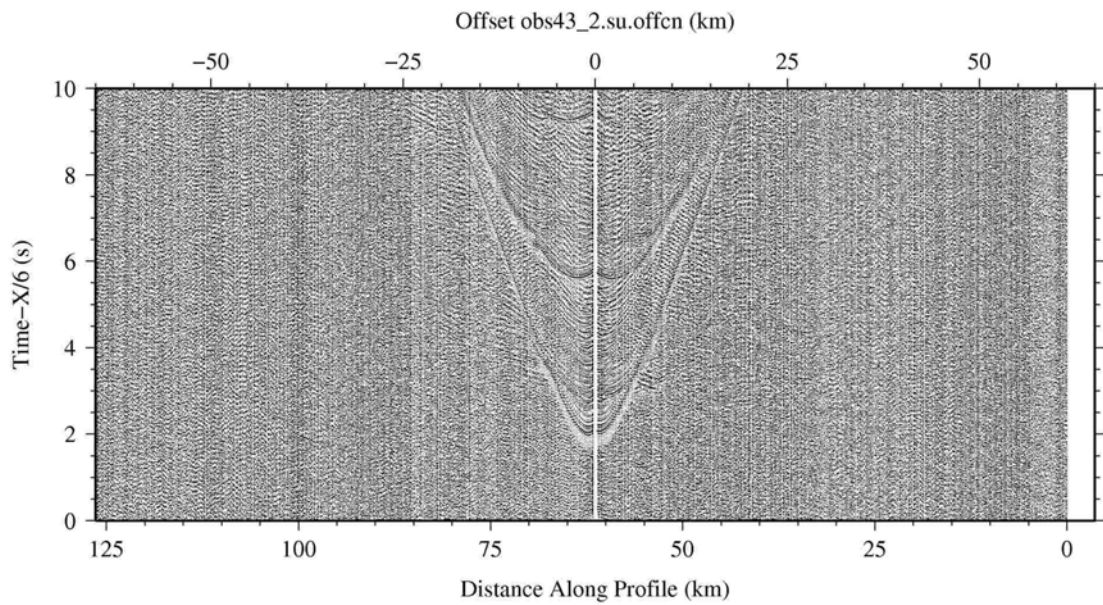


Figure 54.- Record section of OBS43 (up) and OBS44 (bottom) along P2 (vertical component). The OBS model is microOBS.

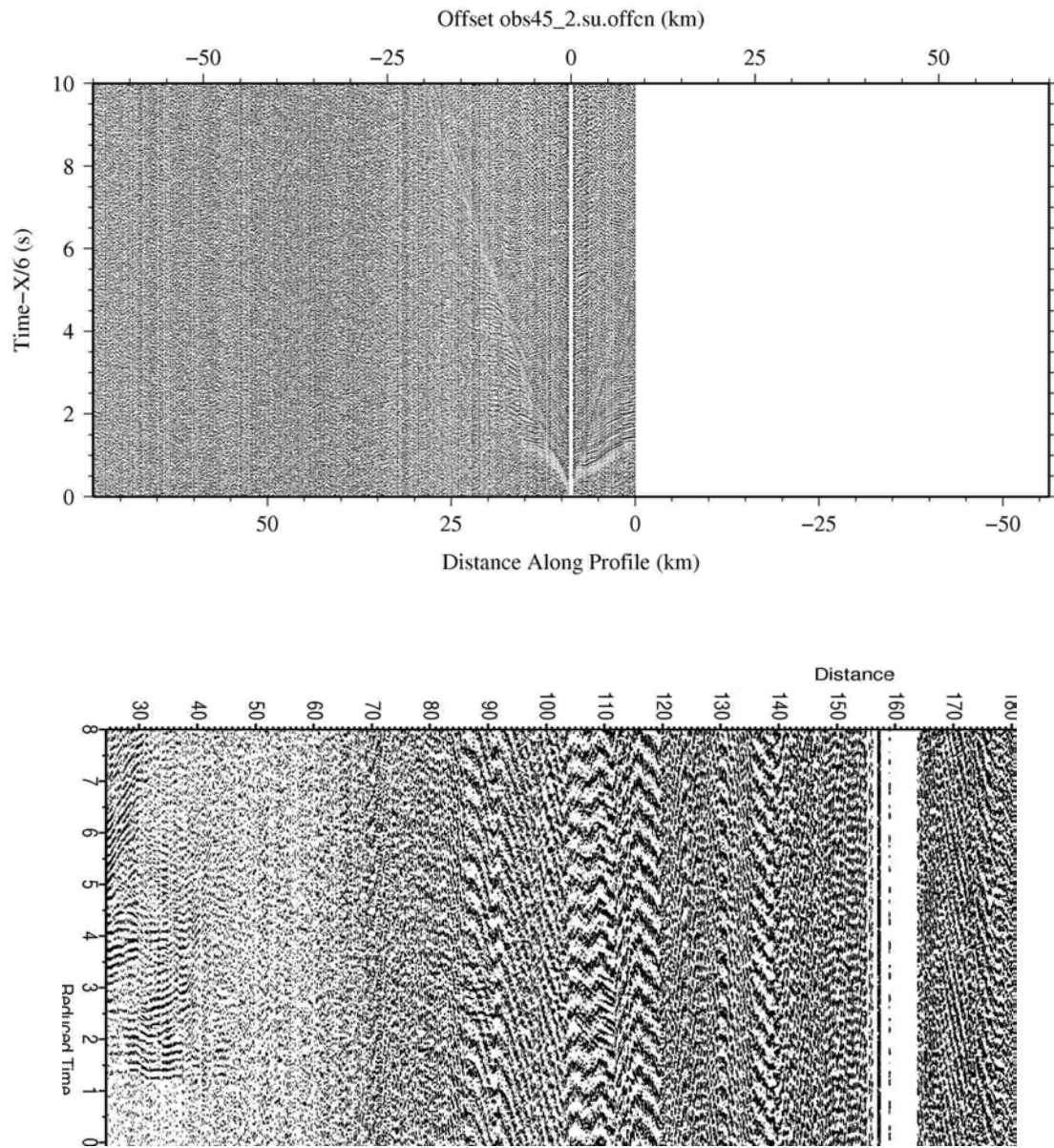


Figure 55.- Record section of OBS45 (up) and landstation L1 (bottom) along P2 (vertical component). The OBS model is micrOBS, and the landstation is Hathor.

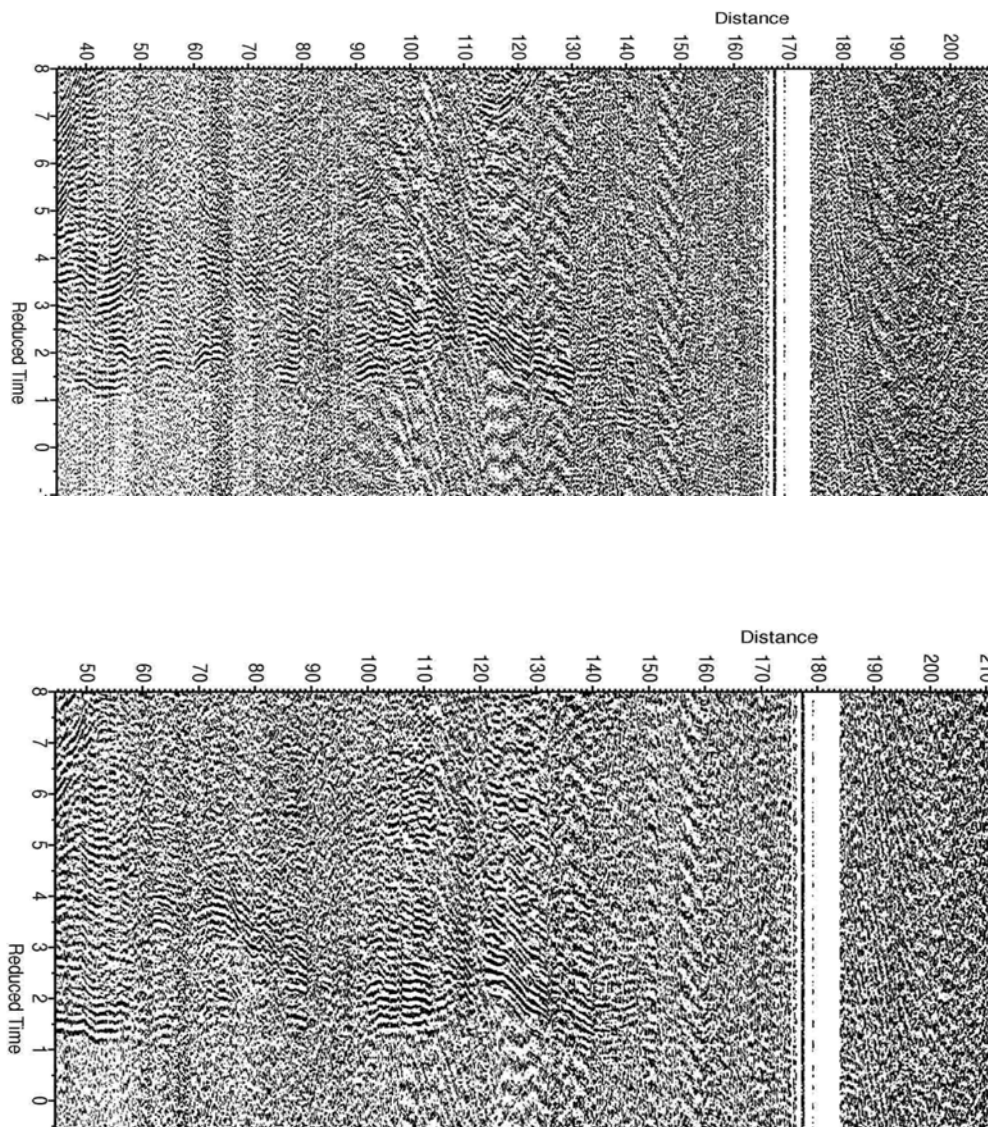


Figure 56.- Record section of landstgations L2 (up) and L3 (bottom) along P2 (vertical component). The landstation model is Hathor.

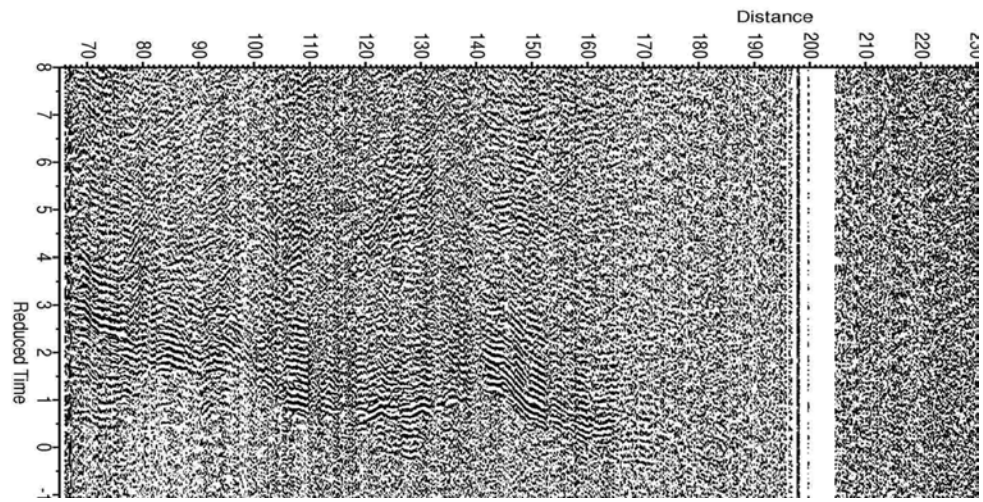
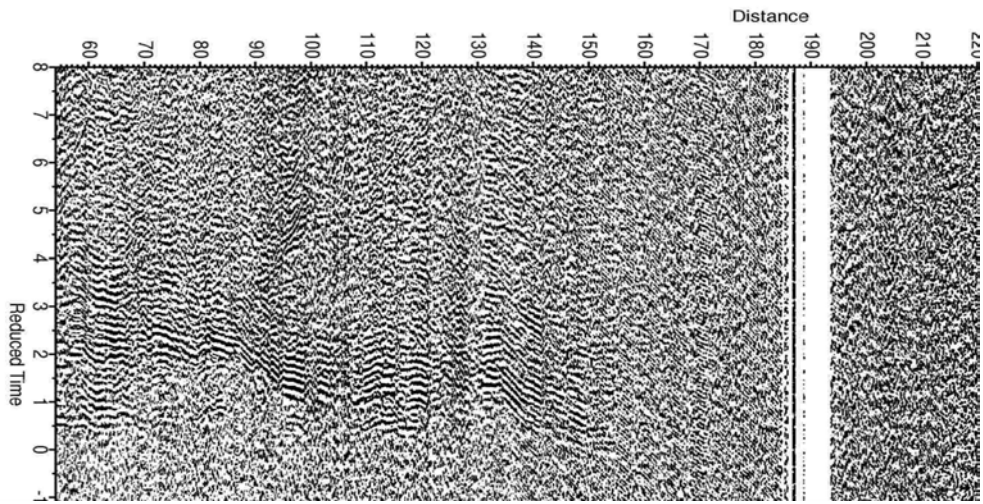


Figure 57.- Record section of landstgations L4 (up) and L5 (bottom) along P2 (vertical component). The landstation model is Hathor.

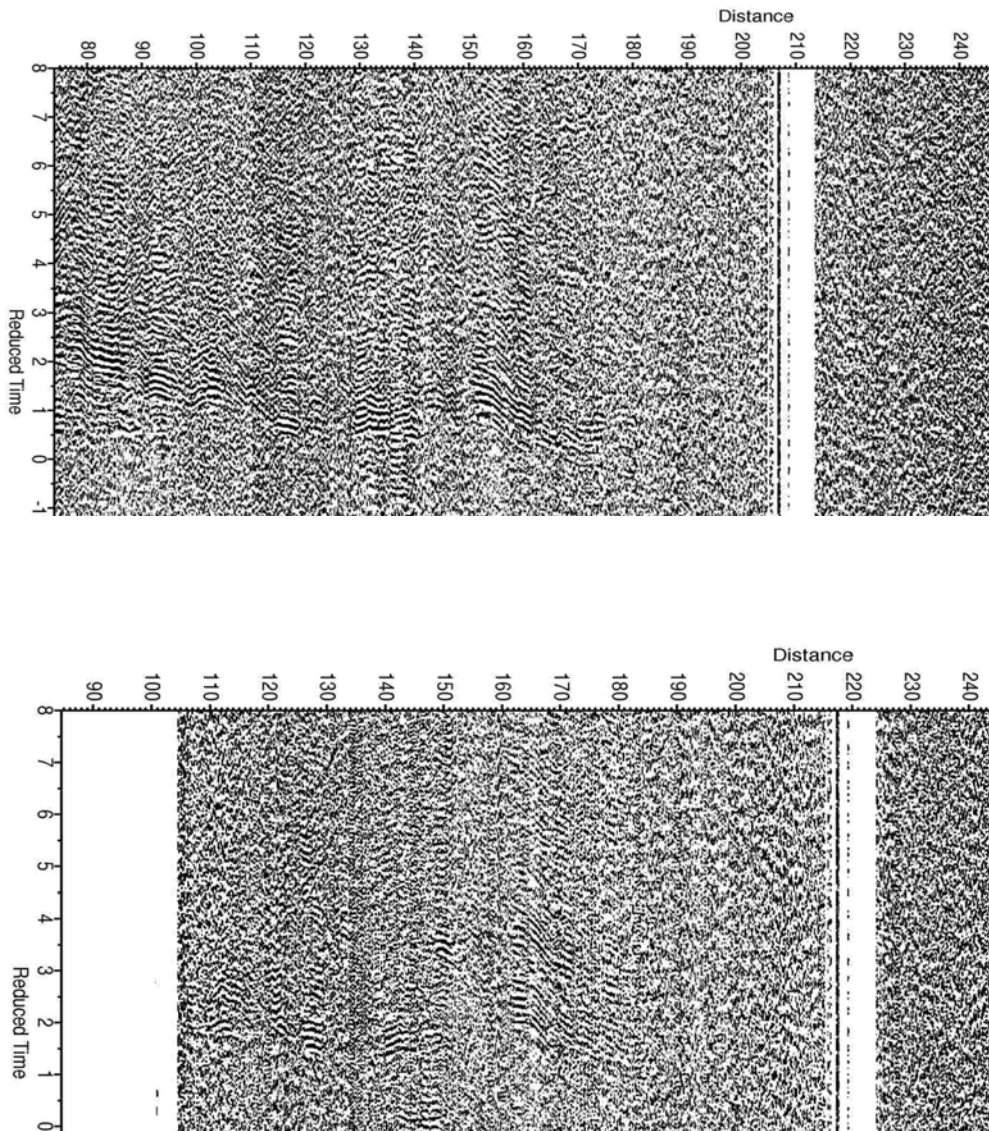


Figure 58.- Record section of landstgations L6 (up) and L7 (bottom) along P2 (vertical component). The landstation model is Hathor.

10.3. Local earthquakes recorded by OBS

In recent times no significant earthquakes occurred in the area of the NEAREST-SEIS experiment. The seismicity appears to be concentrated on particular, localized sectors of the active deformation zone, namely the Gorringe Bank, the Horseshoe plain, the Marques the Pombal, and the Guadalquivir-Portimao Bank (Figure 5 left), with magnitude not exceeding ML 6.1.

The low magnitude earthquake occurrence in the study area is almost continuous. As example, for the period of the NEAREST OBS network experiment (*NEAREST 2008 Cruise Preliminary Report r/v Urania*), from the 29th August 2007 till the 31st July 2008 (335 days), in the proximity of the network were located 276 seismic event (Fig. 13, right). Their magnitude (ML), computed by Instituto de Metereologia, Portugal) ranges from 0.5 to 4.7. So it is not surprising that also during the few days of the NEAREST-SEIS experiment low magnitude events were detected by land seismic networks, and reported on national and international bulletins as located off-shore or near coast (Table 1).

<u>Date (TU)</u>	<u>Lat N</u>	<u>Lon.W</u>	<u>Depth</u>	<u>Mag.</u>	<u>Epicentral area.</u>
2008-11-09 12:22	37,83	-9,52	31	1,6	SW Sines
2008-11-09 07:58	36,67	-7,50	22	1,6	Golfo de Cádiz
2008-11-08 21:16	33,13	-5,27	13	2,3	SW Fez (MARR)
2008-11-08 11:28	36,30	-8,22	15	1,8	SW Faro
2008-11-08 01:31	36,78	-7,64	28	1,2	Golfo de Cádiz
2008-11-07 20:20	37,31	-8,61	14	2,0	W Monchique
2008-11-06 14:31	37,32	-8,56	6	1,2	NW Monchique
2008-11-06 05:54	36,58	-9,62	20	2,3	SW Cabo S.Vicente
2008-11-06 03:41	36,58	-7,57	17	2,7	Golfo de Cádiz
2008-11-05 21:23	36,55	-7,62	18	2,2	Golfo de Cádiz
2008-11-05 13:57	37,16	-9,28	17	2,1	NW Cabo S.Vicente
2008-11-05 07:07	37,27	-8,65	21	0,9	SW Monchique
2008-11-04 04:50	36,96	-8,00	15	1,3	SW Faro
2008-11-03 20:21	35,75	-10,03	23	2,9	Mar de Marruecos

Figure 3

2008-11-03 07:05	36,61	-9,76	17	1,7	SW Cabo S.Vicente
2008-11-02 16:04	36,32	-8,34	15	1,7	SW Faro
2008-11-01 19:52	36,60	-11,22	30	1,6	Gorringe
2008-11-01 09:17	35,39	-5,95	48	2,1	SW Tanger (MARR)
2008-11-01 06:52	36,69	-11,24	31	1,9	Gorringe

Figure 2

2008-10-31 20:54	36,28	-8,47	16	1,3	SW Albufeira
2008-10-31 02:34	34,85	-5,21	14	2,4	S Tetuan (MARR)

Table 1.- Earthquakes in off-shore and coastal areas occurred during the deployment of the NEAREST-SEIS OBS (from Instituto de Metereologia Portugal, online bulletin – www.meteo.pt). The events reported in figures 2 and 3 are underlined.

The waveforms of these kind of seismic events are generally characterized by high-frequency contents, so the sensors used in the NEAREST-SEIS experiment (4.5 Hz) can record them properly. During the preliminary observation of the seismometers recording, performed during the cruise after the recovery of OBSs, some of these events were recognised. Their detection is

important, as testify the good coupling of instruments to the seafloor. In the first example here reported, the onset of P and S phases is clearly recognisable on waveforms shown in Figure 59 (right) recorded at OBSs 8,13,14 of profile P1, and referred to the 1/11/2008 06:52 (GMT) earthquake with magnitude ML=2.5. The Euro-Mediterranean Seismological Centre (EMSC) located the event on the Gorringe Bank area (Figure 59 left).

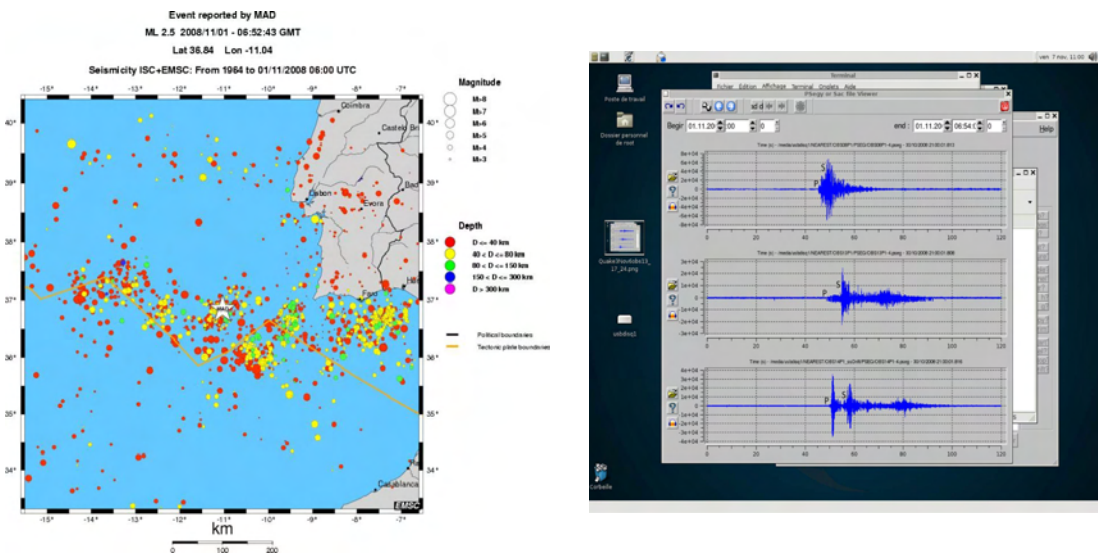


Figure 59.- Epicenter location of 2008/11/01 – 06:52:42 GMT M 2.5 event, as reported by EMSC bulletin; with seismicity overimposed (left). Waveforms from OBSs 8 (top), 13 (mid), 14 (bottom), P1 profile (right). OBS locations are shown in figure 12.

Similarly the earthquake of ML 3.1 occurred the 3/11/2008 at 20:21 (GMT) and located in the Horseshoe Plain (fig 3 left) was well detected from the OBSs. Here waveforms from OBSs 13, 17, 24 are reported in figure 3 (right). In both examples, as expected, the S-P time interval is smaller for the station closer to epicenter.

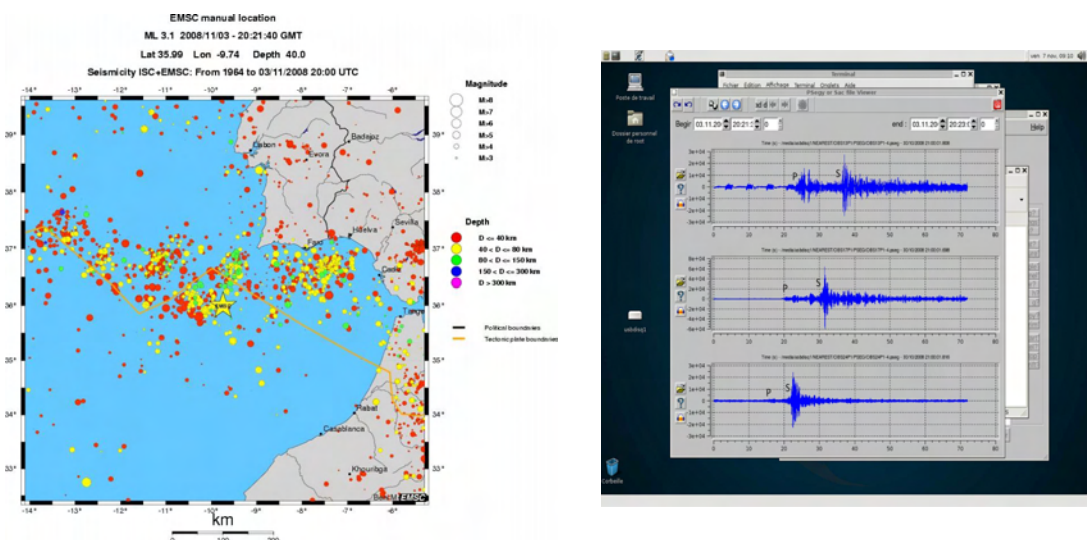


Figure 60.- Epicenter location of 2008/11/03 – 20:21:40 GMT M 3.1 event, as reported by EMSC bulletin; with seismicity overimposed (left). Waveforms from OBSs 13(top), 17 (mid), 24 (bottom), P2 profile (right) . OBS locations are show in figure 12.

Notwithstanding the monitoring of the local seismicity is not the topic of the NEAREST-SEIS experiment, the recorded seismograms will be carefully observed to verify the detection of events located by national networks, or simply recorded by few seismological stations. For each event the available onset of P and S phases observed on off shore sensors, will get better the quality of the data set, as it will increase the number of phases and will reduce the azimuthal gap. Consequently will improve the hypocentral parameters and the contents of seismological bulletins.

11. Conclusions

The NEAREST-SEIS cruise has been a success in the sense that it has allowed acquiring a unique data set of Wide-Angle seismic (WAS) data along two long profiles crossing most of the potentially seismogenic/tsunamigenic structures off the NW Iberian margin. It is worth to note that all the Ocean Bottom Seismometers that were deployed during the full survey (29 in P1 and 15 in P2 for a total of 44) were successfully recovered, and all of them recorded continuously during the airgun shooting phase. Despite the vessel limitations in what concerns size and power of compressors, the airgun array was proved to be efficient enough to produce seismic energy at the low frequencies required to record identifiable signal at the long distances characteristic of WAS experiments. The maximum offset at which seismic energy is recorded enormously varies, however, depending on the place where the instrument was deployed.

The best recordings along P1 are obtained at the Seine Abyssal plain, with clear arrivals corresponding to waves refracted in the sediments, crust and uppermost mantle that are identifiable to more than 75 km from the source. In the Tagus Abyssal plain and the flanks of the Gorringe bank the range of the signal is smaller, varying between 40 and 60 km depending on the OBS, whereas it is 30 to 50 km in the Horseshoe Abyssal plain. Conversely, almost no reflections have been identified (specially at the crust-mantle boundary). The limited recording range in the Horseshoe plain is most probably related to the attenuative nature of the thick gravitational unit that covers the crust. The good overall data quality, as well as the dense OBS sampling along the profile, warrants a good quality tomographic model along P1. This, in turn, must allow to achieve the objectives of providing information about the structure, physical properties and, most important, nature of the different domains. The velocity information will be also used to construct a regional 3D model for earthquake relocation.

The quality of OBS recordings along P2 is systematically lower than along P1. Therefore, only few of the record sections show identifiable signal (first arrivals) to more than 30 km, but still, there are several ones that show refracted phases at the accretionary wedge and underlying crust and reflections at the top of the basement. The lower quality of the data is most likely due to the presence of the extremely attenuative and thick gravitational unit of the eastern Gulf of Cadiz (i.e. the so-called accretionary wedge) and not to the limited energy of the seismic source. Concerning this, it is worth noting that the shots along P1 were recorded on land to more than 150 km from the source. The difference between OBS and landstations is twofold: on one hand, OBS are deployed, without any control of coupling, on top of a *pile of rubble*, whereas landstations are carefully installed in appropriate locations. On the other hand, at OBS the seismic energy should cross the pile of rubble twice, but only once for landstations (roughly half attenuation). Notwithstanding the limited quality of the data along this profile, the identification of refracted phases beneath the wedge in a number of the OBS should give information on the velocity (and in turn on the possible nature) of the underlying crust. This is a key observation in order to prove or disprove some of the proposed tectonic models of the area (e.g. the occurrence or not of ongoing subduction).

Concerning the rest of data acquired during the cruise, they complement the WAS data and will be used during modelling. Swath bathymetry has provided accurate bathymetry along the profiles, which is key for modelling, but during the survey the system was also used to select appropriate locations for OBS deployment. Also, the bathymetry map of the area (Figure 12) was completed in some selected areas. The TOPAS profiles contain relevant information on the detailed structure of the uppermost sediment layers, and therefore on the recent activity of the different faults imaged. Finally, gravity data will be used to constrain velocity-derived density models along the two transects. Having both density and velocity for a given crustal domain will help to better constrain its possible nature than velocity alone.

12. References

- Abe, K. (1989). Size of great earthquakes of 1837-1974 inferred from tsunam data. *J. Geophys. Res.* 84, 1561-1568.
- Alves, T.M.; Gawthorpe, R.L.; Hunt, D.W. and Monteiro, J.H. (2003). Cenozoic tectono-sedimentary evolution of the western Iberian Margin. *Marine Geology*. 195 ;1-4, 75-108.
- Argus, D.F., Gordon, R.G., Demets, C., Stein, S., (1989). Closure of the Africa-Eurasia-North America plate motion circuit and tectonics of the Gloria fault, *J. Geophys. Res.* 94, 5585-5602.
- Banda, E., M. Torné, and IAM Group (1995). Iberian Atlantic Margins group investigates deep structure of ocean margins, *Eos Trans. AGU*, 76 (3), 25-32.
- Baptista, M.A., Heitor, S., Miranda, J.M., Miranda P.M.A., and Mendes Victor, L., (1998a). The 1755 Lisbon; Evaluation of the tsunami parameters, *J. Geodynamics* 25, 143-157.
- Baptista, M.A., Miranda P.M.A., Miranda, J.M., and Mendes Victor, L., (1998b). Constraints on the source of the 1755 Lisbon tsunami inferred from numerical modelling of historical data on the source of the 1755 Lisbon tsunami. *J. Geodynamics* 25: 159-174.
- Baptista, M.A., Miranda P.M.A., Chierici, F., and Zitellini, N. (2003). New study of the 1755 earthquake source based on multi-channel seismic survey data and tsunami modeling. *Natural Hazards and Earth Science Systems* 3, 333-340.
- Bergeron, A., and J. Bonnin, (1999). The deep structure of Goringe Bank (NE Atlantic) and its surrounding area, *Geophys. J. Int.*, 105, 491-502.
- Bonnin, J., J.L. Olivet, and J.M. Auzende, Structure en nappe à l'ouest de Gibraltar, *C. R. Acad. Sci. Paris*, 280, 559-562, 1975.
- Bufo, E.; Beezzechoud, M.; Udias, A.; Pro, C.; (2004). Seismic sources on the Iberia-Africa plate boundary and their tectonic implications. *PAGEOPH*, 161; 3, 623-646
- Dañobeitia, J.J.; Bartolome, R.; Checa, A.; Maldonado, A.; Sloomweg, A.P. (1999). An interpretation of a prominent magnetic anomaly near the boundary between the Eurasian and African plates (Gulf of Cadiz, SW Margin of Iberia). *Marine Geology*, 155, 45-62.
- DeMets, C., R.G. Gordon, D.F. Argus, S. Stein, (1990). Current plate motions. *Geophys. J. Int.* 28, 2121-2124.
- Díez, S.; Gràcia, E.; Gutscher, M.A.; Matias, L.; Mulder, T.; Terrinha, P.; Somoza, L.; Zitellini, N.; De Alteriis, G.; Henriët, J.P.; Dañobeitia, J.J. (2005). Bathymetric map of the Gulf of Cadiz, NE Atlantic Ocean: The SWIM multibeam compilation. 250th Anniversary of the 1755 Lisbon Earthquake, Lisbon (Portugal), 1-4 November.
- Flinch, J.F., A.W. Bally, and S. Wu (1996). Emplacement of a passive-margin evaporitic allochthon in the Betic Cordillera of Spain, *Geology*, 24(1), 67-70.

- González, A., D. Cordoba, R. Vegas, and L.M. Matias, Seismic crustal structure in the southwest of the Iberian Peninsula and the Gulf of Cadiz, *Tectonophysics*, 296, 317-331, 1998.
- Gràcia, E., Danobeitia, J.J., Verges, J., PARSIFAL Team, (2003a). Mapping active faults offshore Portugal (36°N-38°N): Implications for seismic hazard assessment along the southwest Iberian margin. *Geology* 31, 83-86.
- Gràcia, E., Danobeitia, J.J., Verges, J., Bartolome, R. (2003b). Crustal architecture and tectonic evolution of the Gulf of Cadiz (SW Iberian margin) at the convergence of the Eurasian and African plates. *Tectonics* 22, n.4, 1033, doi:10.1029/2001TC901045.
- Grimison, N.L., W.P. Chen, (1986). The Azores-Gibraltar plate boundary: Focal mechanisms, depths of earthquakes and their tectonic implications, *J. Geophys. Res.* 91, 2029-2047.
- Gutscher, M.-A., Malod, J., Rehault, J.-P., Contrucci, I., Klingelhoefer, F., Mendes-Victor, L., Spakman, W. (2002). Evidence for active subduction beneath Gibraltar. *Geology* 30, 1071-1074.
- Gutscher, M.-A. (2004). What caused the Great Lisbon Earthquake?, *Science*, v. 305, p. 1247-1248.
- Gutscher, M.-A., Baptista, M.A., Miranda, J.M. (2006). The Gibraltar Arc seismogenic zone (part 2): constraints on a shallow east dipping fault plane source for the 1755 Lisbon earthquake provided by tsunami modeling and seismic intensity. *Tectonophysics*, Sp. Vol. "Natural laboratories on seismogenic faults", v. 427, p. 153-166, doi:10.1016/j.tecto.2006.02.025.
- Hayward, N., A.B. Watts, G.K. Westbrook, and J. Collier, A seismic reflection and GLORIA study of compressional deformation in the Goringe Bank, eastern North Atlantic, *Geophys. J. Int.*, 138, 831-850, 1999.
- Instituto Geográfico Nacional, Catálogo Sísmico Nacional hasta 2001, IGN, Madrid, Spain (2001). <http://www.geo.ign.es/servidor/sismo/cnis/>
- Hinz K. Hinz, H. Dostmann, J. Fritsch (1982). The continental margin of Morocco : seismic sequences, structural elements and the geological development, in : U. Von Rad, K. Hinz, M. Sarntheim, E. Seibold (Eds.), *Geology of the North West African Continental Margin*, Springer - Verlag, Berlin Heidelberg NewYork, pp. 34-60.
- Iribarren, L., Verges, J., Camurri, F., Fulla, J., Fernandez, M. (2007). The structure of the Atlantic-Mediterranean transition zone from the Alboran Sea to the Horseshoe Abyssal Plain (Iberia – Africa plate boundary). *Marine Geology*, 243, 97-119. doi:10.1016/j.margeo.2007.05.011.
- Johnston, A. (1996). Seismic moment assessment of earthquakes in stable continental regions – III. New Madrid, 1811-1812, Charleston 1886 and Lisbon 1755. *Geophys. J. Int.* 126, 314-344.
- Lajat, D., B. Biju-Duval, R. Gonnard, J. Letouzey, and E. Winnock (1975). Prolongement dans l'Atlantique de la partie externe de l'Arc bético-rifain, *Bull. Soc. Geol. France*, XVII, 481-485.
- Maldonado, A., Somoza, L., and Pallarés, L. (1999). The Betic orogen and the Iberian-African boundary in the Gulf of Cadiz: geological evolution (central North Atlantic). *Mar. Geol.* 155, 9-43.

- Malod, J.A. & Mauffret, A. (1990). Iberian plate motions during the Mesozoic. *Tectonophysics*. 184, 261-278.
- McClusky, S. R. Reilinger, S. Mahmoud, D. Ben Sari, y A Tealeb, (2003). GPS constraints on Africa (Nubia) and Arabia Plate Motions, *Geophysical Journal International*, 155, 1, 126-138.
- Martinez-Solares, J.M., Lopez A., and Mezcuca, J., 1979. Isoleismal map of the 1755 Lisbon earthquake obtained from Spanish data. *Tectonophysics* 53, 301-313.
- Medialdea, T.; R. Vegas L.; Somoza, J.T. Vázquez, A. Maldonado, V. Diaz-del-Rio, A. Maestro, D. Córdoba, M.C. Fernández-Puga. (2004). Structure and evolution of the "Olistostrome" complex of the Gibraltar Arc in the Gulf of Cádiz (eastern Central Atlantic): evidence from two long seismic cross-sections. *Mar. Geol.* 209;1-4, 173-198.
- Mendes-Victor, L., A. Ribeiro, D. Córdoba, S. Persoglia, G. Pellis, R. Sartori, L. Torelli, N. Zitellini, J.J. Dañobeitia, and BIGSETS Team. (1999). BIGSETS: Big Sources of Earthquakes and Tsunami in SW Iberia, *Eos Trans AGU*, Fall meeting, T12B-01.
- Nocquet, J.M., and Calais, E., (2004). Geodetic measurements of crustal deformation in the Western Mediterranean and Europe. *Pure Appl. Geophys.*, 161, 661-681.
- Olivet, J.L., *La cinématique de la Plaque Ibérique* (1996). *Bull. Centres Rech. Explor. Prod. Elf Aquitaine*, 20, 131-195.
- Roberts, D.G., *The Rif-Betic orogen in the Gulf of Cadiz* (1970). *Mar. Geol.*, 9, 31-37.
- Sahabi, M., Aslanian, D., and Olivet, J.-L., (2004). A new starting point for the history of the Central Atlantic, *C.R.A.S. Paris*, 336, 1041-1052.
- Sanz de Galdeano, C., *Geologic evolution of the Betic Cordilleras in the Western Mediterranean, Miocene to present*, *Tectonophysics*, 172, 107-119, 1990
- Sallarès, V., Gràcia, E., Bartolomé, R., Martínez, S., Dañobeitia, J.J., Gutscher, M.-A., Zitellini, N., and the Nearest Project working team (2008). Nearest Project, Deliverable D4: Depth Migrated Multi-Channel Seismic Profiles.
- Sartori, R., L. Torelli, N. Zitellini, D. Peis, E. Lodolo, (1994). Eastern segment of the Azores-Gibraltar line (central-eastern Atlantic): An oceanic plate boundary with diffuse compressional deformation, *Geology*, 22, 555-558.
- Somoza, L., Diaz-del-Rio, V., Leon, R., Ivanov, M., Fernandez-Puga, M.C., Gardner, J.M., Hernandez-Molina, F.J., Pinheiro, L.M., Rodero, J., Lobato, A., Maestro, A., Vazquez, J.T., Medialdea, T., Fernandez-Salas, L.M., (2003). Seabed morphology and hydrocarbon seepage in the Gulf of Cadiz mud volcano area: acoustic imagery, multibeam and ultrahigh resolution seismic data. *Mar. Geol.* 195, 153– 176.
- Srivastava, S.P., H. Schouten, W.R. Roest, K.D. Klitgord, L.C. Kovacs, J. Verhoef, and R. Macnab (1990), Iberian plate kinematics: A jumping plate boundary between Eurasia and Africa. *Nature*, 344, 756-759.
- Stampfli, G.M., von Raumer, J. and Borel, G., (2002). The Paleozoic evolution of pre-Variscan terranes: from Gondwana to the Variscan collision. *Geological Society of America, Special Paper* 364, pp. 263–280.

- Stich, D., Ammon, C.J., Morales, J., (2003). Moment-tensor solutions for small and moderate earthquakes in the Ibero-Maghreb region. *J. Geophys. Res.* 108, 2148.
- Stich, D., Serpelloni, E., Mancilla, F., Morales, J., (2006). Kinematics of the Iberia- Maghreb plate contact from seismic moment tensors and GPS observations. *Tectonophysics* 426, 295-317.
- Stich, D., Mancilla F.d.L., Pondrelli S., Morales, J., (2007). Source analysis of the February 12th 2007, Mw 6.0 Horseshoe earthquake : Implications for the 1755 Lisbon earthquake. *Geophys. Res. Lett.*, v. 34, L12308, doi : 10.1029/2007GL030012.
- Terrinha, P., Pinheiro, L.M., Henriot, J.P., Matias, L., Ivanov, M.K., Monteiro, J.H., Akhmetzhanov, A., Volkonskaya, A., Cunha, T., Shaskin, P., and Rovere, M.(2003). Tsunamigenic-seismogenic structures, neotectonics, sedimentary processes and slope instability on the southwest Portuguese Margin. *Mar. Geol.* 195; 1-4, 55-73.
- Terrinha, P., Valadares, V., Duarte, J., Roque, C., Duarte, H., Vicente, J., Rosas, F., and Matias, L. 2008. Nearest Project, Deliverable D1: Review of tectonic Sources.
- Thiebot, E., and Gutscher, M.-A., 2006. The Gibraltar Arc seismogenic zone (part1): constraints on a shallow east dipping fault plane source for the 1755 Lisbon earthquake provided by seismic data, gravity and thermal modeling. *Tectonophysics Sp. Vol. "Natural laboratories on seismogenic faults"*, v. 427, p. 135-152, doi:10.1016/j.tecto.2006.02.024.
- Torelli, L., Sartori, R., and Zitellini, N. (1997). The giant chaotic body in the Atlantic Ocean off Gibraltar: new results from a deep seismic reflection survey: *Mar. Pet. Geol.*, 14, 125-138.
- Vilanova, S.P., Nunes, C.F., Fonseca, J.F.B.D. (2003). Lisbon 1755: A case of triggered onshore rupture? *Bull. Seism. Society of America.* 93; 5, 2056-2068.
- Verhoef, J., Collette, B. J., Danobeitia, J. J., Roeser, H. A., & Roest, W. R. (1991). Magnetic anomalies off West-Africa, *Mar. Geophys. Res.*, 13, 81-103.
- Vizcaino, A., Gràcia, E., Pallàs, R., Terrinha, P., Escutia, C., Dañoibeitia, J.J., Jacobs, C., & HITS cruise party (2004). Estudio de alta resolución de las fallas activas y procesos sedimentarios asociados al Cañón de São Vicente, margen Sudoeste de Iberia. *Geo-temas*, 6 (5), 215-218.
- Wells, D., and Coppersmith, K., (1994). New empirical relationships among magnitude, rupture length, rupture width, rupture area and surface displacement. *Bull. Seism. Soc. Am.* 84, 974-1002.
- Zitellini, N., et al. (2001). Source of 1755 Lisbon earthquake and tsunami investigated. *Eos (Transactions, American Geophysical Union)* 82, 285-291.
- Zitellini, N., Rovere, M., Terrinha, P., Chierici, F., Matias, L., and BIGSETS Team (2004). Neogene through Quaternary tectonic reactivation of SW Iberian passive margin. *Pure Appl. Geophys.* 161, 565-587.
- Zitellini, N., Gracia, E., Matias, L., Terrinha, P., Abreu, M.A., DeAlteriis, G., Henriot, J.P., Danobeitia, JJ., Masson, D., Mulder, T., Ramella, R., Somoza, L., and Diez, S. (2009). The quest for NWAfrica-SW Eurasia

plate boundary west of Gibraltar. Earth Planet. Sci. Lett. DOI:
10.1016/j.epsl.2008.12.005. (in press).

Annex I: Diary of activities

Day 1 - 27/10/2008

At 18:00 of the 27th of November of 2008 the Vessel Hesperides departed from the Cartagena Arsenal Militar Harbour for the NEAREST-SEIS cruise to be carried out in the Gulf of Cadiz area. The Hesperides started a transit of approximately 45 hours to the Tagus Abyssal Plain to begin the deployment of the OBS's of Profile P1. At 21:00 the acquisition of multibeam swath bathymetry and gravimetry was initiated. The sub-bottom profile TOPAS was also connected but it was not working properly due to the high speed of the vessel.

Day 2 - 27/10/2008

At the second day of the cruise the vessel was still on transit to the Tagus Abyssal Plain. There was a problem with the multibeam echosounder that was frequently losing the seafloor. In order to solve this problem the experts decided to change the acquisition angle from to 65° to 50°, and later to 60°. However, due to the high speed of the vessel, the multibeam continued to lose the seafloor intermittently. At 10:30, when the Hesperides was passing through the Strait of Gibraltar, a positive bathymetric feature, with a negative gravimetric anomaly, was detected. At 20:15 the vessel crossed an E-W trending channel of the Cadiz Contourite Depositional System.

Day 3 - 29/10/2008

During the first two days the weather conditions were bad and at the third day of the cruise they got worst. The wind was blowing from north at around 20 kn and there were waves up to 5 meters in high. During the transit to the Tagus Abyssal Plain the vessel crossed the São Vicente Canyon, the southern flank of the Marquês de Pombal Fault and the Gorringe Bank at 09:45, 10:30 and 13:15, respectively. At 15.30 the Hesperides started the manoeuvres to test the UTM OBS's and at 16:08 the vessel stopped and initiated the acoustic tests. The multibeam echosounder and the EA-600 sub-bottom profiler were disconnected in order to avoid interferences with the transducer that communicates with the OBS's. During the tests the XBT cable was broken and it had to be replaced.

At 17:54 started the communication with the acoustic rosette that was deployed at a depth of approximately 5000 meters. The noise produced by the vessel engines disturbed the communication and thus they had to be disconnected. Consequently, the vessel had drift 5 nm south. The acoustic tests were concluded successfully at 19:13. At this time the multibeam echosounder and the sub-bottom profiler were connected. The rosette with the acoustic instruments was on deck at 22:10. At 20:45 the vessel had to stop due to a mechanic malfunction. The problem was solved at 22:30. Afterwards, the Hesperides started the transit to site OBS01-p1 of the Profile 1.

Day 4 - 30/10/2008

The deployment of 30 OBS's of the Profile 1 started during the night. In total were deployed 14 OBS's of UTM and 16 of IFREMER (Figure AI.1).

The UTM OBS's sites were: OBS01-p1, OBS02-p1, OBS03-p1, OBS04-p1, OBS05-p1, OBS06-p1, OBS16-p1, OBS20-p1, OBS25-p1, OBS26-p1, OBS27-p1, OBS28-p1, OBS29-p1, OBS30-p1.

The IFREMER OBS's sites were: OBS08-p1, OBS09-p1, OBS10-p1, OBS11-p1, OBS12-p1, OBS13-p1, OBS14-p1, OBS15-p1, OBS17-p1, OBS18-p1, OBS19-p1, OBS21-p1, OBS22-p1, OBS23-p1, OBS24-p1.



Figure AI.1.- a) UTM OBS; b) IFREMER OBS

At 01:01 the first OBS was deployed at site OBS01-p1 (at the location: 37°11.80'N; 11°39.19'W; 5208 m) and at 01:15 a checking test was performed (Figure AI.2). The test consisted in sending a signal to the OBS with a transducer immersed around 5 meters in the water. Then the OBS sends a signal back to the transducer. This allows calculating its position in depth and its velocity (Figure AI.3). The operation was performed for all the following OBS's at the given times:

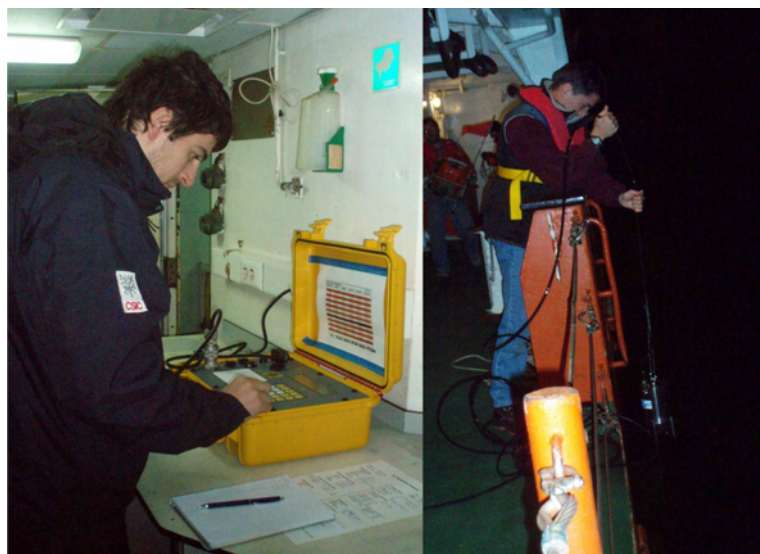


Figure AI.2.- Technicians making the acoustic test

02:08 Deployment at site OBS02-p1 (37°07.53'N; 11°36.63'W; 5151 m) and corresponding checking.

03:09 Deployment at site OBS03-p1 (37°03.07'N; 11°34.02'W; 5191 m) and corresponding checking.

04:17 Deployment at site OBS04-p1 (36°58.77'N; 11°31.49'W; 5197 m) and corresponding checking.

05:22 Deployment at site OBS05-p1 (36°53.80'N; 11°28.51'W; 4787 m) and corresponding checking.

06:26 Deployment at site OBS06-p1 (36°49.59'N; 11°26.01'W; 3764 m) and corresponding checking.

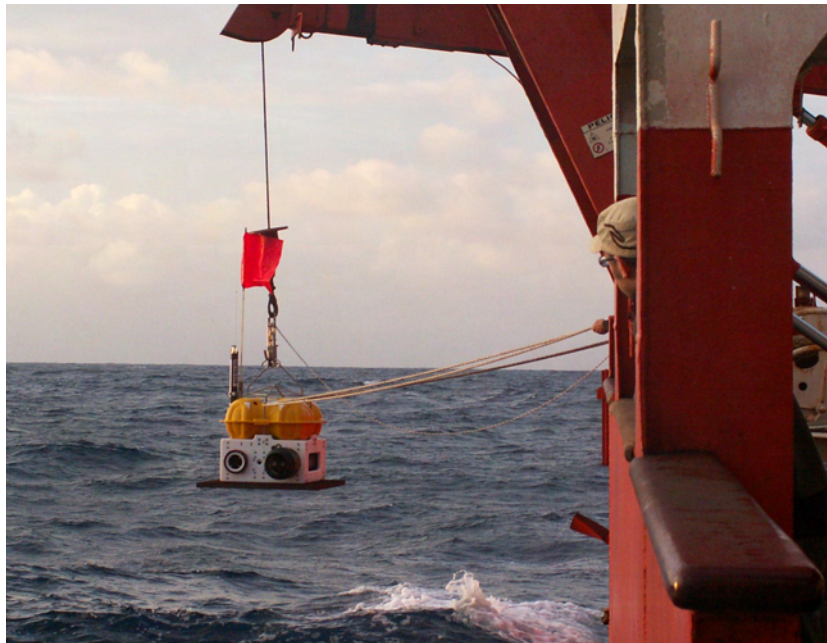


Figure AI.3. - Operation of OBS's deployment.

At 07:15 was made the acoustic test of IFREMER OBS's. This test terminated successfully at 07:50 and the operations of deployment continued:

08:53 Deployment at site OBS08-p1 (36°39.85'N; 11°20.18'W; 998 m) and corresponding checking.

09:30 Deployment at site OBS09-p1 (36°36.22'N; 11°18.11'W; 1173 m) and corresponding checking.

10:00 Deployment at site OBS10-p1 (36°32.48'N; 11°15.90'W; 2132 m) and corresponding checking.

11:00 Deployment at site OBS11-p1 (36°27.49'N; 11°12.92'W; 3256 m) and corresponding checking.

11:45 Deployment at site OBS12-p1 (36°22.74'N; 11°10.13'W; 3725 m) and corresponding checking.

12:37 Deployment at site OBS13-p1 (36°18.02'N; 11°07.46'W; 4101 m) and corresponding checking.

13:19 Deployment at site OBS14-p1 (36°13.67'N; 11°04.80'W; 4676 m) and corresponding checking.

14:03 Deployment at site OBS15-p1 (36°09.14'N; 11°02.14'W; 4926 m) and corresponding checking.

14:51 Deployment at site OBS16-p1 (36°04.61'N; 10°59.35'W; 4866 m) and corresponding checking.

15:35 Deployment at site OBS17-p1 (36°00.0435'N; 10°56.5727'W; 4945 m) and corresponding checking.

16:11 Deployment at site OBS18-p1 (35°55.4304'N; 10°53.8790'W; 4943 m) and corresponding checking.

16:49 Deployment at site OBS19-p1 (35°50.9557'N; 10°51.2694'W; 4895 m) and corresponding checking.

17:34 Deployment at site OBS20-p1 (35°46.4877'N; 10°48.6505'W; 4937 m) and corresponding checking.

18:22 Deployment at site OBS21-p1 (35°41.8181'N; 10°45.9114'W; 4937 m) and corresponding checking.

19:00 Deployment at site OBS22-p1 (35°37.7770'N; 10°43.3260'W; 4940 m) and corresponding checking.

19:47 Deployment at site OBS23-p1 (35°32.4609'N; 10°40.3804'W; 4597 m) and corresponding checking.

20:32 Deployment at site OBS24-p1 (35°28.12'N; 10°37.55'W; 4483 m) and corresponding checking.

21:15 Deployment at site OBS25-p1 (35°23.55'N; 10°35.05'W; 4258 m) and corresponding checking.

22:04 Deployment at site OBS26-p1 (35°19.0508'N; 10°32.3350'W; 4323 m) and corresponding checking.

22:52 Deployment at site OBS27-p1 (35°14.4960'N; 10°29.5832'W; 4436 m) and corresponding checking.

23:45 Deployment at site OBS28-p1 (35°10.04'N; 10°26.90'W; 4524 m) and corresponding checking.

Day 5 - 31/10/2008

00:34 Deployment at site OBS29-p1 (35°05.48'N; 10°24.26'W; 4327 m) and corresponding checking.

01:22 Deployment at site OBS30-p1 (35°00.91'N; 10°21.39'W; 4432 m) and corresponding checking.

At 01:30 the vessel was heading to the point B that corresponded to the start of line (SOL) of the Profile 1, in order to start shooting.

At 05:15 the airguns tests started with a shot interval of 60 seconds (Figure AI. 4). At 5:25 during the shoot number 11 an air lost on gun number 1 was

detected. All airguns were recovered from the water and the subsequent deployment was delayed due to the bad weather conditions.



Figure AI.4. – Details of airguns, airgun array and cluster used during the survey.

At 16:00 the manoeuvres to deploy the airguns restarted. All the airguns were on the water at 16:15 (Figure AI.5).



Figure AI.5.- Airgun array in the water.

At 16:24 the shooting tests started (TAG=375). Problems with the air tube were detected and at 17:17 (TAG=392) all the airguns had to be recovered to the vessel to be repaired.

At 16:11 TOPAS was connected and started to acquire data (file: 160834).

The airguns were finally deployed with success at 18.38.

The Profile 1 started at 19:20 at the position 34°34.2498N; 9°57.84W further away from the planned starting point B (TAG=421; TOPAS file:192005). At 23:04 the vessel crossed the point B (34°43.7882N; 10°11.3732W).

Day 6 - 01/11/2008

At 01:30 there was a problem with the synchronization of airguns. The shot interval had been 60 seconds during 20 shots (TAG=172).

At 03:25 the calibration of airguns was complete (TAG=253). The shot cadence was 60 seconds for the following 20 shots.

The TAG and Shot Number were than annotated for all the OBS's position at the given times has following:

03:49 Passed over site OBS30-p1 (TAG=382; shot=382).

04:50 Passed over site OBS29-p1 (TAG=315; shot=425).

05:56 Passed over site OBS28-p1 (TAG=359; shot=468).

06:55 Passed over site OBS27-p1 (TAG=399; shot=507).

At 07:45 the coverage angle of the multibeam echosounder was changed from 50° to 70°.

08:16 Passed over site OBS26-p1 (TAG=452; shot=561).

09:32 Passed over site OBS25-p1 (TAG=003; shot=611).

10:54 Passed over site OBS24-p1 (TAG=058; shot=667).

12:03 Passed over site OBS23-p1 (TAG=104).

13:38 Passed over site OBS22-p1 (TAG=167shot=776).

At 14:40 the airgun number 7 had to be recovered from the water in order to be repaired. At 14:52 the airgun number 7 was repair and was deployed in the water (TAG=216; shot=822).

14:42 Passed over site OBS21-p1 (TAG=210).

At 16:00 there were detected problems in the air tube of airgun number 7. The air tube was broken and had to be repaired (TAG=262; shot=871). At 16:35 the airgun number 7 was deployed in water (TAG=285; shot=896).

17:06 Passed over site OBS19-p1 (TAG=306; shot=915).

At 18:15 there were problems with the synchronization of the airgun number 5.

18:25 Passed over site OBS18-p1 (TAG=358; shot=967).

19:44 Passed over site OBS17-p1 (TAG=411; shot=1019).

21:00 Passed over site OBS16-p1 (TAG=465; shot=1072).

22:15 Passed over site OBS15-p1 (TAG=012).

23:38 Passed over site OBS14-p1 (TAG=068; shot=1178).

Day 7 - 02/11/2008

00:58 Passed over site OBS13-p1 (TAG=121; shot=1230).

02:18 Passed over site OBS12-p1 (TAG=175; shot=1284).

03:46 Passed over site OBS11-p1 (TAG=233; shot=1339).

04:56 Passed over site OBS10-p1 (TAG=280; shot=1389).

06:03 Passed over site OBS09-p1 (TAG=325; shot=1433).

07:07 Passed over site OBS08-p1 (TAG=368; shot=1476).

08:30 Passed over site OBS07-p1 (TAG=423).

09:45 Passed over site OBS06-p1 (TAG=473; shot=1584).

11:00 Passed over site OBS05-p1 (TAG=023; shot=1635).

12:47 Passed over site OBS04-p1 (TAG=094).

14:23 Passed over site OBS03-p1 (TAG=158; shot=1766).

15:48 Passed over site OBS02-p1 (TAG=215; shot=1823).

16:58 Passed over site OBS01-p1 (TAG=261; shot=1871).

At 19:00 there was malfunction in the airgun number 6 (stopped shooting).

At 20:41 the Hesperides ended the profile P1 and the shooting was stopped (37°25.09'N; 11°47.06'W; TAG=411; shot=1120). At 21:15 ended the TOPAS acquisition.

At 20:57 the airgun number 7 was recovered and at 21:25 all the airguns were on deck. The rough weather had difficult the manoeuvre (Figure AI.6).

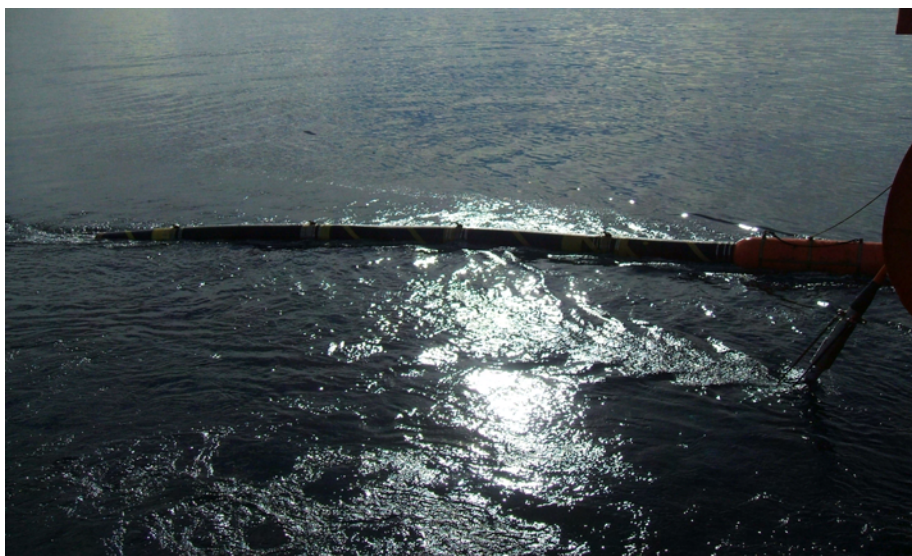


Figure AI.6. - Operations of Airguns recovery.

At 21:30 the vessel was heading to the site OBS01-p1 in order to start the recouplement of the OBS's. Due to bad weather conditions was decided to start by the site OBS-08-p1. During the recouplement manoeuvres the multibeam echosounder, the EA600 sub-bottom profiler and TOPAS were stopped to facilitate the communication between the transducer and the OBS's.

Day 8 - 03/11/2008

At 04:12 was made a first attempt to communicate with OBS08-p1 at the position 36°40.0373'N-11°20.3110'W; a second attempt at 04:27 in position 36°39.7997'N-11°19.9895'W; and a last one at 04:41 in position 36°39.8104'N-11°20.2634'W. At 04:45 the OBS08-p1 was sighted on the surface and at 04:50 the OBS was onboard the vessel (36°39.8140'N-11°20.2964'W; 980 m).

At 05:12 was made the first attempt to communicate with OBS09-p1 at the position 36°38.0667'N-11°19.3916'W and a second one at 05:40 in the position 36°36.3935'N-11°18.3809'W. At 05:47 the OBS was sighted at the surface, and at 06:11 was onboard the Hesperides (36°36.2495'N-11°18.4240'W; 898 m).

At 06:37 was made the first attempt to communicate with the OBS10-p1 at the position 36°33.9037'N-11°16.9692'W; a second attempt at 07:06 in position 36°32.32'N-11°15.60'W; and the last one at 07:23 in position 36°32.09'N-11°15.73'W. At 07:30 the OBS10-p1 was sighted on surface, and at 07:51 was onboard (36°31.99'N-11°15.86'W; 2085 m).

At 07:51 as made the first attempt to communicate with OBS11-p1 at the position 36°31.99'N-11°15.86'W; a second at 08:30 in position 36°30.06'N-11°14.47'W; a third attempt at 08:45 in position 36°28.01'N-11°13.27'W; and the last one at 09:00 in position 36°27.58'N-11°12.75'W. At 09:50 the OBS11-p1 was sighted on surface, and at 10:00 was onboard (36°27.44'N-11°13.30'W; 3211 m).

At 10:15 was made the first attempt to communicate with OBS12-p1 at the position 36°26.44'N-11°12.33'W; a second attempt at 10:42 in position 36°24.56'N-11°11.12'W; a third one at 11:05 in position 36°22.88'N-11°10.24'W; a fourth at 11:19 in position 36°22.71'N-11°09.81'N and the last one at 11:36 in position 36°22.47'N-11°10.08'W. At 11:52 the OBS12-p1 was sighted on surface, and at 11:58 was on board (36°22.65'N-11°10.35'W; 3836 m).

At 12:15 was made the first attempt to communicate with OBS13-p1 at the position 36°21.54'N-11°09.51'W; a second attempt at 12:37 in position 36°19.79'N-11°08.46'W; and a last one at 12:57 in position 36°18.07'N-11°07.49'W. At 15:15 was decided to go to site OBS14-p1 since the OBS13 did not came to the surface.

At 15:16 was made the first attempt to communicate with OBS14-p1 at the position 36°17.8242'N-11°07.5763'W; a second attempt at 15:37 in position 36°15.3550'N-11°05.8844'W; a third one at 15:58 in position 36°13.6846'N-11°04.8604'W; a fourth at 16:06 in position 36°13.5903'N-11°04.8318'N; a fifth at 16:20 in position 36°13.5619'N-11°04.8296'N; and the last one at 11:31 in position

36°13.6646'N-11°04.7909'W. At 17:12 the OBS14-p1 was sighted on surface, and at 17:29 was onboard (36°13.2765'N-11°05.2723'W; 4467 m).

At 17:30 was made the first attempt to communicate with OBS15-p1 at the position 36°13.2723'N-11°05.2499'W; a second attempt at 17:59 in position 36°10.8452'N-11°03.2465'W; a third at 18:21 in position 36°09.1096'N-11°02.0896'W; a fourth attempt at 18:30 in position 36°09.0123'N-11°02.2568'N; a fifth at 18:42 in position 36°09.1809'N-11°02.2174'N; and the last one at 18:53 in position 36°09.11'N-11°01.87'W. At 19:36 the OBS15-p1 was sighted on surface, and at 19:51 was onboard (36°08.55'N-11°02.53'W; 4863 m).

At 19:53 was made the first attempt to communicate with OBS16-p1 at the position 36°08.48'N-11°02.49'W; a second attempt at 20:40 in position 36°05.78'N-11°00.89'W; and the last one at 21:30 in position 36°04.13'N-10°59.19'W. At 22:23 the OBS16-p1 was sighted on surface, and at 22:55 was on board (36°03.59'N-10°59.56'W).

At 23:15 was made the first attempt of communicate with OBS17-p1 at the position 36°03.04'N-10°59.08'W; a second attempt at 23:32 in position 36°01.59'N-10°57.92'W; a third tempt at 23:56 in position 36°00.04'N-10°56.58'W; a attempt fourth at 00:13 in position 36°00.16'N-10°56.28'N; and the last one at 00:35 in position 35°59.79'N-10°56.48'W. At 01:10 the OBS17-p1 was sighted on surface, and at 01:20 was onboard (35°59.70'N-10°56.70'W; 4871 m).

Day 9 - 04/11/2008

At 01:27 was made a first attempt to communicate with OBS18-p1 the position 35°59.57'N-10°56.90'W; a second attempt at 01:57 in position 35°57.15'N-10°55.12'W; a third one at 02:20 in position 35°55.52'N-10°53.95'W; a fourth at 02:46 in position 35°55.44'N-10°53.65'N; and the last one at 03:04 in position 35°55.28'N-10°54.12'W. At 03:28 the OBS18-p1 was sighted on surface, and at 03:38 was onboard (35°55.3392'N-10°53.6534'W; 4874 m).

At 03:40 was made the first attempt to communicate with OBS19-p1 at the position 35°55.3030'N-10°53.6462'W; a second attempt at 04:12 in position 35°52.9238'N-10°52.0399'W; a third at 04:41 in position 35°51.1802'N-10°51.1802'W; a fourth at 04:50 in position 35°50.9633'N-10°50.9494'N; a fifth at 05:02 in position 35°50.7540'N-10°51.1775'N; and the last one at 05:15 in position 35°50.8960'N-10°51.4042'W. At 05:48 the OBS19-p1 was sighted on surface, and at 05:57 was onboard (35°51.0933'N-10°50.8418'W; 4875 m).

At 06:07 was made the first attempt of communication with OBS20-p1 on position 35°51.1715'N-10°50.7355'W; a second attempt at 06:50 in position 35°48.4860'N-10°49.1800'W; and the last one at 07:32 in position 35°46.49'N-10°48.54'W. At 08:09 the OBS20-p1 was sighted on surface, and at 08:42 was onboard (35°46.48'N-10°47.47'W; 4877 m).

At 08:42 was made the first attempt to communicate with OBS21-p1 at the position 35°46.48'N-10°47.47'W; a second attempt at 09:10 in position 35°43.66'N-10°46.16'W; and the last one at 09:34 in position

35°42.05'N-10°45.82'W. At 10:47 the OBS21-p1 was sighted on surface, and at 10:52 was onboard (35°41.91'N-10°45.32'W; 4879 m).

At 10:59 was made a first attempt of communication with OBS22-p1 at the position 35°42.01'N-10°45.08'W; the second at 11:22 in position 35°38.67'N-10°43.75'W; and the last one at 11:50 in position 35°37.78'N-10°42.97'W. At 12:33 the OBS22-p1 was sighted on surface, and at 13:12 was onboard (35°37.79'N-10°42.56'W; 4733 m).

At 13:12 was made the first attempt to communicate with OBS23-p1 at the position 35°37.79'N-10°42.56'W; a second attempt at 14:24 in position 35°32.37'N-10°40.31'W; and the last one at 14:55 in position 35°32.52'N-10°40.39'W. At 15:15 the OBS23-p1 was sighted on surface, and at 15:23 was onboard (35°32.5314'N-10°39.4805'W; 4842 m).

At 15:25 was made a first attempt to communicate with OBS24-p1 at the position 35°32.4872'N-10°39.3871'W; a second attempt at 15:51 in position 35°29.9094'N-10°38.1095'W; a third at 16:12 in position 35°28.2066'N-10°37.3523'W; a fourth at 16:25 in position 35°28.2741'N-10°37.5461'N; a fifth attempt at 16:36 in position 35°28.0252'N-10°37.7269'N; and the last one at 16:48 in position 35°28.0518'N-10°37.2718'W. At 17:17 the OBS24-p1 was sighted on surface, and at 17:23 was onboard (35°28.2388'N-10°36.5290'W; 4415 m).

At 17:29 was made a first attempt to communicate with OBS25-p1 at the position 35°28.2645'N-10°36.4746'W; the second attempt at 17:58 in position 35°25.3920'N-10°35.3792'W; a third at 18:24 in position 35°23.6449'N-10°35.0554'W; a fourth at 18:33 in position 35°23.5344'N-10°34.9010'N; a fifth attempt at 19:17 in position 35°23.41'N-10°34.93'N; and the last one at 19:39 in position 35°23.06'N-10°34.54'W. At 19:42 the OBS25-p1 was sighted on surface, and at 19:59 was onboard (35°23.41'N-10°34.01'W; 4415 m).

At 19:59 was made a first attempt to communicate with OBS26-p1 at the position 35°23.41'N-10°34.01'W; the second attempt at 20:48 in position 35°21.09'N-10°32.97'W; and the last one at 21:18 in position 35°19.15'N-10°32.28'W. At 21:45 the OBS26-p1 was sighted on surface, and at 22:03 was onboard (35°18.72'N-10°31.50'W; 4293 m).

At 22:10 was made the first attempt to communicate with OBS27-p1 at the position 35°18.68'N-10°31.38'W; a second attempt at 22:10 in position 35°16.44'N-10°30.52'W; a third at 23:05 in position 35°16.24'N-10°30.11'W; and the last one at 23:30 at the position 35°14.14'N-10°29.43'W. At 23:58 the OBS27-p1 was sighted on surface, and at 00:21 was onboard (35°13.98'N-10°29.03'W; 4179 m).

At 23:40 was made the first attempt to communicate with OBS28-p1 at the position 35°13.09'N-10°39.28'W; and a second one at 00:42 in position 35°11.87'N-10°07.77'W. At 01:15 the OBS28-p1 was sighted on surface, and at 01:46 was onboard (35°09.44'N-10°26.85'W; 4287 m).

Day 10 - 05/11/2008

At 01:20 was made the first attempt to communicate with OBS29-p1 at the position 35°09.69'N-10°27.07'W; and the second one at 02:12 in position 35°07.17'N-10°25.26'W. At 02:59 the OBS29-p1 was sighted on surface, and at 03:25 was onboard (35°04.9697'N-10°24.4265'W; 4921 m).

At 03:04 was made the first attempt to communicate with OBS30-p1 at the position 35°05.0914'N-10°23.9215'W; the second tempt at 03:30 in position 35°04.9566'N-10°24.3521'W; the third tempt at 03:59 in position 35°02.5586'N-10°22.8852'W; and the last one at 04:29 in position 35°00.9155'N-10°21.6233'W. At 04:41 the OBS30-p1 was sight on surface, and at 05:03 was onboard (35°00.5380'N-10°21.7502'W; 4331 m).

At 05:07 the vessel went back to the site OBS13-p1 to recover the OBS that had an automatic release triggering device. At 12:12 was made the first attempt to communicate with OBS13-p1 at the position 36°16.43'N-11°05.98'W. At 14:09 the OBS13-p1 was sighted on surface, and at 14:52 was onboard (36°13.04'N-11°08.96'W; 4317 m).

At 18:05 was made the first attempt to communication with OBS06-p1 at the position 36°46.8328'N-11°25.1015'W; a second attempt at 19:03 in position 36°49.5388'N-11°26.0122'W; a third attempt at 19:44 in position 36°48.9830'N-11°25.7987'W; and the last one at 20:08 in position 36°49.61'N-11°25.94'N. At 20:33 the OBS06-p1 was sighted on surface, and at 20:57 was onboard (36°49.44'N-11°25.97'W; 3764 m).

At 20:33 was made the first attempt to communicate with OBS05-p1 at the position 36°49.39'N-11°25.79'W; a second attempt at 21:21 in position 36°52.13'N-11°27.41'W; and the last one at 21:49 in position 36°53.87'N-11°28.49'W. At 22:25 the OBS05-p1 was sighted on surface, and at 22:47 was onboard (36°54.05'N-11°27.76'W; 4787 m).

At 21:49 was made the first attempt to communicate with OBS04-p1 at the position 36°53.87'N-11°28.49'W; and the second one at 23:20 in position 36°57.05'N-11°30.33'W. At 23:51 the OBS04-p1 was sighted on surface, and at 00:07 was onboard (36°58.90'N-11°30.68'W; 5259 m).

Day 11 - 06/11/2008

At 00:07 was made a first attempt to communicate with OBS03-p1 at the position 36°58.90'N-11°30.68'W; and a second one at 01:03 in position 37°01.13'N-11°32.69'W. At 02:12 the OBS03-p1 was sighted on surface, and at 02:27 was onboard (37°02.99'N-11°33.27'W; 5150 m).

At 02:27 was made a first attempt of communicate with OBS02-p1 at the position 37°02.99'N-11°33.27'W; and the second one at 02:58 in position 37°05.86'N-11°35.47'W. At 03:29 the OBS02-p1 was sighted on surface, and at 03:53 was onboard (37°07.3566'N-11°35.8130'W; 5130 m).

At 03:45 was made a first attempt of communication with OBS01-p1 on position 37°07.33'N-11°36.12'W; and the second one at 04:24 in position 37°10.2075'N-11°37.8653'W. At 05:09 the OBS01-p1 was sighted on surface, and at 05:26 was onboard (37°11.7787'N-11°38.5372'W; 5129 m).

At 05:29 the vessel started the transit to point C (next to the start of the Profile 2 to initiate the deployment of OBS31-p2). The multibeam echosounder was restarted. TOPAS was restarted at 06:34 (file:063340). Due to the high speed of the vessel during the transit to point C none of the two instruments were working correctly.

At 18:10 the Hesperides arrived to the point C and was heading to site OBS31-p2. The velocity of the vessel was reduced from 12.5 to 8 kn to enable the acquisition of TOPAS data in the deformation front of the Gulf of Cadiz Accretionary Wedge south of the Coral Patch Ridge.

The deployment of the 15 OBS's of the Profile 2 started during the afternoon. In total were deployed 4 OBS's of UTM and 11 of IFREMER.

The UTM OBS's sites were: OBS35-P2, OBS36-P2, OBS41-P2, OBS42-P2.

The IFREMER OBS's sites were: OBS31-P2, OBS32-P2, OBS33-P2, OBS34-P2, OBS37-P2, OBS38-P2, OBS39-P2, OBS40-P2, OBS43-P2, OBS44-P2, OBS45-P2.

19:43 Deployment at site OBS31-p2 (35°01.35'N; 9°14.69'W; 3755 m) and corresponding checking.

20:28 Deployment at site OBS32-p2 (35°08.38'N; 9°11.70'W; 3676 m) and corresponding checking.

21:15 Deployment at site OBS33-p2 (35°15.16'N; 9°09.16'W; 3416 m) and corresponding checking.

21:53 Deployment at site OBS34-p2 (35°21.91'N; 9°06.39'W; 3328 m) and corresponding checking.

21:31 Deployment at site OBS35-p2 (35°28.59'N; 9°03.58'W; 3711 m) and corresponding checking.

23:15 Deployment at site OBS36-p2 (35°35.47'N; 9°00.80'W; 3347 m) and corresponding checking.

23:59 Deployment at site OBS37-p2 (35°42.54'N; 8°57.96'W; 3352 m) and corresponding checking.

00:35 Deployment at site OBS38-p2 (35°48.76'N; 8°59.23'W; 3372 m) and corresponding checking.

Day 12 - 07/11/2008

01:19 Deployment at site OBS39-p2 (35°55.48'N; 8°52.16'W; 3504 m) and corresponding checking.

02:00 Deployment at site OBS40-p2 (36°02.08'N; 8°49.57'W; 3435 m) and corresponding checking.

02:47 Deployment at site OBS41-p2 (36°08.77'N; 8°46.75'W; 3357 m) and corresponding checking.

03:35 Deployment at site OBS42-p2 (36°15.4296'N; 8°44.32'W; 2315 m) and corresponding checking.

04:21 Deployment at site OBS43-p2 (36°21.9004'N; 8°41.85'W; 2796 m) and corresponding checking.

06:05 Deployment at site OBS44-p2 (36°37.7120'N; 8°36.48'W; 2221 m) and corresponding checking.

07:19 Deployment at site OBS45-p2 (36°48.81'N; 8°30.46'W; 2238 m) and corresponding checking.

At 07:30 the vessel started the transit to the starting point of the profile P2 (point E). At 08:15 the Hesperides arrived to point D but had to wait for the land stations to be connected to start shooting the line.

At 09:15 the airgun tests started on the deck. At 09:54 the airguns were in water to be tested. All tests were accomplished successfully.

At 11:05 the airguns started shooting and the Profile 2. At 11:37 the airguns were aligned with the Profile P2 (shot= 22; TAG=113).

At 11:12 TOPAS started logging (file= 111139).

The TAG and Shot Number were than annotated for all the OBS's position at the given times has following:

12:45 Pass over site OBS45-p2 (TAG=159; shot=65).

15:15 Pass over site OBS44-p2 (TAG=259; shot=168).

19:00 Pass over site OBS43-p2 (TAG=409; shot=317).

20:27 Pass over site OBS42-p2 (TAG=467; shot=375).

21:58 Pass over site OBS41-p2 (TAG=27; shot=436).

23:36 Pass over site OBS40-p2 (TAG=93; shot=501).

Day 13 - 08/11/2008

01:11 Pass over site OBS39-p2 (TAG=156; shot=565).

02:48 Pass over site OBS38-p2 (TAG=221; shot=629).

At 03:25 there was a problem with the airgun number 2, the air tube was broken. Airguns stopped shooting at 03:33. At 03:45 started the manoeuvres to recover the airguns in order to repair the airgun number 2. The problem was solved at 05:07 and the air guns return to the water at 05:48. Then the airguns started shooting (shot=661; TAG=263). Due to this problem there was a small segment of the profile that was not shooted

05:55 Pass over site OBS37-p2 (TAG=263; shot=661).

07:28 Pass over site OBS36-p2 (TAG=324; shot=702).

09:08 Pass over site OBS35-p2 (TAG=391; shot=787).

10:45 Pass over site OBS34-p2 (TAG=456; shot=852).

12:19 Pass over site OBS33-p2 (TAG=18; shot=915).

13:54 Pass over site OBS32-p2 (TAG=82; shot=978).

New problem with the airgun number 2 at 14:10 (1000 c.i.). Since the profile was almost ending it was decided not repair the airgun and end the profile with a total energy of 3520 c.i.

15:15 Pass over site OBS31-p2 (TAG=136; shot=1032).

At 15:15 the TOPAS stopped working and was restarted a quarter of an hour later (file=154202). Due to this problem the printed TOPAS profile P2 is divided in two parts.

End of Line of the profile P2 at 20:15 (TAG=336; shot=1233). At 20:42 all airguns were on deck and the vessel started the transit to recover the OBS31-p2. The TOPAS final file is the number:195745. The multibeam was turned off at 21:30 and the sub-bottom profiler EA-600 was disconnected at 22:30.

At 22:30 was made a first attempt to communicate with OBS31-p2 at the position 34°56.65'N-9°17.24'W; the second attempt at 22:58 in position 34°59.53'N-9°15.78'W; a third at 23:24 in position 35°01.53'N-9°14.55'W; and the last one at 23:45 in position 35°01.16'N-9°14.80'W. At 00:04 the OBS31-p2 was sighted on surface, and at 00:24 was onboard (35°01.08'N-9°14.92'W; 4396 m).

Day 14 - 09/11/2008

At 00:47 was made a first attempt to communicate with OBS32-p2 at the position 35°03.65'N-9°14.02'W; the second attempt at 01:15 in position 35°06.33'N-9°12.90'W; a third at 01:41 in position 35°08.45'N-9°11.64'W; and the last one at 02:00 in position 35°08.24'N-9°11.94'W. At 02:34 the OBS-32-p2 was onboard (35°08.40'N-9°11.80'W; 3854 m).

At 02:34 was made a first attempt to communicate with OBS33-p2 at the position 35°08.40'N-9°11.80'W; the second attempt at 03:19 in position 35°13.3975'N-9°10.00'W; and the last one at 03:57 in position 35°14.8214'N-9°09.14'W. At 03:59 the OBS33-p2 was sighted on surface, and at 04:16 was onboard (35°14.8982'N-9°09.92'W; 3858 m).

At 04:21 was made a first attempt to communicate with OBS34-p2 at the position 35°14.8649'N-9°09.31'W; the second attempt at 04:50 in position 35°17.3195'N-9°08.44'W; and the last one at 05:21 in position 35°20.1772'N-9°07.32'W. At 05:49 the OBS34-p2 was sighted on surface, and at 06:06 was onboard (35°21.7120'N-9°06.72'W; 2747 m).

At 06:06 was made a first attempt to communicate with OBS35-p2 at the position 35°21.7120'N-9°06.72'W; the second attempt at 06:40 in position 35°23.9303'N-9°05.89'W; and the last one at 07:17 in position 35°26.82'N-9°05.73'W. At 07:30 the OBS35-p2 was sighted on surface, and at 07:54 was onboard (35°28.41'N-9°03.89'W; 3549 m) (Figure A1.6.).



Figure AI.6.- Spanish OBS's recovering operations

At 07:54 was made a first attempt to communicate with OBS36-p2 at the position $35^{\circ}28.41'N-9^{\circ}38.89'W$; and the second one at 08:42 in position $35^{\circ}28.34'N-9^{\circ}02.60'W$. At 09:49 the OBS36-p2 was onboard ($35^{\circ}35.59'N-9^{\circ}01.35'W$; 3525 m). The zodiac was on water during the recovering.

At 10:15 was made a first attempt to communicate with OBS37-p2 at the position $35^{\circ}35.39'N-9^{\circ}01.34'W$; the second attempt at 10:39 in position $35^{\circ}37.68'N-9^{\circ}08.59'W$; and the last one at 11:12 in position $35^{\circ}40.43'N-8^{\circ}59.47'W$. At 11:46 the OBS37-p2 was sighted on surface, and at 11:52 was onboard ($35^{\circ}42.28'N-8^{\circ}58.12'W$).

At 11:52 was made a first attempt to communicate with OBS38-p2 at the position $35^{\circ}42.28'N-8^{\circ}58.12'W$; the second attempt at 12:31 in position $35^{\circ}44.22'N-8^{\circ}57.93'W$; and the last one at 13:01 in position $35^{\circ}47.16'N-8^{\circ}56.49'W$. At 13:37 the OBS38-p2 was sighted on surface, and at 13:44 was onboard ($34^{\circ}48.90'N-8^{\circ}55.60'W$).

At 13:48 was made a first attempt to communicate with OBS39-p2 at the position $35^{\circ}48.92'N-8^{\circ}55.51'W$; the second attempt at 14:13 in position $35^{\circ}51.07'N-8^{\circ}54.20'W$; and the last one at 14:37 in position $35^{\circ}54.02'N-8^{\circ}54.04'W$. At 15:18 the OBS39-p2 was sighted on surface, and at 15:26 was onboard ($35^{\circ}55.6404'N-8^{\circ}52.52'W$; 4167 m).

At 15:26 was made a first attempt to communicate with OBS40-p2 at the position $35^{\circ}55.6404'N-8^{\circ}52.52'W$; the second attempt at 15:51 in position $35^{\circ}57.5374'N-8^{\circ}52.00'W$; a third at 16:22 in position $36^{\circ}00.2907'N-8^{\circ}10.50'W$; and the last one at 16:51 in position $36^{\circ}02.1357'N-8^{\circ}49.63'W$. At 17:23 the

OBS40-p2 was sighted on surface, and at 17:30 was onboard (36°02.1066'N-8°49.57'W; 4188 m).

At 17:39 was made a first attempt to communicate with OBS41-p2 at the position 36°02.0944'N-8°49.60'W; the second attempt at 18:26 in position 36°06.9694'N-8°47.50'W; and the last one at 19:09 in position 36°08.64'N-8°46.93'W. At 19:35 the OBS41-p2 was sighted on surface, and at 19:49 was onboard (36°08.68'N-8°46.69'W; 4476 m).

At 19:49 was made a first attempt to communicate with OBS42-p2 at the position 36°08.68'N-8°46.69'W; the second attempt at 20:38 in position 36°12.18'N-8°45.66'W; and the last one at 20:51 in position 36°13.54'N-8°45.10'W. At 21:29 the OBS42-p2 was sighted on surface, and at 21:42 was onboard (36°15.33'N-8°44.28'W; 3639 m).

At 21:42 was made a first attempt to communicate with OBS43-p2 at the position 36°15.33'N-8°44.28'W; and the second one at 22:31 in position 36°20.04'N-8°42.66'W. At 23:10 the OBS43-p2 was sighted on surface, and at 23:21 was onboard (36°21.88'N-8°41.09'W; 954 m).

At 23:00 was made at test with the XBT cable (Figure Al.7).



Figure Al.7. – Throwing an XBT

Day 15 - 10/10/2008

At 00:37 was made a first attempt to communicate with OBS44-p2 at the position 36°36.00'N-8°36.98'W; and the second one at 00:50 in position 36°36.89'N-8°36.68'W. At 01:10 the OBS44-p2 was sighted on surface, and at 01:19 was onboard (36°37.59'N-8°36.36'W; 414 m).

And finally at 02:38 OBS45-p2 was sighted on surface, and at 02:43 was onboard (36°48.72'N-8°30.43'W; 280 m).

At 03:03 the vessel started a transit to the Guadalquivir Bank and Cadiz Fault area for a bathymetric survey. At 03:15 the vessel restart the acquisition of data with the multibeam echosounder (file=211) and the sub-bottom profiler TOPAS (file=031151).

At 04:24 the Hesperides arrived at point 1 and Started the Line 1-2. At 7:14 the vessel arrived at point 2 and changed the head to start of line 2-3. At 09:00

passed through the point 3 and started the line 3-4. Start of line 4-5 was at 11:43; the start of line 5-6 was at 14:16; and of line 7-8 at 14:24; line 8-9 at 17:00. The BIO Hesperides arrived in Cadiz on 11/10/2008 at 9:00 local time.

Annex II: Technical report (in spanish)

All.1. Batimetría multihaz y backscatter acústico

Características técnicas

See chapter 6

Incidencias

Sin incidencias técnicas.

All.2. Perfilador de sedimentos

Características técnicas

Ver capítulo 7

Incidencias

Al iniciar la campaña el equipo no transmitía con la potencia deseada, esto era debido a un fallo interno en una de las fuentes de alimentación del rack de electrónica (Power 1).

Se ha sustituido el elemento defectuoso y se ha comprobado su correcto funcionamiento.

All.3. Sonda hidrográfica Simrad EA-600

Características técnicas

Sonda monohaz de doble frecuencia. Las frecuencias de trabajo son:

- 12 kHz en modo activo o pasivo activo, (PINGER) utilizado en combinación con el Pinger Benthos
- 200 kHz.

La sonda dispone de salidas serie, Ethernet y Centronics para impresora. Los datos se presentan en pantalla y por impresora, a los que se añaden los datos de navegación y hora. Los datos de navegación, tiempo y actitud le llegan del Seapath 200, mediante una líneas serie cuya configuración es la siguiente:

Telegrama	Puerto	Baudios	Bits Datos	Bits Stop	Paridad
Navegación y tiempo	COM1	4800	8	1	No
Actitud	COM3	19600	8	1	No

La profundidad se envía al sistema de navegación Konmap y a la sonda paramétrica Topas a través de la red Ethernet por el puerto UDP:2020 mediante un programa llamado Data Distribution.

Esta sonda se utiliza para navegación.

Incidencias

Sin incidencias técnicas.

All.4. Sondas batitermogáficas

Características técnicas

El sistema de adquisición de datos oceanográficos SIPPICAN MK-21 utiliza un PC estándar y un conjunto de sondas desechables para medir y visualizar parámetros físico-químicos del océano, tales como temperatura (sondas XBT),

velocidad del sonido (sondas XSV), conductividad y salinidad (XCTD). El sistema realiza la adquisición, presentación y almacenamiento de los datos en tiempo quasi-real, permitiendo una presentación posterior de los datos para su análisis.

Sonda	Parámetro	Profundidad máxima	Velocidad máxima de lanzamiento	Precisión	Resolución vertical
T-4	Temperatura	460 m	30 nudos	2% de la profundidad o $\pm 0.15^{\circ}\text{C}$	65 cm.
T-5	Temperatura	1830 m	6 nudos	2% de la profundidad o $\pm 0.15^{\circ}\text{C}$	65 cm.
T-7	Temperatura	760 m	15 nudos	2% de la profundidad o $\pm 0.15^{\circ}\text{C}$	65 cm.
SV-02	Vel. Del sonido	2000 m	8 nudos	2% de la profundidad o $\pm 0.25\text{m/s}$	32 cm.
XCTD	Temperatura, conductividad y salinidad	1000 m	10 nudos	2% de la profundidad o $\pm 0.3^{\circ}\text{C}$	No especificada

Calibración

Las sondas vienen ya calibradas de fábrica, según el fabricante para las sondas T-7 la precisión en la medida de temperatura es mejor del 2% de la profundidad o de $\pm 0.15^{\circ}\text{C}$, lo que sea peor.

Metodología

Los lanzamientos realizados han sido de sondas XBT de los modelos XSV-02 Los perfiles realizados se hacen pasar por el programa SVP Manager de forma que este los transforma en ficheros .asvp. Una vez transformados se pasan por la red Ethernet a las sondas, las cuales aplican el perfil para corregir las profundidades.

En la presente campaña se ha utilizado tres sondas XSV-02, para toda la zona de trabajo.

Las localizaciones de lanzamiento de las sondas fueron las siguientes:

Xbt1: 37° 4.52686N ---- 11° 21.51489W

Xbt2: 35° 12.05322N --- 9° 10.50916W

Xbt3: 36° 21.99097N --- 8° 41.83875W

All.5. Seapath 200

Introducción

El Seapath200 es el alma de los sensores de actitud del barco. Consta de dos antenas GPS, separadas 4 metros, una unidad central y su pantalla, situadas en el rack de proa del laboratorio de Equipos Electrónicos Proa (Sondas).

El equipo toma datos del GPS y de la VRU (Unidad de referencia vertical) que da información sobre la actitud del barco, cabeceo, balanceo, oleaje. Procesa

los datos y genera telegramas NMEA heading, actitud y de posición, que se reparten por todo el barco a través de un sistema de distribución de datos situado tras los racks de EEPROA.

Su configuración (fichero *hesperides.par*) incluye la posición de los sensores respecto al centro del barco, que se considera está en la MRU, local de gravimetría.

La posición que proporciona el Seapath 200 corresponde al centro de gravedad del Barco (MRU en el local de gravimetría).

Technical characteristics

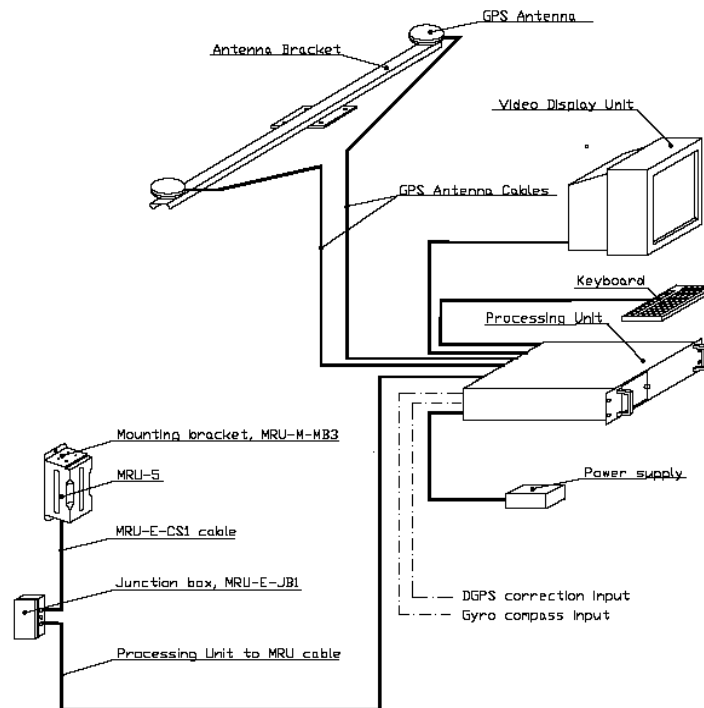


Figure All.1.- Esquema de funcionamiento del sistema Seapath 200

Las antenas GPS proporcionan la información de Heading, velocidad, posición y tiempo, mientras que la MRU proporciona la información de actitud.

Para asegurar que las marcas de tiempo son correctas, el PPS del GPS se utiliza como tiempo de referencia tanto para la unidad central como la MRU.

La información de Seapath está disponible en la pantalla y en 4 Leds situados en la unidad central. Los Leds indican el estado de la unidad de forma que el color amarillo indica que el sistema funciona correctamente, el color naranja indica que las prestaciones no son del todo precisas y el color rojo indica que los datos son malos.

Los Leds empezando de izquierda a derecha representan:

Velocidad/Posición Heave Roll/Pitch Heading.

Cuando no hay correcciones diferenciales DGPS el primer led (Vel/Pos) queda en **Naranja**.

Roll and pitch accuracy: 0.05° RMS
 Heading accuracy with 2.5 meter Antenna baseline: 0.075° RMS
 Heading accuracy with 4 meter Antenna baseline: 0.05° RMS
 Scale factor error on heading (typical): 0.2%
 Heave accuracy: 0.05 m RMS
 Position accuracy: 2.5 m (95% CEP)
 Velocity accuracy: 0.03 m/s 1 σ or 0.07 m/s (95% CEP)

Las posiciones que da el GPS de Seapath están referenciadas al centro del barco, en la imagen se observa la distancia entre la antena GPS y el centro del barco (que coincide con la posición de la MRU5). La distancia del centro del barco al espejo de popa es de 50 metros.

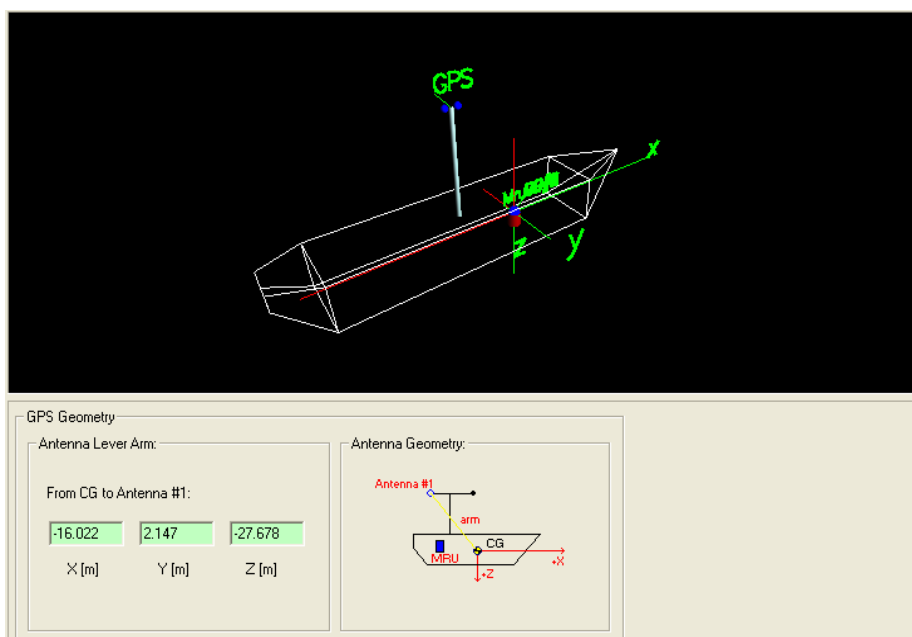


Figure All.2.- Geometría GPS-Centro del barco

All.8. Gravímetro marino BGM-3

Características técnicas

El gravímetro BGM-3 es un sistema de adquisición de datos de gravimetría aerotrasportado y marino.

El sistema tiene un sensor montado en una plataforma giro-estabilizada, Los datos en bruto se procesan, filtran y escalan en un ordenador HP-486/50 mediante el software BGM, que a su vez almacena los datos en disco duro y los envía por la red Ethernet, para que sean capturados por el integrador de datos. El formato de los datos es el siguiente:

Datos brutos:

\$PRAWGRV,Día,Hora,Flag,Valor Medido

Datos que se envían por la red:

\$PHESGRV,Día,Hora,Flag,Valor Medido,Valor GRS67,Corrección
 $E^{\wedge}tv^{\wedge}s, \sin v, \sin v$

Flag: Valor que indica el estado del gravímetro. 0: normal, 2: error, 5: arrancando.

El sistema está compuesto por los siguientes elementos:

Subsistema sensor: Consta de un rack con los dispositivos electrónicos de alimentación, de acondicionamiento de señal y baterías de emergencia. El subsistema sensor genera un tren de pulsos cuya frecuencia es proporcional a la gravedad en el rango del instrumento y una señal de referencia para contarlos. También generan los bits de status correspondientes a un mal funcionamiento.

Plataforma estabilizada: Aísla el sensor de gravedad de las posibles influencias de los movimientos del buque y lo alinea con la vertical. Consiste en una plataforma estabilizada, de una electrónica de control y alimentación del sistema.

Subsistema de adquisición: Está formado por un PC HP-486/50.

Calibración

El gravímetro BELL AEROSPACE-TEXTRON BGM-3 (actualmente Lockheed Martin Federal Systems) viene calibrado de fábrica, pero es conveniente una comprobación periódica para ajustar las posibles derivas. Las medidas de recalibración se realizan con un gravímetro portátil WORDEN mod. MASTER de la UTM

HOJA DE CALIBRACIÓN

GRAVÍMETRO:	BGM-3	
	BIO	
BUQUE:	HESPÉRIDES	

Fecha:	25/10/2008	Hora:	
Referencia BASE:	Cartagena Base ZEE		
Localización BASE:	Muelle carenero Navantia		
Localización BIO	Arsenal		
Campaña:	NEAREST- SEIS		
Operador / es:	Jose Luis Pozo/Toni Bermúdez		
Gravímetro portátil:	Worden		
(0) Valor BASE (mgal):	980017,915		

DATOS DE CAMPO			
Medidas	Hora GMT	Lectura (div.)	Altura (m)
(1) BIO 1	14:07	1452,40	0,69
(2) BASE1	14:22	1451,80	
(3) BIO2	14:33	1452,80	0,69
(4) BASE2	14:43	1450,70	
(5) BIO3	14:54	1453,00	0,68
Núm medidas BASE	2		
Núm. medidas BIO	3		

CÁLCULOS

(6) Valor medio en BIO:	1452,73	div.
(7) Valor medio en BASE:	1451,25	div.
(8) Diferencia medias (6)-(7):	1,48	div.
(9) Cte Calibración WORDEN :	0,08590	mgal.
(10) Diferencia en mgal (8)*(9):	0,12742	mgal.
(11) G _{muelle} (mgal):	980018,042	mgal.

(12) Altura del muelle (m):	0,69	m
(13) Distancia BGM-3 a línea flotación:	2,3	m
(14) Distancia total:	2,99	m
(15) Cte. por correcc. por Aire Libre:	0,3086	mgal. / m
(16) Correc. total por Aire Libre (mgal.):	0,92169	mgal.
(17) G. calculada en Local gravimetría:	980018,964	mgal.

(18) Valor medio BGM-3 (G medida):	980018,1355	mgal.
(19) Bias en BGM-3	852014,17	mgal.

(20) Diferencia a corregir (17) - (18)	0,8286	mgal.	Offset resp/ arranque anterior
(21) Nuevo BIAS teórico (calculado) (19)+(20):	852015,00	mgal.	Nuevo Bias entrado
(22) Bias p/ adquisición (Arranque):	852015,00	mgal.	

All.9. Sistema de cañones de aire comprimido

Características técnicas

ver apartado 9.4 para los cañones y el Anexo IV para el sistema de adquisición de registros.

Incidencias

En el Perfil P1 el despliegue de los cañones se realizó el día 30/10/2008 a las 18:15, y se comienza a disparar en modo softstart que consiste en añadir un cañón en cada disparo. El intervalo de disparo durante esta fase es de 60 segundos y se dispara en modo interno (el controlador de cañones genera su propio trigger). EL disparo número 9 y 10 son disparos de calibración, no se registran. En el disparo número 11, a las 18:25 se detecta una fuga en el cañón número 1 (1000 p.c.). Se para de disparar y se sacan los cañones del agua para reparar la fuga. Se largan de nuevo los cañones y se comienza a disparar. Se realizan 12 disparos de calibración y en el disparo número 16 se detecta una nueva fuga de aire en el cañón número 1 y se decide volver a recoger el array principal.

Por el mal estado de la mar se decide aplazar la maniobra de largado de cañones ya que con esas condiciones el peligro tanto para los equipos como para el personal es inminente.

El día 1/11/2006 se vuelven a largar los cañones una vez ha mejorado el estado de la mar y se comienza a disparar. Después de 5 disparos la línea de aire se vuelve a romper (probablemente debido a la dificultad de la maniobra

de largado), pero se decide dejar los cañones en el agua y continuar disparando, las posibilidades de que se vuelva a romper son altas y se ha perdido demasiado tiempo.

En el disparo 340 se produce una desincronización del cañón n° 5 de mas de 500 milisegundos, debido a un problema en el transductor de la solenoide. Una vez se ha corregido esta desincronización hasta un nivel de 2 milisegundos se pone el cañón en modo estático para evitar que se vuelva a producir esa desincronización.

En el disparo 808 se recoge el cañón de cruja para alargar el cable de la boya. Debido a la tensión del cabo de la boya el cañón está mas en superficie de lo que debería y la burbuja interfiere con las del array principal.

En el disparo 1922 se rompe la línea de aire del cañón n° 6. Como el final de la línea está cercana se decide no sacarlos y continuar disparando con un volumen menor.

En el perfil P2 e despliegan los cañones a las 10:30 de la mañana, sin incidencias que destacar. Se realizan 20 disparos de calibración y se dejan los cañones en Stand-By. Se comienza a disparar a las 12:00 de la mañana.

A las 4:30 (disparo 655) se detecta un fallo electrico en el cañón n° 2 (1000 c.i.) y se recogen los cañones para reparar. El fallo es una rotura en el "pigtail" de la solenoide que ha dejado inservible la solenoide (Figura AII.3). Se cambia la solenoide y se aprovecha para repasar el resto del array. Se vuelven a desplegar los cañones a las 6:56. Se continua la secuencia de disparo.

El día siguiente a las 14:15 se produce un error de continuidad en el cañón n° 2, probablemente por rotura en el pigtail ya que al recoger los cañones a final de la línea no se detecta ningun daño en la solenoide. Se deja de disparar ese cañón hasta final de línea.



Figura AII.3.- Rotura de la solenoide y el pigtail cañón n° 2 de 1000 cu.in

Annex III: Report on filming done by ZDF

Team members: Bertram Kropac, Camera
Thomas Mailänder, Assistant
Heike Schmidt, Script

The scheduled ZDF-project “Lisbon 1755” is a documentary about the great earthquake that destroyed most of Lisbon in the 18th century. The documentary will combine re-enactments with the documentation of modern science dedicated to the research of seismic activities from different fields, plus interviews with the associated scientists. One of the mayor scientific parts of the documentary will be the work on the Hespérides in the Gulf of Cadiz – the very place, where the epicentre of the earthquake of 1755 must be located somewhere.

The storyline of the drama will unfold not only the main events from 1755 but also the timeline of the cruise with all its scientific components. Therefore the filming on board covered most of the scientific work executed during the cruise.

gaining bathymetric data
preparing and deploying the OBS
preparation of the airguns
shooting with the airguns
recovering the OBS
processing the acquired data
in addition different shots where taken of some of the scientific team members during shifts.

Furthermore interviews have been taken with Valenti Sallares, Scientific Leader of the Mission and Mark-André Gutscher, with whom we have worked already before.

The interviews covered not only the scientific campaign on board of the Hespérides but also some questions about the Lisbon earthquake in particular and seismic hazards in the Gulf of Cadiz in general.

All the scientists were more than helpful to fulfil our mission.

Thanks a lot!

Annex IV: Scripts and configuration parameters (in Spanish)

AIV.1. Sistema de adquisición de registros

El sistema de navegación y generación de eventos genera 4 diferentes telegramas de los cuales 3 son registrados localmente por el sistema de navegación y el cuarto es enviado por puerto serie a diferentes sistemas, uno de ellos registra el telegrama correspondiente a cada uno de los eventos o disparos.

Hasta esta campaña, para generar la secuencia de disparo se ha utilizado o bien el sistema de navegación Konmap o el EIVA. En esta campaña se ha utilizado un GPS Modelo Fei-Zyfer GPS Starplus. Este GPS se programa para que produzca un pulso de trigger cada 90 segundos que es recibido por el controlador de cañones por el puerto Trigger A y este, a su vez, comienza la secuencia de disparo descrita más arriba. El controlador de cañones da la orden de disparo y cuando todos los cañones disparan, en el momento denominado Fire Time Break se genera un pulso a través del puerto FTB del controlador de cañones que se envía al GPS y se obtiene un telegrama con el tiempo exacto del disparo.

Formato de los ficheros de registros

Fichero telegrama de evento de disparo resultante del Minipulse

```
$HYDRA 1 NearestL1 03 I 02/01/07 19:42:38 0 2 7 0 0 0 0 0 0 0 0 1 S P 1 N
0 0 0 000 0 2 S P 1 N 0 0 0 000 0 3 S P 1 N 0 0 0 000 0 4 S P 1 N 0 0 0 000
0 5 S P 1 N 0 0 0 000 0 6 S P 1 N 0 0 0 000 0 7 S P 1 N 0 0 0 000 0
$GPGGA,050504.273,3439.90062,N,01009.11131,W,2,6,1.3,40.4,M,0.0,M,
0,0000*40
```

Interpretación: En el instante del disparo el controlador de cañones genera un telegrama resultado de unir el telegrama de navegación procedente del EIVA con uno propio en el que se genera con información referente al disparo, e información de cada uno de los cañones, además del numero de disparo. Este telegrama se envia por el puerto COM2 a otro host. El mismo puerto COM2 recibe la navegación procedente del EIVA.

Format	Description	No. of Bytes	Position
A	“\$HYDRA”	7	0
N	N' mero de Disparo	-	1
A	Nombre de Linea-	-	2
XX	N' mero de Array	3	3
A	Modo de Disparo I= Internal, E=External	2	4
YY/MM/DD	Fecha	9	6
HH:MM:SS	Hora	9	7
N	Pattern Point	-	7
N	Numero de Sub- Arrays	-	8

N	N' mero máximo de cañones en el Array	-	9
N	N' mero de cañones activos	-	10
N	Numero de errores	-	11
N	Numero de Auto-Disparos	-	12
N	Numero de disparos omitidos	-	13
N	Delta Spread	-	14
N	Volumen de disparo total	-	15

La secuencia siguiente se repite para cada cañón en el array:

Format	Description	No. of Bytes	Position
N	N' mero de cañón	-	0
A	Modo de disparo	-	1
A	Tipo de sincronización	-	2
A	Gun Fire Pattern	-	3
A	Estado de autodisparo 'Y' o 'N'	-	4
NNNN	Offset estático total (Cañón + retardo del Array)	-	5
NNN	Offset Dinámico Total	-	6
NNN	Tiempo de disparo	-	7
NNN	Delta Offset	-	9
NNN	Profundidad del cañón	-	10

La segunda parte del telegrama combinado, la formada por la información procedente del sistema de navegación EIVA comienza con la palabra \$GPGGA y está formado por los siguientes campos:

Formato	Descripción	No de Bytes	Posición
A	"\$GPGGA"	7	1
NNNN.NNN	Latitud	8	2
A	Etiqueta Latitud	1	3
NNNN.NNN	Longitud	8	4
A	Etiqueta Longitud	1	5

DDMMAAA	Fecha	8	6
A			
HHMMSS	Hora	6	7
N	Rumbo	-	8
N	Dirección	-	9
N	Velocidad	-	10
N	Profundidad	-	11
A	Nombre Linea	-	12
N	Fix Number	-	13
A	Código de Control	-	14

A) Fichero telegrama de evento de disparo resultante del GPS Fei-Zyfer

New Tag [375]: 305:16:26:00.1558857 Latitude 34:33.4229 N Longitude 10:0.4551 W Altitude 69.21 metres

B) Fichero telegrama de evento de disparo registrado en SADO

A la vez que se producen estos dos telegramas, se produce un tercer telegrama que es enviado a través de la trama 3008 UDP en Broadcast al sistema de adquisición de datos oceanográficos, dando lugar al siguiente telegrama:

\$PHESOBS,108,306,00,00,30,1552576,34,46.9652,N,10,13.2593,W,68.98,00,00,30,4152.5,34.7830151,-10.2210676,336.07,4.3,01112008,000029

Descripción: \$PHESOBS, número de evento, día juliano, hora, minuto,segundo, partes de segundo, latitud (grados), latitud (minutos centesimales), marca de latitud, longitud (grados), longitud (minutos centesimales), marca de longitud, rumbo, hora del sistema, minuto del sistema, segundo del sistema, profundidad, latitud (grados centesimales), longitud (grados centesimales), rumbo, velocidad, fecha SADO, minuto SADO.

AIV.2. Sistema de Navegación y generación de disparos

Introducción

Hasta este momento se ha utilizado como sistema navegador de sísmica y generador de eventos al Konmap, un sistema de Kongsberg, que no se adecuaba a las necesidades de precisión que se requería la sísmica embarcada en el Hesperides.

Se ha buscado un sistema que fuera a la vez fiable y no desmesuradamente caro. En la industria petrolera comercial existen sistemas muy precisos, pero extremadamente caros. Como consecuencia de exposiciones como el Oceanology, o de la adquisición de nuevos equipos para el Sarmiento de Gamboa, contactamos con la gente de EIVA y se propuso probar su sistema de sísmica en una campaña, en este caso la MARSIBAL_I (HE117) y si los resultados eran satisfactorios se adquiriría un sistema para el BIO Hesperides.

Descripción

El sistema esta formado por los siguientes elementos.

- PC de adquisición y control.
- Software: NaviPac y NaviEdit
- Multipuesto den entrada y salida
- Caja con 4 salidas de eventos

Configuración

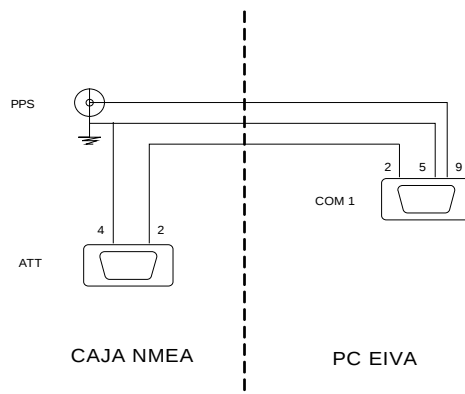
Red: Dirección IP: 192.168.1.33

Entradas: Todas las entradas vienen de la caja NMEA de datos del Seapath 200

GPS: COM4, 4800, 8, N, 1

- GYRO: COM 5, 9600, 8, N, 1
- PPS+ZDA: COM1, 9600, 8, N, 1

El conexionado del PPS+ZDA es el siguiente:



Salidas

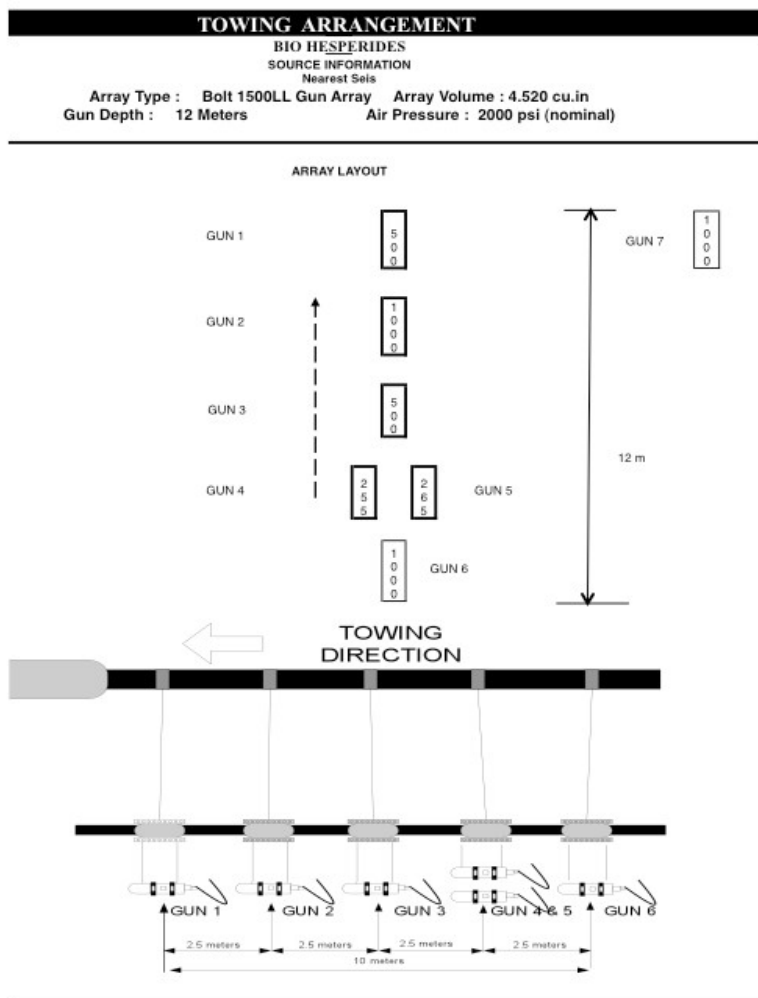
- Posición to trigger: COM 6, 9600, 8, N, 1
 - o Formato: Telegrama NMEA \$GPGGA
 - o Este telegrama va al controlador de cañones Hydra
- Telegrama de sísmica: COM 7,9600, 8, N, 1
 - o Formato: Line_name, Día, Hora, Evento, X (grid), Y (grid), Latitud, Longitud, Heading, Dirección de la línea, Velocidad, COM-DAQ+
 - o Este telegrama se graba con un Terminal y contiene toda la información del evento.
- Posición to Delph: COM 9, 9600, 8, N, 1
 - o Formato: Telegrama NMEA \$GPGGA
 - o Este telegrama va al controlador de cañones

NaviPac

Consta de dos programas principales que controlan al resto.

- NaviPac config este software es el de configuración de todos los elementos del sistema. Desde aquí se activan el resto de programas
- NaviPac Online, este programa es que controla la navegación, la adquisición, los eventos y la visualización. Tiene, entre otros, los siguientes programas asociados.

- o Definición de eventos
- o GPS Status.
- o Input Monitor
- o Log Data
- o Helsen Display
 - Generación de líneas
 - Selección de líneas
 - Inicio de la adquisición
 - Control de la navegación



AIV.4. Script for OBS data processing

Script for OBS relocation

```
#
# By IFREMER
#/bin/csh

awk 'BEGIN{a=0} {if ($2 <= a) print $1,-$2 ; if ($2 > a) print $1,$2 ; a = 0}'
obs14_4.water.picks >! tmp
awk '{if ($2 < 1720) print $1,$2}' tmp >! water.picks

\rm tmp*
#set BATHYGRD = /home/gailler/NEAREST/GMT/gridone.grd
set BATHYGRD = /home/gailler/NEAREST/GMT/Compil12.grd
set FICHNAV = ./nav_p1.dat
set VWAT = 1.500
set LONOBSSORIG = -11.0799
set LATOBSSORIG = 36.2279
#set LONOBSSORIG = -11.0799
#set LATOBSSORIG = 36.2279
set INT = 0.001          ##### 0.001 apres 0.0002
set TICK = 0.005       ##### 0.005

set CALC = y

gmtset D_FORMAT %f
echo $LONOBSSORIG $LATOBSSORIG > obs.dat
#set INC = 1.5          ##### valeur de INC pour gridone.grd
#set INT2 = 0.0020/0.0020  ##### valeur de INT2 pour gridone.grd
set INC = 0.5
set INT2 = 0.0010/0.0010

grdsample -I${INT2} $BATHYGRD -Gobs.grd `minmax -I${INC} obs.dat`

awk '{printf ("%5d %8.6f %8.6f \n", $1, $5, $4 )}' ${FICHNAV} >! nav.dat

##### Calculate Travel Times

if ($CALC == y) then

\rm chi.dat

awk '{printf ("%5d %8.6f \n", $2, $1-0.000)}' water.picks | sort -u -n >! water_sort.picks

paste /home/gailler/NEAREST/PROFIL1/RAW_SU/obs14/offset_obs14.dat $FICHNAV >
temp
awk '{printf ("%5d %8.6f %8.6f \n", $1, $6, $5 )}' temp >! shots

\rm tmp
awk '{print "grep -w " ($1) " shots >> tmp1"}' water_sort.picks >! ordre1
source ordre1
paste water_sort.picks tmp1 >! tmp2
awk '{print $4, $5}' tmp2 >! pick.ll

awk '{print "grep -w " ($2) " nav.dat >> tmp3"}' pick.ll >! ordre1b
source ordre1b
awk '{print $1}' tmp3 >! offshots
```

```

set numlon = -5
while ( $numlon < 5 )

set LONOBBS = $LONOBBSORIG

awk '{CONVFMT="%8.5f" ; OFMT="%8.5f" ; print "set LONOBBS = " (" $
{LONOBBS}'+$numlon*${INT}'))' obs.dat >! ordre2
source ordre2

set numlat = -5
while ( $numlat < 5 )

##### * -1 to get negative latitudes...
set LATOBBS = $LATOBBSORIG
awk '{CONVFMT="%8.5f" ; OFMT="%8.5f" ; print "set LATOBBS = " (" ${LATOBBS}'+$numlat*${
INT}'))' obs.dat >! ordre3
source ordre3

\rm gmt.dat dist.dat tmp*
echo $LONOBBS $LATOBBS >! tmp
grdtrack -Gobs.grd `minmax -I${INC} obs.dat` tmp >! obs.depth
awk '{print "set DOBS = " $3/1000}' obs.depth >! ordre4
source ordre4

echo "LON LAT DEPTH" $LONOBBS $LATOBBS $DOBS

awk '{CONVFMT="%8.5f" ; OFMT="%8.5f" ; print "project -G10000 -Q -C" (" ${LONOBBS}"/" (" $
{LATOBBS}"/" -E"$1"/"$2" >> gmt.dat"')} pick.ll >! ordre5
source ordre5

awk '{CONVFMT="%8.5f" ; OFMT="%8.5f" ; if ($3 != 0) print $0}' gmt.dat >! dist.dat
echo $DOBS $LONOBBS $LATOBBS $VWAT
paste dist.dat water_sort.picks | awk '{CONVFMT="%8.5f" ; OFMT="%8.4f" ; print $4, $3, $5,
$1, $2}' >> tmp1
awk '{CONVFMT="%8.5f" ; OFMT="%8.5f" ; print $1, (sqrt(($2^2) +
((-1*$DOBS)^2))/$VWAT) , $3 }' tmp1 >> tmp2
awk ' BEGIN {a=0}{ CONVFMT="%8.5f" ; OFMT="%8.5f" ; b =((($2 - $3)^2); a=a+b } END
{print sqrt(a/NR), "${LONOBBS}', "${LATOBBS}'}' tmp2 >> chi.dat

awk 'BEGIN {a=999} {CONVFMT="%8.5f" ; OFMT="%8.5f" ; if ($1 < a) b = $2 ; if ($1 < a) c =
$3 ; if ($1 < a) a = $1} END {print b, c, a}' chi.dat > final.dat

set numlat=`expr $numlat + 1`
end

set numlon=`expr $numlon + 1`
end

endif ### $CALC == y

##### Plot
# gmtset D_FORMAT %lg
gmtset D_FORMAT %f
gmtset PAPER_MEDIA a4+
gmtset PAGE_ORIENTATION portrait
gmtset HEADER_FONT Helvetica-Bold
gmtset HEADER_FONT_SIZE 14
gmtset ANOT_OFFSET 0.1
gmtset TICK_LENGTH 0.1
gmtset ANOT_FONT_SIZE 10

```

```

gmtset LABEL_FONT_SIZE 10
gmtset DOTS_PR_INCH 400
gmtset MEASURE_UNIT cm

awk '{print $2, $3, $1}' chi.dat > chi2.dat

minmax -C -I${INT} chi2.dat > tmp
awk '{print "set LON1 = " $1}' tmp > ordre6
awk '{print "set LON2 = " $2}' tmp >> ordre6
awk '{print "set LAT1 = " $3}' tmp >> ordre6
awk '{print "set LAT2 = " $4}' tmp >> ordre6
source ordre6

set SCALE = X7

grdsample obs.grd `minmax -I${INC} obs.dat` -I${INT} -Gtmp0.grd
grdcut tmp0.grd -R${LON1}/${LON2}/${LAT1}/${LAT2} -Gtmp1.grd
grd2cpt tmp1.grd -Cocean > chi.cpt
grdimage -J${SCALE} -R${LON1}/${LON2}/${LAT1}/${LAT2} -C tmp1.grd -Cchi.cpt -Ba$
{TICK}/a${TICK}:. "":WeSn -G5 -K -Y16 > reloc.ps
awk '{CONVFMT="%8.5f" ; OFMT="%8.5f" ; print $2, $3}' nav.dat | psxy -J${SCALE} -R$
{LON1}/${LON2}/${LAT1}/${LAT2} -O -W1/255/0/0 -K -N >> reloc.ps
awk '{CONVFMT="%8.5f" ; OFMT="%8.5f" ; print $2, $3}' nav.dat | psxy -J${SCALE} -R$
{LON1}/${LON2}/${LAT1}/${LAT2} -O -Sc0.1 -G255/0/0 -K >> reloc.ps

awk '{CONVFMT="%8.5f" ; OFMT="%8.5f" ; print $2, $3 " 6 0 1 BL " $1}' nav.dat |\
    pstext -J${SCALE} -R${LON1}/${LON2}/${LAT1}/${LAT2} -O -K -W255/255/255 >>
reloc.ps

psxy -J${SCALE} -R${LON1}/${LON2}/${LAT1}/${LAT2} obs.dat -O -Si0.2 -G255/0/0 -K -N >>
reloc.ps

xyz2grd chi2.dat -R${LON1}/${LON2}/${LAT1}/${LAT2} -I${INT}/${INT} -Gchi.grd
grd2cpt chi.grd -Crainbow > chi.cpt

grdimage -J${SCALE} -R${LON1}/${LON2}/${LAT1}/${LAT2} -C chi.grd -Cchi.cpt -Ba$
{TICK}/a${TICK}:. "":WesN -G5 -K -X10 -O >> reloc.ps
awk '{CONVFMT="%8.5f" ; OFMT="%8.5f" ; print $2, $3}' nav.dat | psxy -J${SCALE} -R$
{LON1}/${LON2}/${LAT1}/${LAT2} -O -W1/255/0/0 -K -N >> reloc.ps
awk '{CONVFMT="%8.5f" ; OFMT="%8.5f" ; print $2, $3}' nav.dat | psxy -J${SCALE} -R$
{LON1}/${LON2}/${LAT1}/${LAT2} -O -Sc0.1 -G255/0/0 -K >> reloc.ps
psxy -J${SCALE} -R${LON1}/${LON2}/${LAT1}/${LAT2} obs.dat -O -Si0.2 -G255/0/0 -K -N >>
reloc.ps
psxy -J${SCALE} -R${LON1}/${LON2}/${LAT1}/${LAT2} final.dat -O -Si0.5 -G255/255/0 -K -N
>> reloc.ps
psxy -J${SCALE} -R${LON1}/${LON2}/${LAT1}/${LAT2} chi2.dat -O -Sc0.05 -G0/0/255 -K -N
>> reloc.ps
echo -1 1.4 12 0 5 "LT `more final.dat`" | pstext -J${SCALE} -R-1/1/-1/1 -O -V -W255/255/255
-N -K >> reloc.ps

gmtset D_FORMAT %lg
\rm gmt.dat dist.dat

echo $LONOBSORIG $LATOBSORIG >! obstemp.dat
echo $LONOBSORIG $LATOBSORIG
grdtrack -Gobs.grd `minmax -I${INC} obs.dat` obstemp.dat >! obs.depth
awk '{print "set DOBS = " $3/1000}' obs.depth >! ordre7
source ordre7

```

```

awk '{print "project -G10000 -Q -C${LONOBSORIG}/${LATOBSORIG} -E"$1/"$2" >>
gmt.dat"}' pick.ll >! ordre8
source ordre8
awk '{if ($3 != 0) print $0}' gmt.dat >! dist.dat
paste dist.dat water_sort.picks | awk '{print $4, $3, $5, $1, $2}' | awk '{print $1, (sqrt(($2^2) +
((-1*$DOBS)^2))/$VWAT) , $3 } >! obsorig.dat

paste offshots obsorig.dat | sort -u -n >! obsorig.shot
set SHOTMIN=`awk '{if (NR==1) {print $1-2}}' obsorig.shot`
set SHOTMAX=`awk '{if (NR==1) {print $1+22}}' obsorig.shot`

echo ${SHOTMIN} ${SHOTMAX}

awk '{print $1, $4, 0.040}' obsorig.shot | psxy -J$SCALE -R${SHOTMIN}/${SHOTMAX}/2/5
-Sc0.001 -Ey0.001/3/0/0/0 -Ba5f1:"Pick number":/a0.5f0.1:"Time [s]":WnSe -O -K -X-10 -Y-10
>> reloc.ps
awk '{print $1, $3, 0.040}' obsorig.shot | psxy -J$SCALE -R${SHOTMIN}/${SHOTMAX}/2/5 -
W1/255/0/0 -O -K >> reloc.ps

##### ATTENTION obs.dat changed from final.dat
awk '{print "set FINLON = " $1}' final.dat >! finobs
awk '{print "set FINLAT = " $2}' final.dat >> finobs
source finobs

echo $FINLON $FINLAT >! obstemp.dat
echo $FINLON $FINLAT
grdtrack -Gobs.grd `minmax -I${INC} obs.dat` obstemp.dat >! obs.depth
awk '{print "set DOBS = " $3/1000}' obs.depth >! ordre9
source ordre9

\rm gmt.dat dist.dat
awk '{print "project -G10000 -Q -C${FINLON}/${FINLAT} -E"$1/"$2" >> gmt.dat"}' pick.ll >!
ordre10
source ordre10
awk '{if ($3 != 0) print $0}' gmt.dat >! dist.dat
paste dist.dat water_sort.picks | awk '{print $4, $3, $5, $1, $2}' | awk '{print $1, (sqrt(($2^2) +
((-1*$DOBS)^2))/$VWAT) , $3 } >! obsfin.dat

paste offshots obsfin.dat | sort -u -n >! obsfin.shot
set SHOTMIN=`awk '{if (NR==1) {print $1-2}}' obsfin.shot`
set SHOTMAX=`awk '{if (NR==1) {print $1+22}}' obsfin.shot`

echo ${SHOTMIN} ${SHOTMAX}

\rm tmp*

awk '{print $1, $4, 0.040}' obsfin.shot | psxy -J$SCALE -R${SHOTMIN}/${SHOTMAX}/2/5
-Sc0.001 -Ey0.001/3/0/0/0 -Ba5f1:"Pick number":/a0.5f0.1:"Time [s]":WnSe -O -K -X10 >>
reloc.ps
awk '{print $1, $3, 0.040}' obsfin.shot | psxy -J$SCALE -R${SHOTMIN}/${SHOTMAX}/2/5
-W1/255/0/0 -O >> reloc.ps

#/usr/local/stow-dir/cwp_su_all_41/bin/psmerge in=reloc.ps scale=0.75,0.75 >! test2.ps
\rm ordre* tmp* temp* gmt.dat dist.dat chi* *.shot obs.grd obstemp* *obs obsfin.dat
obsorig.dat
gv reloc.ps

```

Script for record section representation

```
#!/bin/ksh
#####PROGRAMA PARA PROCESAR Y PLOTEAR LOS OBS #####
#####DE LA UTM Y LOS MICROBS IFREMER/UBO #####
#####CAMPAÑA NEAREST-SEIS. AUTOR:RAFA BARTOLOME, 2008 #####

#--- Origen OBS: French=f UTM=u -----
fig=f
#fig=u
#-----
#
if [[ $fig = f ]]; then
perfil=2
num=38
component=4
obs=obs$num_"_$component.su.off
DIR=/media/LaCie/nearest/OBS-Data/FrenchOBS/Profil-P$perfil/OffsetSU/obs$num
DIRps=/media/LaCie/nearest/OBS-Data/FrenchOBS/Profil-P$perfil/Plots
#
suchw <$DIR/$obs key1=d2 key2=sx | suchw key1=sx key2=sy b=0.36 | suchw key1=sy
key2=d2 b=0.36 > tmpkk
suchw < tmpkk key1=d2 key2=gx | suchw key1=gx key2=gy b=0.36 | suchw key1=gy
key2=d2 b=0.36 > tmpsu
fi
#
#
if [[ $fig = u ]]; then
perfil=2
num=42
component=Z
obs=obs$num-p$perfil"_NearestL"$perfil"_L28"$component
#obs=obs$num-p$perfil"_NearestL"$perfil"_HYD"
DIR=/media/LaCie/nearest/OBS-Data/SpanishOBS/Profil-P$perfil/SEGYPData/obs$num-p
$perfil/segyp
DIRps=/media/LaCie/nearest/OBS-Data/SpanishOBS/Profil-P$perfil/Plots
sgyfile=$DIR/$obs.segy
echo sgyfile=$sgyfile
segypread tape=$sgyfile endian=0 | segypclean > tmpsu
#
fi
#
#####
#
#####
#
#----- OPCIO NOU OFFSET -----
### Calcul del offset en funcio de la posicio de l'OBS i lat/lon dels tirs ###

# -----1er pas -----
# Extraccio de lat/lon dels tirs dels headers

    sugethw key=sx,sy output=geom < tmpsu | \
    awk '{printf("%9.5f %7.5f\n", $1/3600., $2/3600.)}' > latlon.asc.tmp
#
#
# -----2on pas -----
# Posicion de l'OBS
```

```

    sugethw key=gx,gy output=geom < tmpsu | \
    awk '{printf("%9.5f %7.5f\n", $1/3600, $2/3600)}' > OBSpos.asc.tmp

lonOBS=`awk '{if (NR==1) print $1}' OBSpos.asc.tmp`
latOBS=`awk '{if (NR==1) print $2}' OBSpos.asc.tmp`
echo 'lonOBS' $lonOBS
echo 'latOBS' $latOBS

# -----3er pas -----
# Calcul de la distancia entre els shots i l'obs en metres

project latlon.asc.tmp -Fxy pq -Dd -Q -C$lonOBS/$latOBS -A90 |
awk '{print $1,$2,(sqrt(($3*$3)+($4*$4)))*1000}' > $obs".offset.tmp"

#-----4art pas -----
# Busco el shot que te la distancia mes propera al OBS: cap al Sud sera -, cap al nord +

awk '{ if (NR==1) xant=$3;
      {if (NR>1)
        {if ($3<xant) print $1,$2,$3,xant; xant=$3}
      }
    }' $obs".offset.tmp" > offset_petit.asc.tmp
#
offset_petit=`tail -1 offset_petit.asc.tmp | awk '{print $3}`
lonoffset_petit=`tail -1 offset_petit.asc.tmp | awk '{print $1}`
latoffset_petit=`tail -1 offset_petit.asc.tmp | awk '{print $2}`
#
echo 'punt mes a prop al OBS'
echo 'en metres, offset_petit=$offset_petit
echo 'lonoffset_petit=$lonoffset_petit
echo 'latoffset_petit=$latoffset_petit
#
echo $latoffset_petit | cat - $obs.offset.tmp |
awk '{ if (NR==1) h=$1;
      {if (NR>1)
        {if ($2<=h) print -int($3); else print int($3)}
      }
    }' > $obs.offset.tmp

#-----5e pas -----
#---inserto la distancia OBS-shot al header offset del file *.su--
a2b < $obs.offset.tmp n1=1 > $obs.offset.bin.tmp
sushw < tmpsu infile=$obs.offset.bin.tmp key=offset > $obs.su
#
#
#####
#####
#
psfile=$DIRps/$obs.ps
scalex=0.16
scaley=0.9
minof=-65000
maxof=65000
mnof=$(echo "$minof/1000." | bc -l)
mxof=$(echo "$maxof/1000." | bc -l)
tmn=0
tmx=10
rv=6
region=$mnof/$mxof/$tmn/$tmx
#

```

```

gmtset ANOT_FONT Times-Roman HEADER_FONT Times-Roman LABEL_FONT_SIZE
14p \
    LABEL_FONT Times-Roman ANOT_FONT_SIZE 14p HEADER_FONT_SIZE 14p
PAPER_MEDIA a4
#
segyclean < $obs.su |
sugethw key=fldr,offset output=geom > tmp.shot
distin=`head -1 tmp.shot| awk '{print (sqrt($2*$2))/1000.}'`
distmin=$(echo "$distin+$mnof" | bc -l)
distmax=$(echo "$distin+$mxof" | bc -l)
region2=$distmin/$distmax/$tmn/$tmx
#
segyclean < $obs.su |
suwind key=offset min=$minof max=$maxof tmin=0 tmax=25 |
sugethw key=fldr,sy,sx output=geom > tmp.shotminmax
shotmin=`head -1 tmp.shotminmax | awk '{print $1}'`
shotmax=`tail -1 tmp.shotminmax | awk '{print $1}'`
latmin=`head -1 tmp.shotminmax | awk '{print $2}'`
latmax=`tail -1 tmp.shotminmax | awk '{print $2}'`
#
echo 'shotmin=$shotmin
echo 'shotmax=$shotmax
echo 'latmin=$latmin
echo 'latmax=$latmax
#region2=$shotmin/$shotmax/$tmn/$tmx
echo 'mxof=$mxof
echo 'mnof=$mnof
echo $mxof > tmp.mxof
echo $mnof > tmp.mnof
echo $shotmax > tmp.shotmax
echo $shotmin > tmp.shotmin
echo $scalex > tmp.scalex
echo $latmin > tmp.latmin
echo $latmax > tmp.latmax
#
scalex2=`paste tmp.scalex tmp.mxof tmp.mnof tmp.shotmax tmp.shotmin | awk '{print
$1*((($2-$3)/($4-$5))}'`
signlat=`paste tmp.latmin tmp.latmax | awk '{if ($1>$2) print -1.; else print 1.}'`
echo 'signlat=$signlat
scalex2=$(echo "$signlat*$scalex2" | bc -l)
#
segyclean < $obs.su |
suwind key=offset min=$minof max=$maxof tmin=0 tmax=25 |
subfilt zerophase=0 fstplo=5.5 fpasslo=8 fpasshi=22 fstphi=25 |
suchw key1=d2 key2=offset a=0 b=.001 |
sugain agc=1 waggc=0.5 pbal=1 |
sureduce rv=$rv |
suascii bare=5 key=d2 sep=">" >tmp.xyz
#
echo 'perfil reduit a v=$rv
#
echo 'pintare pswiggle'
#
pswiggle tmp.xyz -R$region -Jx$scalex/$scaley -M -G0 -Z100 -K -Y5 -X3 > $psfile
psbasemap -B25f5:"Offset $obs (km)"/:2f0.5:"Time-X/$rv (s)":WeN \
-Jx -R -V -O -K >> $psfile
#
scalex2=$(echo "$scalex*$signlat" | bc -l)
psbasemap -B25f5:"Distance Along Profile (km)"/:2f0.5:"Time-X/$rv (s)":S \
-Jx$scalex2/$scaley -R$region2 -V -O >> $psfile

```

```
#  
rm tmp* *tmp *.su  
#  
echo 'pinto' $psfile  
#  
#  
gv $psfile &
```